



Stability of Viscous St. Venant Roll Waves: From Onset to Infinite Froude Number Limit

Blake Barker¹ · Mathew A. Johnson² · Pascal Noble³ ·
L. Miguel Rodrigues⁴ · Kevin Zumbrun⁵

Received: 9 December 2015 / Accepted: 27 August 2016 / Published online: 23 September 2016
© Springer Science+Business Media New York 2016

Abstract We study the spectral stability of roll wave solutions of the viscous St. Venant equations modeling inclined shallow water flow, both at onset in the small Froude number or “weakly unstable” limit $F \rightarrow 2^+$ and for general values of the Froude number F , including the limit $F \rightarrow +\infty$. In the former, $F \rightarrow 2^+$,

Communicated by Arnd Scheel.

Research of B.B. was partially supported under NSF Grants DMS-1400872, DMS-0300487, DMS-0801745, and CNS-0723054. Research of M.J. was partially supported under NSF Grant No. DMS-1211183. Research of P.N. was partially supported by the French ANR Project No. ANR-09-JCJC-0103-01. Research of M.R. was partially supported by the ANR project BoND ANR-13-BS01-0009-01. Research of K.Z. was partially supported under NSF Grant No. DMS-1400555.

✉ Mathew A. Johnson
matjohn@ku.edu

Blake Barker
blake@math.byu.edu

Pascal Noble
pascal.noble@math.univ-toulouse.fr

L. Miguel Rodrigues
luis-miguel.rodrigues@univ-rennes1.fr

Kevin Zumbrun
kzumbrun@indiana.edu

- 1 Brigham Young University, Provo, UT 84602, USA
- 2 University of Kansas, Lawrence, KS 66045, USA
- 3 Institut de Mathématiques de Toulouse, Toulouse, France
- 4 Université de Rennes 1, IRMAR, Rennes, France
- 5 Indiana University, Bloomington, IN 47405, USA

limit, the shallow water equations are formally approximated by a Korteweg-de Vries/Kuramoto–Sivashinsky (KdV–KS) equation that is a singular perturbation of the standard Korteweg-de Vries (KdV) equation modeling horizontal shallow water flow. Our main analytical result is to rigorously validate this formal limit, showing that stability as $F \rightarrow 2^+$ is equivalent to stability of the corresponding KdV–KS waves in the KdV limit. Together with recent results obtained for KdV–KS by Johnson–Noble–Rodrigues–Zumbrun and Barker, this gives not only the first rigorous verification of stability for any single viscous St. Venant roll wave, but a complete classification of stability in the weakly unstable limit. In the remainder of the paper, we investigate numerically and analytically the evolution of the stability diagram as Froude number increases to infinity. Notably, we find transition at around $F = 2.3$ from weakly unstable to different, large- F behavior, with stability determined by simple power-law relations. The latter stability criteria are potentially useful in hydraulic engineering applications, for which typically $2.5 \leq F \leq 6.0$.

1 Introduction

In this paper, we investigate the stability of periodic wavetrain, or *roll wave*, solutions of the inclined viscous shallow water equations of St. Venant, appearing in nondimensional Eulerian form as

$$\partial_t h + \partial_x(hu) = 0, \quad \partial_t(hu) + \partial_x\left(hu^2 + \frac{h^2}{2F^2}\right) = h - |u|u + \nu \partial_x(h \partial_x u), \quad (1.1)$$

where F is a Froude number, given by the ratio between (a chosen reference) speed of the fluid and speed of gravity waves, and $\nu = R_e^{-1}$, with R_e the Reynolds number of the fluid. System (1.1) describes the motion of a thin layer of fluid flowing down an inclined plane, with h denoting fluid height, u fluid velocity averaged with respect to height, x longitudinal distance along the plane, and t time. The terms h and $|u|u$ on the right-hand side of the second equation model, respectively, are gravitational force and turbulent friction along the bottom.¹

Roll waves are well-known hydrodynamic instabilities of (1.1), arising in the region $F > 2$ for which constant solutions, corresponding to parallel flow, are unstable. They appear in the modeling of such diverse phenomena as landslides, river and spillway flow, and the topography of sand dunes and sea beds; see Fig. 1a, b for physical examples of roll waves and Fig. 1c for a typical wavetrain solution of (1.1). As motivated by these applications, their stability properties have been studied formally, numerically, and experimentally in various physically interesting regimes; see, for example, Balmforth and Mandre (2004) for a useful survey of this literature. However, up until now, there has been no complete rigorous stability analysis of viscous St. Venant roll waves either at the linear (spectral) or nonlinear level.

Over the last several years, the authors, in various combinations, have developed a theoretical framework for the study of nonlinear stability of these and related peri-

¹ For simplicity, henceforth we restrict to cases where $u \geq 0$ and write the latter term simply as u^2 .



Fig. 1 Roll waves **a** on a spillway and **b** in the laboratory: pictures courtesy of Neil Balmforth, UBC. **c** Periodic profile of (1.1), $F = \sqrt{6}$, $\nu = 0.1$, $q = 1.5745$, $X = 17.15$. For better comparison to experiment, we extended the profile here as constant in transverse direction

odic waves. Specifically, for the model at hand, it was shown in [Johnson et al. \(2011\)](#) that, under standard *diffusive spectral stability assumptions* [conditions (D1)–(D3) in Sect. 1.1.1] together with a technical “slope condition” [(1.4) below] satisfied for “moderate” values $2 < F \lesssim 3.5$ of F and a genericity assumption [(H1) below] satisfied almost everywhere in parameter space,² *roll waves are nonlinearly stable in the sense that localized perturbations converge to localized spatial modulations of the background periodic wave*. More recently, the technical slope condition was removed ([Rodrigues and Zumbrun 2016](#)) as a necessary hypothesis, opening the possibility to consider nonlinear stability of waves for arbitrary Froude numbers F . See also [Barker et al. \(2012, 2013\)](#) for discussions in the related context of the Kuramoto–Sivashinsky equation ([Kuramoto 1984; Kuramoto and Tsuzuki 1975; Sivashinsky 1977, 1983](#)). Going further, for general (partially) parabolic systems, detailed nonlinear asymptotic behavior under localized and nonlocalized perturbations has been established in [Johnson et al. \(2014\)](#) in terms of certain formal modulation, or “Whitham,” equations.³

This reduces the study of stability and asymptotic behavior to verification of the spectral stability conditions (D1)–(D3), concerning Floquet spectrum of the associated eigenvalue ODE. However, it is in general a hard problem to verify such spectral assumptions analytically. Indeed, up to now, spectral stability has not been rigorously verified for *any* roll wave solution of the viscous St. Venant equations (1.1).

In some particular situations, for example, at the onset of hydrodynamical instability, analytical proof of spectral stability may be possible using perturbation techniques. However, most of the known examples concern reaction diffusion equations and related models like the Swift Hohenberg equations, Rayleigh Bénard convection or Taylor Couette flows that are all described, near the instability threshold of a background constant solution, by a Ginzburg–Landau equation derived as an amplitude equation ([Mielke 2002](#)). Associated with classical Hopf bifurcation, this normal form may be rigorously validated in terms of existence and stability by Lyapunov–Schmidt reduction about a limiting constant-coefficient operator ([Collet and Eckmann 1990; Mielke 1997a, b](#)).

By contrast, the corresponding model for onset of hydrodynamic (roll wave) instability in (1.1) is, at least formally, the *Korteweg-de Vries/Kuramoto–Sivashinsky equation* (KdV–KS)

$$\partial_S v + v \partial_Y v + \varepsilon \partial_Y^3 v + \delta (\partial_Y^2 v + \partial_Y^4 v) = 0, \quad \forall S > 0, \forall Y \in \mathbb{R}, \quad (1.2)$$

with $0 < \delta \ll 1$, $\varepsilon > 0$, a singular perturbation of the Korteweg-de Vries (KdV) equation.⁴ Equation (1.2) is derived as an amplitude equation for the shallow water system (1.1) near the critical value $F = 2$ above which steady constant-height flows are unstable, in the small-amplitude limit $h = \bar{h} + \delta^2 v$ and in the KdV time and space scaling $(Y, S) = (\delta(x - c_0 t), \delta^3 t)$ with $\delta = \sqrt{F - 2}$, where c_0 is an appropriate reference wave speed: see Sect. 2.1 below for details in the Lagrangian formulation. Alterna-

² Indeed, this appears numerically to be satisfied for all profiles.

³ See [Oh and Zumbrun \(2010\)](#) for the easier multidimensional case, in which behavior is asymptotically linear due to faster decay of the linearized propagator.

⁴ Without loss of generality, one can assume that $\varepsilon^2 + \delta^2 = 1$. See [Barker et al. \(2013\)](#).

tively, it may be derived from the full Navier–Stokes equations with free boundary from which (1.1) is derived in the shallow water limit, for Reynolds number R near the critical value R_c above which steady Nusselt flows are unstable; see Aung Win (1993), Jun and Yang (2003).

In this case, neither existence nor stability reduce to computations involving constant-coefficient operators; rather, the reference states are arbitrary amplitude periodic solutions of KdV, and the relevant operators (variable-coefficient) linearizations thereof. *This makes behavior considerably richer and both analysis and validation of the amplitude equations considerably more complicated than in the Ginzburg–Landau case mentioned above.* Likewise, onset occurs for (1.1) not through Hopf bifurcation from a single equilibrium, but through Bogdanov–Takens, or *saddle-node* bifurcation involving collision of two equilibria, as discussed, for example, in Hong Hwang and Chang (1987), Barker et al. (2011), with limiting period thus $+\infty$, consistent with the $1/\delta$ spatial scaling of the formal model. (The standard unfolding of a Bogdanov–Takens bifurcation as a perturbed Hamiltonian system is also consistent with KdV–KS; see Remark 2.1.)

Nevertheless, similarly as in previous works by Mielke (1997a, b) in the reaction diffusion setting, where the stability of periodic waves for the amplitude (Ginzburg–Landau) equation provides a stability result for periodic waves of the full system (Swift Hohenberg equation or Rayleigh Bénard convection), we may expect that stability for the amplitude equation, here the KdV–KS equation (1.2) will provide some information on the stability of periodic waves for the viscous St. Venant system (1.1), at least in the weakly unstable limit $F \rightarrow 2^+$. Our first main goal is to rigorously validate this conjecture, showing that stability of roll waves in the weakly unstable limit $F \rightarrow 2^+$ is determined by stability of corresponding solutions of (1.2) under the rescaling described above. Together with previous results (Bar and Nepomnyashchy 1995; Johnson et al. 2015; Barker 2014) on stability for (1.2), this gives the first complete nonlinear stability results for roll waves of (1.1): *More, it gives a complete classification of stability in the weakly unstable limit.*

This gives at the same time a rigorous justification in a particular instance of the much more generally applicable and better-studied (1.2) as a canonical model for weak hydrodynamic instability in inclined thin-film flow; see, for example, Bar and Nepomnyashchy (1995), Chang and Demekhin (2002), Chang et al. (1993), Pego et al. (2007). Looked at from this opposite point of view, (1.1) gives an interesting extension in a specific case of (1.2) into the large-amplitude, strongly unstable regime. Our second main goal is, by a combination of rigorous analysis and (nonrigorous but numerically well conditioned) numerical experiment, to continue our analysis into this large-amplitude regime, performing a systematic stability analysis for F on the entire range of existence $F > 2$ of periodic roll wave solutions of (1.1). Our main finding here is a remarkably simple power-law description of curves bounding the region of stability in parameter space from above and below, across which particular high-frequency and low-frequency stability transitions occur. These curves eventually meet, yielding instability for F sufficiently large. The large- F description is quite different from the small- F description of weakly unstable theory; indeed, there is a dramatic transition from small- to large- F behavior at $F \approx 2.3$, with behavior governed thereafter by the large- F version. This distinction appears important for

hydraulic engineering applications, where F is typically 2.5–6.0 and sometimes 10–20 or higher (Jeffreys 1925; Brock 1969, 1970; Abd-el Malek. 1991; Richard and Gavriluk 2012, 2013; Freeze et al. 2003).

1.1 Summary of Previous Work

We begin by recalling some known results that will be relied upon throughout our analysis. In particular, we begin by recalling how spectral stability (in a suitable diffusive sense) may provide a detailed nonlinear stability result, a fact that strongly underpins and motivates our spectral studies. We then recall the relevant numerical and analytical results for the amplitude Eq. (1.2), upon which our entire weakly unstable analysis for $0 < F - 2 \ll 1$ hinges.

1.1.1 Diffusive Spectral Stability Conditions

We first recall the standard diffusive spectral stability conditions as defined in various contexts in, for example, Schneider (1998, 1996), Johnson and Zumbrun (2011, 2010), Johnson et al. (2011), Barker et al. (2013), Johnson et al. (2014).

Given an appropriately smooth nonlinear map \mathcal{F} between Banach spaces⁵, let $u(x, t) = \bar{u}(x - ct)$ define a spatially periodic traveling wave solution of a general partial differential equation $\partial_t u = \mathcal{F}(u)$ with period (without loss of generality) one, or, equivalently, \bar{u} be a stationary solution of $\partial_t u = \mathcal{F} + c\partial_x u$ with period one. Let $L := (d\mathcal{F}/du)(\bar{u}) + c\partial_x$ denote the associated linearized operator about \bar{u} . As L is a linear differential operator with 1-periodic coefficients, standard results from Floquet theory dictate that nontrivial solutions of $Lv = \lambda v$ cannot be integrable on \mathbb{R} , more generally they cannot have finite norm in $L^p(\mathbb{R})$ for any $1 \leq p < \infty$. Indeed, it follows by standard arguments that the $L^2(\mathbb{R})$ -spectrum of L is purely continuous and that $\lambda \in \sigma_{L^2(\mathbb{R})}(L)$ if and only if the spectral problem $Lv = \lambda v$ has an $L^\infty(\mathbb{R})$ -eigenfunction of the form

$$v(x; \lambda, \xi) = e^{i\xi x} w(x; \lambda, \xi)$$

for some $\xi \in [\pi, \pi)$ and $w \in L^2_{\text{per}}([0, 1])$; see Gardner (1993), Kapitula and Promislow (2013, Chapter 3.3), Reed and Simon (1978, Chapter XIII.16), or Rodrigues (2013, pp. 30–31) for details. In particular, $\lambda \in \sigma_{L^2(\mathbb{R})}(L)$ if and only if there exists a $\xi \in [-\pi, \pi)$ such that there is a nontrivial 1-periodic solution of the equation

$$L_\xi w = \lambda w, \quad \text{where} \quad (L_\xi w)(x) := e^{-i\xi x} L \left[e^{i\xi \cdot} w(\cdot) \right] (x).$$

⁵ We are being intentionally vague for this general discussion, but interested readers may consult, for instance, Kapitula and Promislow (2013).

and

$$\sigma_{L^2(\mathbb{R})}(L) = \sigma_{L^\infty(\mathbb{R})}(L) = \bigcup_{\xi \in [-\pi, \pi]} \sigma_{L^2_{\text{per}}([0, 1])}(L_\xi).$$

The parameter ξ is referred to as the Bloch or Floquet frequency, and the operators L_ξ are the Bloch operators associated with L . Since the Bloch operators have compactly embedded domains in $L^2_{\text{per}}([0, 1])$, their spectrum consists entirely of discrete eigenvalues that depend continuously on the Bloch parameter ξ . Thus, the spectrum of L consists entirely of $L^\infty(\mathbb{R})$ -eigenvalues and may be decomposed into countably many curves $\lambda(\xi)$ such that $\lambda(\xi) \in \sigma_{L^2_{\text{per}}([0, 1])}(L_\xi)$ for $\xi \in [-\pi, \pi)$.

Suppose, further, that \bar{u} is a transversal⁶ orbit of the traveling wave ODE $\mathcal{F}(u) + c\partial_x u = 0$. Then, near \bar{u} , the implicit function theorem guarantees a smooth manifold of nearby 1-periodic traveling wave solutions of (possibly) different speeds, with some dimension $N \in \mathbb{N}$,⁷ not accounting for invariance under translations. Then, the *diffusive spectral stability conditions* are:

- (D1) $\sigma_{L^2(\mathbb{R})}(L) \subset \{\lambda \mid \Re\lambda < 0\} \cup \{0\}$.
- (D2) There exists a $\theta > 0$ such that for all $\xi \in [-\pi, \pi)$ we have $\sigma_{L^2_{\text{per}}([0, 1])}(L_\xi) \subset \{\lambda \mid \Re\lambda \leq -\theta|\xi|^2\}$.
- (D3) $\lambda = 0$ is an eigenvalue of L_0 with generalized eigenspace $\Sigma_0 \subset L^2_{\text{per}}([0, 1])$ of dimension N .

Under mild additional technical hypotheses to do with regularity of the coefficients of \mathcal{F} , hyperbolic–parabolic structure, etc., conditions (D1)–(D3) have been shown in all of the above-mentioned settings—in particular for periodic waves of either (1.1) or (1.2)—to imply *nonlinear modulation stability, at Gaussian rate*: More precisely, provided $\|(\tilde{u} - \bar{u})|_{t=0}\|_{L^1(\mathbb{R}) \cap H^s(\mathbb{R})}$ is sufficiently small for some s sufficiently large, there exists a function $\psi(x, t)$ with $\psi(x, 0) \equiv 0$ such that the solution satisfies

$$\|\tilde{u}(\cdot, t) - \bar{u}(\cdot - \psi(\cdot, t) - ct)\|_{L^p(\mathbb{R})} + \|\nabla_{x,t}\psi(\cdot, t)\|_{L^p(\mathbb{R})} \leq C(1+t)^{-\frac{1}{2}(1-1/p)},$$

$$2 \leq p \leq \infty, \tag{1.3}$$

valid for all $t > 0$; see Johnson and Zumbrun (2011, 2010), Johnson et al. (2011), Barker et al. (2013), Johnson et al. (2014), Rodrigues and Zumbrun (2016). In the case of (1.1), (1.2), for which coefficients depend analytically on the solution, essentially there suffices the single technical hypothesis:

(H1) The N zero eigenvalues of L_0 split linearly as ξ is varied with $|\xi|$ sufficiently small, in the sense that they may be expanded as $\lambda_j(\xi) = \alpha_j\xi + o(\xi)$ for some constants $\alpha_j \in \mathbb{C}$ distinct.

We note that, since the existence of the expansion $\lambda_j(\xi) = \alpha_j\xi + o(\xi)$ in (H1) may be proved independently, the hypothesis (H1) really concerns distinctness of the α_j ,

⁶ In a sense compatible with the algebraic structure of the system.

⁷ For both (1.1) and (1.2), an easy dimensional count gives $N = 2$ (Johnson et al. 2011; Barker et al. 2010) because of the presence of one local conservation law in the respective sets of equations.

which is equivalent to the condition that the characteristics of a (formally) related first-order Whitham modulation system be distinct, a condition that, in the case of analytic dependence of the underlying equations, as here, either holds generically with respect to nondegenerate parametrizations of the manifold of periodic traveling waves, or else uniformly fails. In the original nonlinear analysis (Johnson et al. 2011) of (1.1), there appeared an additional *slope condition*

$$h_x/h < (c\nu F)^{-2}, \quad (1.4)$$

used to obtain hyperbolic–parabolic damping and high-frequency resolvent estimates by Kawashima-type energy estimates, which in turn were necessary to obtain the desired nonlinear modulational stability result; see Johnson et al. (2011, Section 4.3). More recently, a subset of the authors has shown through a modified energy approach that these damping and resolvent estimates may be obtained provided the slope condition holds in the averaged sense $0 < (c\nu F)^{-1}$ and hence may be dropped from the nonlinear analysis: see Rodrigues and Zumbrun (2016).

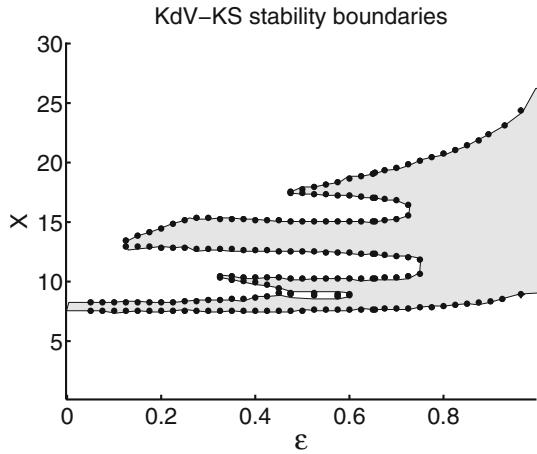
The above nonlinear stability results motivate a detailed analytical inspection of the conditions (D1)–(D3) and (H1), which is precisely the intent of the weakly nonlinear analysis presented in Sect. 2 below. We note that these conditions may be readily checked numerically, in a well-conditioned way, using either *Hill’s method* (Galerkin approximation), or *numerical Evans function analysis* (shooting/continuous orthogonalization); see Barker et al. (2012, 2013, 2010).

1.1.2 Numerical Evaluation for Viscous St. Venant and KdV–KS

The diffusive spectral stability conditions (D1)–(D3) have been studied numerically for the viscous St. Venant equations (1.1) in Barker et al. (2010) for certain “typical” waves and Froude numbers F , with results indicating existence of both stable and unstable waves: More precisely, the existence of a single “band” of stable waves as period is varied for fixed F . This echoes the much earlier numerical study of roll waves of the classical Kuramoto–Sivashinsky equation (KS) [$\varepsilon = 0$ for (1.2)] in Frisch et al. (1986) and elsewhere that obtained similar results.

Equations (1.2) have received substantially more attention, as canonical models for hydrodynamical instability in a variety of thin-film settings; as derived formally in Chang et al. (1993), see also Rodrigues (2013, p. 16, footnote 10), the model (1.2) with the addition of a further term $D(v_Y^2)_Y$, D constant, gives a general form for such instabilities in the weakly unstable regime. A systematic numerical study of this more general model was carried out in Chang et al. (1993), across all values of ε , δ , D , and the period X of the wave, and, by different methods in Barker et al. (2013), for the value $D = 0$ only; see Fig. 2, reprinted from Barker et al. (2013) (in close agreement also with the results of Chang et al. 1993). As noted in Chang et al. (1993), it may be observed from Fig. 2 that the small stable band for $\varepsilon/\delta \ll 1$ enlarges with addition of dispersion/decrease in δ , reaching its largest size at $\delta/\varepsilon = 0$ (corresponding to the singular KdV) limit. For intermediate ratios of δ/ε , behavior can be considerably more complicated, with bifurcation to multiple stable bands as this ratio is varied.

Fig. 2 Stability boundaries (in period X) versus parameter ε for the KdV–KS equation (1.2) with $\varepsilon^2 + \delta^2 = 1$. Here, the shaded regions correspond to spectrally stable periodic traveling waves of the KdV–KS equation. Note the KdV limit corresponds to $\varepsilon \rightarrow 1^-$



1.1.3 The KdV Limit $\delta \rightarrow 0^+$ for KdV–KS

Of special interest for us is the KdV limit $\delta \rightarrow 0^+$ for (1.2), treated with varying degrees of rigor in Ercolani et al. (1993), Bar and Nepomnyashchy (1995), Noble and Rodrigues (2013), Johnson et al. (2014), Barker (2014): a singularly perturbed Hamiltonian—indeed, *completely integrable*—system. We cite briefly the relevant results; for details, see Johnson et al. (2015), Barker (2014).

Proposition 1.1 (Existence Ercolani et al. 1993) *Given any positive integer $r \geq 1$, there exists $\delta_0 > 0$ such that there exist periodic traveling wave solutions $v_\delta(\theta)$, $\theta = Y - \sigma_\delta S$, of (1.2) (with $\epsilon = 1$) that are analytic functions of $\theta \in \mathbb{R}$ and C^r functions of $\delta \in [0, \delta_0)$. When $r \geq 3$, profiles v_δ expand as $\delta \rightarrow 0^+$ as a 2-parameter family*

$$\begin{cases} v_\delta(\theta; a_0, k) = T_0(\theta; a_0, k, \kappa) + \delta T_1(\theta) + \delta^2 T_2(\theta) + O(\delta^3), \\ \sigma_\delta = \sigma_0(a_0, k, \kappa) + \delta^2 \sigma_2 + O(\delta^3), \end{cases} \tag{1.5}$$

where

$$T_0(\theta; a_0, k, \kappa) = a_0 + 12k^2\kappa^2 \operatorname{cn}^2(\kappa\theta, k), \quad \sigma_0 = a_0 + 4\kappa^2(2k^2 - 1),$$

comprise the 3-parameter family (up to translation) of periodic KdV profiles and their speeds; $\operatorname{cn}(\cdot, k)$ is the Jacobi elliptic cosine function with elliptic modulus $k \in (0, 1)$; a_0 is a parameter related to Galilean invariance; and $\kappa = \mathcal{G}(k)$ is determined via the selection principle

$$\left(\frac{K(k)\mathcal{G}(k)}{\pi} \right)^2 = \frac{7}{20} \frac{2(k^4 - k^2 + 1)E(k) - (1 - k^2)(2 - k^2)K(k)}{(-2 + 3k^2 + 3k^4 - 2k^6)E(k) + (k^6 + k^4 - 4k^2 + 2)K(k)},$$

where $K(k)$ and $E(k)$ are the complete elliptic integrals of the first and second kind. The period $X(k) = 2K(k)/\mathcal{G}(k)$ is in one-to-one correspondence with k . More-

over, the functions $(T_i)_{i=1,2}$ are (respectively, odd and even) solutions of the linear equations

$$\mathcal{L}_0[T_0]T_1 = T_0'' + T_0'''' , \quad \mathcal{L}_0[T_0]T_2 = \left(\frac{T_1^2}{2} - \sigma_2 T_0 \right)' + T_1'' + T_1'''' , \quad (1.6)$$

on $(0, 2K(k)/\mathcal{G}(k))$ with periodic boundary conditions, where $\mathcal{L}_0[T_0] := -\partial_\theta^3 - \partial_\theta(T_0 - \sigma_0)$ denotes the linearized KdV operator about T_0 .

Throughout this manuscript, we let $v_\delta(\cdot; a_0, k)$ and $\sigma_\delta(a_0, k)$ denote the periodic traveling wave profiles and wave speeds, respectively, as described in Proposition 1.5.

Remark 1.2 The additional parameter κ for periodic KdV waves as compared to KdV–KS waves reflects the existence of the additional conserved quantity of the Hamiltonian at $\delta = 0$. The selection principle $\kappa = \mathcal{G}(k)$ is precisely the condition that the periodic Hamiltonian orbits at $\delta = 0$ persist, to first order, for $0 < \delta \ll 1$. Alternatively, this condition can be written explicitly as $\int_0^{2K(k)/\kappa} T_0 (T_0'' + T_0''') dx = 0$.

By Galilean invariance of the underling Eq. (1.2), the stability properties of the above-described $X = X(k)$ -periodic solutions are independent of the parameter a_0 . Hence, for stability purposes one may identify waves with a common period, fixing a_0 and studying stability of a one-parameter family in k . It is known (Kuznetsov et al. 1984; Spektor 1988; Bottman and Deconinck 2009) that the spectra of the linearized operator $\mathcal{L}[T_0]$, considered on $L^2(\mathbb{R})$, about a periodic KdV wave T_0 is spectrally stable in the neutral, Hamiltonian, sense, i.e., all eigenvalues of the Bloch operators

$$\mathcal{L}_\xi[T_0] := (\partial_Y + i\xi) \left(-(\partial_Y + i\xi)^2 - T_0 + \sigma_0 \right) : L^2_{\text{per}}(0, X) \rightarrow L^2_{\text{per}}(0, X),$$

considered with compactly embedded domain $H^3_{\text{per}}(0, X)$, are purely imaginary for each $\xi \in [-\pi/X, \pi/X)$. Moreover, the explicit description of the spectrum obtained in Bottman and Deconinck (2009) also yields⁸ that $\lambda = 0$ is an eigenvalue of $\mathcal{L}_0[T_0]$ of algebraic multiplicity three, that $\lambda = 0$ is an eigenvalue of $\mathcal{L}_\xi[T_0]$ only if $\xi = 0$, and that the three zero eigenvalues of $\mathcal{L}_0[T_0(\cdot; a_0, k, \mathcal{G}(k))]$ expand about for $|\xi| \ll 1$ as

$$\lambda_j(\xi) = i\alpha_j(\xi)\xi = i\xi\alpha_j + O(\xi^2), \quad j = 1, 2, 3 \quad \text{with } \alpha_j \in \mathbb{R} \text{ distinct.} \quad (1.7)$$

We introduce one final technical condition, first observed then proved numerically to hold, at least for KdV waves that are limits as $\delta \rightarrow 0$ of stable waves of (1.2) (Bottman and Deconinck 2009; Johnson et al. 2015; Barker 2014):⁹

⁸ In Johnson et al. (2015), Barker (2014), some of these facts remained unnoticed to the authors. In particular, in Johnson et al. (2015), the condition that only $\xi = 0$ yields $\lambda = 0$ was gathered to condition (A) below to form condition (A1) and distinctness of the α_j was identified as condition (A2).

⁹ In fact (A) has been verified (see Proposition 1.4 below) on essentially the entire range $k \in (0, 1)$; we know of no instance where it fails.

(A) A given parameter $k \in (0, 1)$ is said to satisfy condition (A) if the nonzero eigenvalues of the linearized (Bloch) KdV operator $\mathcal{L}_\xi[T_0]$ about $T_0(\cdot; a_0, k, \mathcal{G}(k))$ are simple for each $\xi \in [-\pi/X, \pi/X)$.

Note that the set of $k \in (0, 1)$ for which property (A) holds is open.

Given a periodic traveling wave solution $T_0(\cdot; a_0, k, \mathcal{G}(k))$ of the KdV equation with elliptic modulus $k \in (0, 1)$ satisfying condition (A) above, we now consider the spectral stability of the associated family of periodic traveling wave solutions $v_\delta(\cdot; a_0, k)$, defined for $\delta \in [0, \delta_0)$, with δ_0 as in Proposition 1.5, as solutions of the KdV–KS equation (1.2). To this end, notice that, assuming $k \in (0, 1)$ satisfies condition (A), the nonzero Bloch eigenvalues $\lambda(\xi)$ of the linearized KdV–KS operator

$$L_\xi[v_\delta] = e^{-i\xi \cdot} \left[-\delta \left(\partial_Y^4 + \partial_Y^2 \right) - \partial_Y^3 - \partial_Y (v_\delta - \sigma_\delta) \right] e^{i\xi \cdot} : L^2_{\text{per}}(0, X) \rightarrow L^2_{\text{per}}(0, X)$$

admit a smooth¹⁰ expansion in δ for $0 < \delta \ll 1$. In particular, for each pair (ξ, λ_0) with $\lambda_0 \in \sigma(\mathcal{L}_\xi[T_0]) \setminus \{0\}$ and $\xi \in [-\pi/X, \pi/X)$, there is a unique spectral curve $\lambda(\xi, \lambda_0, \delta)$ bifurcating from λ_0 smoothly in δ , and it takes the form

$$\lambda(\delta; \xi, \lambda_0) = \lambda_0 + \delta \lambda_1(\xi, \lambda_0) + O(\delta^2) \tag{1.8}$$

for some $\lambda_1(\xi, \lambda_0)$. It is then natural to expect that the signs of the real parts of the first-order correctors $\lambda_1(\xi, \lambda_0)$ in the above expansion be indicative of stability or instability of the near-KdV profiles u_δ for $0 < \delta \ll 1$. With this motivation in mind, for any $k \in (0, 1)$ that satisfies condition (A) above,¹¹ we define the index

$$\text{Ind}(k) := \sup_{\substack{\lambda_0 \in \sigma(\mathcal{L}_\xi[T_0(\cdot; a_0, k, \mathcal{G}(k))]) \setminus \{0\} \\ \xi \in [-\pi/X(k), \pi/X(k))}} \Re(\lambda_1(\xi, \lambda_0)). \tag{1.9}$$

Evidently, $\text{Ind}(k) > 0$ is a sufficient condition for the spectral instability for $0 < \delta \ll 1$ of the near-KdV waves v_δ bifurcating from T_0 . The next proposition states that the condition $\text{Ind}(k) < 0$ is also sufficient for the diffusive spectral stability of the v_δ , for $0 < \delta \ll 1$. Define the open set

$$\mathcal{P} := \{ k \in (0, 1) \mid \text{condition (A) holds for } k \text{ and } \text{Ind}(k) < 0 \}. \tag{1.10}$$

Proposition 1.3 [Limiting stability conditions (Johnson et al. 2015)] *For each $k \in \mathcal{P}$ there exists a neighborhood $\Omega_k \subset (0, 1)$ of k and $\delta_0(k) > 0$ such that $\Omega_k \subset \mathcal{P}$ and for any $(a_0, \tilde{k}, \delta) \in \mathbb{R} \times \Omega_k \times (0, \delta_0(k))$ the nondegeneracy and spectral stability conditions (H1) and (D1)–(D3) hold for the solutions $v_\delta(\cdot; \tilde{a}_0, \tilde{k})$ of (1.2) discussed above. In particular, \mathcal{P} is open and $\delta_0(\cdot)$ can be chosen uniformly on compact subsets of \mathcal{P} .*

¹⁰ In the sense of Proposition 1.1 that one can reach arbitrary prescribed regularity.

¹¹ Condition (A) is independent of a_0 , holding for every a_0 or for none. Likewise, $\text{Ind}(k)$ is independent of a_0 .

Proposition 1.3 reduces the question of diffusive spectral stability and nonlinear stability—in the sense defined in Sect. 1.1.1—of the near-KdV profiles constructed in Proposition 1.5 to the verification of the structural condition (A) and the evaluation of the function $\text{Ind}(k)$. Note condition (A) is concerned only with the spectrum of the linearized KdV operator about the limiting KdV profile v_0 ; its validity is discussed in detail in Johnson et al. (2015, Section 1). Further, note that due to the triple eigenvalue of the KdV linearized operator at the origin, the fact that $\text{Ind}(k) < 0$ is sufficient for stability is far from a foregone conclusion, and this represents the main contribution of Johnson et al. (2015).

To evaluate $\text{Ind}(k)$, using the complete integrability of the KdV equation to find an explicit parametrization of the KdV spectrum and eigenfunctions about v_0 (Bottman and Deconinck 2009; Deconinck and Kapitula 2010), one can construct a continuous multi-valued mapping¹²

$$[-\pi/X, \pi/X] \times \mathbb{R}i \ni (\xi, \lambda_0) \mapsto \Re(\lambda_1(\xi, \lambda_0)) \in \mathbb{R}$$

that is explicitly computable in terms of Jacobi elliptic functions; see Bar and Nepomnyashchy (1995) or Barker et al. (2013, Appendix A.1). This mapping may then be analyzed numerically. Numerical investigations of Bar and Nepomnyashchy (1995), Barker et al. (2013) suggest stability for limiting periods $X = X(k)$ in an open interval (X_m, X_M) and instability for X outside $[X_m, X_M]$, with $X_m \approx 8.45$ and $X_M \approx 26.1$, thus completely classifying stability for $0 < \delta \ll 1$. The following result of Barker (2014), established by numerical proof using interval arithmetic, gives rigorous validation of these observations for all limiting periods $X(k)$ except for a set near the boundaries of the domain of existence $X(k) \in (2\pi, +\infty) \approx (6.2832, +\infty)$ corresponding to the limits $k \rightarrow 0, 1$.

Proposition 1.4 (Numerical proof Barker 2014) *With $k_{\min} = 0.199910210210210$ and $k_{\max} = 0.999999999997$, corresponding to $X_{\min} \approx 6.284$ and $X_{\max} \approx 48.3$, condition (A) holds on $[k_{\min}, k_{\max}]$. Moreover, there are $k_l \in [0.9421, 0.9426]$ and $k_r \in [0.99999838520, 0.99999838527]$, corresponding to $X_l \in [8.43, 8.45]$ and $X_r \in [26.0573, 26.0575]$, such that $\mathcal{P} \cap [k_{\min}, k_{\max}] = (k_l, k_r)$ and Ind takes positive values on $[k_{\min}, k_{\max}] \setminus [k_l, k_r]$.*

As noted in Barker (2014), the limits $k \rightarrow 0$ and $k \rightarrow 1$ not treated in Proposition 1.4, corresponding to Hopf and homoclinic limits, though inaccessible by the numerical methods of Barker (2014), should be treatable by asymptotics relating spectra to those of (unstable Barker et al. 2011, 2010) limiting constant and homoclinic profiles; see the related analyses (Hărăguș and Kapitula 2008; Mikyoung Hur and Johnson 2015; Yang and Zumbrun 2016).

¹² While $\lambda_1(\xi, \lambda_0)$ is defined above only when λ_0 is a simple eigenvalue of the limiting linearized KdV operator $\mathcal{L}_\xi[v_0]$, it possesses an explicit expression in terms of k and an auxiliary Lax spectral parameter that extend this function to points where simplicity fails. Note in particular that this extension is triple-valued at $(0, 0)$.

1.2 Description of Main Results

As mentioned previously, the fact that the KdV–KS equation (1.2) serves as an amplitude equation for the shallow water system (1.1) in the weakly nonlinear regime $0 < \delta = \sqrt{F - 2} \ll 1$ suggests that Propositions 1.3 and 1.4 should have natural counterparts for the stability of roll waves in (1.1). To explore this connection, following (Johnson et al. 2011, 2014; Barker et al. 2011), we find it convenient to rewrite the viscous St. Venant equations (1.1) in their equivalent Lagrangian form:

$$\partial_t \tau - \partial_x u = 0, \quad \partial_t u + \partial_x \left(\frac{\tau^{-2}}{2F^2} \right) = 1 - \tau u^2 + \nu \partial_x (\tau^{-2} \partial_x u), \tag{1.11}$$

where $\tau := 1/h$ and x denotes now a Lagrangian marker rather than a physical location \tilde{x} , satisfying the relations $dt/d\tilde{x} = u(\tilde{x}, t)$ and $dx/d\tilde{x} = \tau(\tilde{x}, t)$. In these coordinates, observe that the (now unnecessary Rodrigues and Zumbrun 2016) slope condition (1.4) takes the form

$$2\nu u_x < F^{-2}. \tag{1.12}$$

Hereafter, we will work exclusively with the formulation (1.11).

Remark 1.5 Though nontrivial, the one-to-one correspondence between periodic waves of the Eulerian and Lagrangian forms is a well-known fact. A fact that seems to have remained unnoticed until very recently is that this correspondence extends to the spectral level even in its Floquet-by-Floquet description. In particular, without loss of generality one may safely study spectral stability in either formulation. See, for instance, Benzoni-Gavage et al. (2014) for an explicit description of the former correspondence and [BGMR] for the spectral connection, both in the closely related context of the Euler–Korteweg system.

1.2.1 The Weakly Unstable Limit $F \rightarrow 2^+$

Our first three results, and the main analytical results of this paper, comprise a rigorous validation of KdV–KS as a description of roll wave behavior in the weakly unstable limit $F \rightarrow 2^+$. Let (τ_0, u_0) , $u_0 = \tau_0^{-1/2}$, be a constant solution of (1.11), and $c_0 := \tau_0^{-3/2}/2$. Setting $\delta = \sqrt{F - 2}$, we introduce the rescaled dependent and independent variables

$$\tilde{\tau} = 3\delta^{-2} \left(\frac{\tau}{\tau_0} - 1 \right), \quad \tilde{u} = 6\delta^{-2} \left(\frac{u}{u_0} - 1 \right), \quad Y = \frac{\tau_0^{5/4} \delta (x - c_0 t)}{\nu^{1/2}}, \quad S := \frac{\delta^3 t}{4\tau_0^{1/4} \nu^{1/2}}. \tag{1.13}$$

Our first result concerns existence of small-amplitude periodic traveling wave solutions in the limit $\delta \rightarrow 0^+$. Seeking traveling wave solutions $(\tilde{\tau}, \tilde{u})(Y - \tilde{c}S)$, in Sect. 2.1 below we will show that, up to a further near-identity change in the dependent variable

$\tilde{\tau}$, the rescaled $\tilde{\tau}(\cdot)$ solves the profile equation for the KdV–KS equation (1.2), forced by higher-order terms in δ : see (2.4)–(2.6) for details. Together with an appropriate perturbation argument, this leads to the following existence result.

Theorem 1.6 (Existence) *There exists $\delta_0 > 0$ such that there exist periodic traveling wave solutions of (1.11), in the rescaled coordinates (1.13) $(\tilde{\tau}, \tilde{u})_\delta(\theta)$, $\theta = Y - \tilde{c}_\delta(a_0, k)S$, that are analytic functions of $\theta \in \mathbb{R}$, $(a_0, k) \in \mathbb{R} \times (0, 1)$ and $\delta \in [0, \delta_0)$ and that, in the limit $\delta \rightarrow 0^+$, expand as a 2-parameter family*

$$\begin{cases} \tilde{\tau}_\delta(\theta; a_0, k) = -v_{\tilde{\delta}}(\theta; a_0, k) + O(\delta^2), \\ \tilde{u}_\delta(\theta; a_0, k) = -\tilde{\tau}_\delta(\theta; a_0, k) + \frac{\delta^2}{2}(\tilde{q}(a_0, k) - 3\tau_0^{-1}\tilde{c}_\delta(a_0, k)\tilde{\tau}_\delta(\theta; a_0, k)), \\ \tilde{c}_\delta(a_0, k) = \sigma_{\tilde{\delta}}(a_0, k) + O(\delta^2), \end{cases} \tag{1.14}$$

where $\tilde{\delta} = \delta/(2\tau_0^{1/4}v^{1/2})$, $v_\delta(\theta; a_0, k)$ and $\sigma_\delta(a_0, k)$ are the small- δ traveling wave profiles and speeds of KdV–KS described in (1.5) and

$$\begin{aligned} \tilde{q}(a_0, k) &= 24k^2(1 - k^2)(\mathcal{G}(k))^4 - a_0\left(\frac{1}{2}a_0 + 4(\mathcal{G}(k))^2(2k^2 - 1)\right) \\ &\equiv v_0^2/2 - \sigma_0v_0 + v_0'' \end{aligned}$$

is a constant of integration in the limiting KdV traveling wave ODE (see (2.7)).

For brevity, throughout the paper we shall often leave implicit the dependence on (a_0, k) or a_0 .

Remark 1.7 As we will see in the analysis below, the weakly unstable limit for the St. Venant equations (1.11) is a regular perturbation of KdV, rather than a singular perturbation as in the KdV–KS case, a fact reflected in the stronger regularity conclusions of Theorem 1.6 as compared to Proposition 1.1.

Our next result concerns the spectral stability of the small-amplitude periodic traveling wave solutions constructed in Theorem 1.6 when subject to arbitrary small localized (i.e., integrable) perturbations on the line.

Theorem 1.8 (Limiting stability conditions) *For each $k \in \mathcal{P}$, \mathcal{P} as in (1.10), there exists a neighborhood $\Omega_k \subset (0, 1)$ of k and $\delta_0(k) > 0$ such that for any $(a_0, \tilde{k}, \delta) \in \mathbb{R} \times \Omega_k \times (0, \delta_0(k))$, the nondegeneracy and spectral stability conditions (H1) and (D1)–(D3) hold for $(\tau, u)_\delta(\cdot; a_0, \tilde{k})$. In particular, $\delta_0(\cdot)$ can be chosen uniformly on compact subsets of \mathcal{P} . Conversely for each $k \in (0, 1)$ such that condition (A) holds but $\text{Ind}(k) > 0$ (where Ind is defined as in (1.9)), there exists a neighborhood $\Omega_k \subset (0, 1)$ of k and $\delta_0(k) > 0$ such that if $(a_0, \tilde{k}, \delta) \in \mathbb{R} \times \Omega_k \times (0, \delta_0(k))$ then $(\tau, u)_\delta(\cdot; a_0, \tilde{k})$ is spectrally unstable.*

From Theorem 1.6, it follows in particular that our roll waves have asymptotic period $\sim \delta^{-1}$ and amplitude $\sim \delta^2$ in the weakly unstable limit $F \rightarrow 2^+$; that is, this is a long-wave, small-amplitude limit.¹³ In Theorems 1.6 and 1.8, rescaling period and

¹³ Observe that, in this limit, $u_x \sim \delta^3$ so that the slope condition (1.12) is automatically satisfied for $\delta \ll 1$. Recall, however, this condition is no longer required for the nonlinear analysis thanks to Rodrigues and Zumbrun (2016).

amplitude to order one, we find that in this regime, *existence and stability* are indeed well described by KdV–KS \rightarrow KdV: to zeroth order by KdV, and to first correction by KdV–KS.

Combining Theorem 1.8 with Proposition 1.4, and untangling coordinate changes, we obtain the following *essentially complete description of stability of viscous St. Venant roll waves in the limit $F \rightarrow 2^+$* .

Corollary 1.9 (Limiting stability region) *For $\delta = \sqrt{F - 2}$ sufficiently small, uniformly for δX on compact sets, periodic traveling waves of (1.11) are stable for (Lagrangian) periods $X \in \frac{v^{1/2}}{\tau_0^{5/4}\delta}(X_l, X_r)$ and unstable for $X \in \frac{v^{1/2}}{\tau_0^{5/4}\delta}[X_{\min}, X_l)$ and $X \in \frac{v^{1/2}}{\tau_0^{5/4}\delta}(X_r, X_{\max}]$ where $X_{\min}, X_l, X_r, X_{\max}$ are as in Proposition 1.4, in particular, $X_{\min} \approx 6.284, X_l \approx 8.44, X_r \approx 26.1,$ and $X_{\max} \approx 48.3$.*

1.2.2 Large Froude Number Limit $F \rightarrow +\infty$

We complement the above weakly nonlinear analysis by continuing into the large-amplitude regime, beginning with a study of the distinguished large Froude number limit $F \rightarrow +\infty$. The description of this limit requires a choice of scaling in the parameters indexing the family of waves. To this end, we first emphasize that a suitable parametrization, available for the full range of Froude numbers, is given by (q, X) , where $q := -c\bar{\tau} - \bar{u}$ is a constant of integration in the associated traveling wave ODE, corresponding to *total outflow*, and X is the *period*. As discussed in Sect. 3.1 below, the associated two-parameter family of possible scalings may be reduced by the requirements that (i) the limiting system be nontrivial and (ii) the limit be a regular perturbation, to a one-parameter family indexed by $\alpha \geq -2$, given explicitly via

$$\tau = aF^\alpha, \quad u = bF^{-\alpha/2}, \quad c = c_0F^{-1-3\alpha/2}, \quad X = X_0F^{-1/2-5\alpha/4}, \quad q = q_0F^{-\alpha/2}, \tag{1.15}$$

where $a, b : \mathbb{R} \rightarrow \mathbb{R}$ and c_0, X_0, q_0 are real constants. Note, from the relation $X = 1/k$ between period and wave number¹⁴ k , that we have also $k = k_0F^{1/2+5\alpha/4}$.

Under this rescaling, moving to the co-moving frame $(x, t) \mapsto (k(x - ct), t)$, we find that X -periodic traveling wave solutions of (1.11) correspond to X_0 -periodic solutions of the *rescaled profile equation*

$$a'' = (-a^2/c_0k_0^2v) \times (k_0a'F^{-3/2-3\alpha/4}(c_0^2 - 1/a^3) - 1 + a(q_0 - c_0F^{-1}a)^2 - 2c_0k_0^2v(a')^2/a^3), \tag{1.16}$$

where b is recovered from a via the identity $b = -q_0 - c_0F^{-1}a$; see Sect. 3.1 below for details. Noting that the behavior of $F^{-3/2-3\alpha/4}$ as $F \rightarrow \infty$ depends on whether

¹⁴ Note that throughout our paper we use notation k for two distinct quantities, wavenumber as here (in study away from $F \approx 2$) and modulus of ellipticity (in study of $F \rightarrow 2^+$) as described in the previous section.

$\alpha = -2$ or $\alpha > -2$, one finds two different limiting profile equations in the limit $F \rightarrow \infty$: a (disguised¹⁵) Hamiltonian equation supporting a selection principle, when $\alpha > -2$, and a non-Hamiltonian equation in the boundary case $\alpha = -2$; see Sect. 3.1 below. Further, by elementary phase plane analysis when $\alpha > -2$ or direct numerical investigation when $\alpha = -2$, periodic solutions of the limiting profile equations are seen to exist as 2-parameter families parametrized by the period X_0 and the discharge rage q_0 . Noting that, by design, the rescaled profile Eq. (1.16) is a *regular perturbation* of the appropriate limiting profile equation for all $\alpha \geq -2$, we readily obtain the following asymptotic description

Theorem 1.10 *For sufficiently large F , generically, X_0 -periodic profiles of (1.16), obtained under the scaling (1.15), emerge for each $\alpha \geq -2$ from X_0 -periodic solutions of the appropriate limiting profile equation obtained by taking $F \rightarrow \infty$ in (1.16) and, when $\alpha > -2$, satisfying a suitable selection principle.*

Next, we study the spectral stability of a pair of fixed periodic profiles (\bar{a}, \bar{b}) constructed above. One may readily check that, under the further rescaling $Fb = \check{b}$ and $F^{1/2+\alpha/4}\lambda = \Lambda$, the linearized spectral problems around such a periodic profile (\bar{a}, \bar{b}) is given by

$$\begin{aligned} \Lambda a - c_0 k_0 a' - k_0 \check{b}' &= 0 \\ F^{-3/2-3\alpha/4} \left(\Lambda \check{b} - c_0 k_0 \check{b}' - k_0 (a/\bar{a}^3)' \right) \\ &= -2F^{-1} \bar{a} \bar{b} \check{b} - \bar{b}^2 a + \nu k_0^2 (\check{b}' \bar{a}^2 + 2c_0 \bar{a}' a / \bar{a}^3)', \end{aligned} \quad (1.17)$$

where (a, b) denotes the perturbation of the underlying state (\bar{a}, \bar{b}) . The limiting spectral problems obtained by taking $F \rightarrow \infty$ again depend on whether $\alpha = -2$ or $\alpha > -2$. In particular, we note the spectral problem is Hamiltonian and hence possesses a natural fourfold symmetry about the real and imaginary axes, when $\alpha > -2$; see 3.1 below for details. Since (1.17) is, again by design, a *regular perturbation* of the appropriate limiting spectral problems for all $\alpha \geq -2$, we obtain by standard perturbation methods (e.g., the spectral/Evans function convergence results of Plaza and Zumbrun 2004) the following sufficient *instability condition*.

Corollary 1.11 *For all $\alpha \geq -2$, under the rescaling (1.15), the profiles of (1.16) converging as $F \rightarrow \infty$ to solutions of the appropriate limiting profile equation, as described in Theorem 1.10 are spectrally unstable if the appropriate limiting spectral problem about the limiting profiles admit $L^2(\mathbb{R})$ -spectrum in Λ with positive real part.*

As clearly discussed in Sect. 3.1.2, for $\alpha > -2$ the limiting profile equation, associated selection principle, and limiting spectral problem are *independent* of the value of α : see (3.11) and (3.14) and surrounding discussion. Thus, the above instability criterion for $F \rightarrow +\infty$ can be determined by the study of just two model equations: one for $\alpha = -2$ and one for any other fixed $\alpha > -2$. Both regimes include particularly physically interesting choices since $\alpha = 0$ corresponds to holding the outflow q constant as $F \rightarrow \infty$, while $\alpha = -2$ corresponds to holding the Eulerian period $\Xi(X_0)$

¹⁵ Indeed, the profile equation in this case is Hamiltonian in the unknown $h = \frac{1}{a}$.

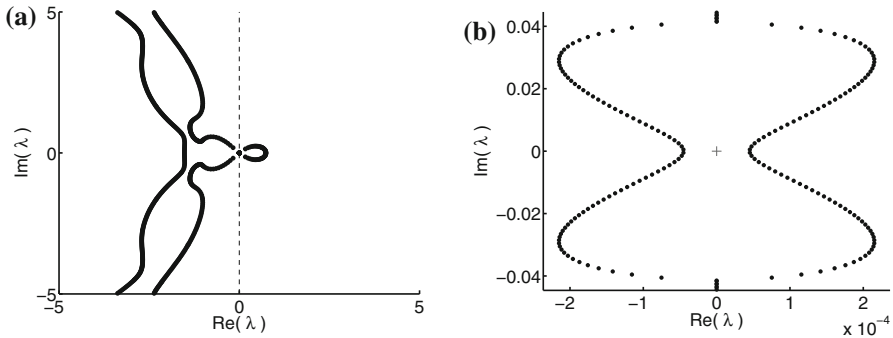


Fig. 3 In **a**, **b**, we plot a numerical sampling of the (unstable) spectrum corresponding to the $F \rightarrow \infty$ limiting spectral problems for the cases $\alpha = -2$ and $\alpha > -2$, respectively, for a representative periodic stationary solution of the appropriate limiting profile equation

constant as $F \rightarrow \infty$.¹⁶ In Sect. 3.2, we investigate numerically the stability of the limiting spectral problems in both the cases $\alpha = -2$ and $\alpha = 0$. This numerical study indicates that, in both these cases, all periodic solutions of the appropriate limiting profile equations are *spectrally unstable* and hence, by Corollary 1.11, that spectrally stable periodic traveling wave solutions of the viscous St. Venant system (1.11) do not exist for sufficiently large Froude numbers; see Figs. 3 and 6.

Numerical Observation 1 *For both $\alpha > -2$ and $\alpha = -2$, the limiting eigenvalue equations have strictly unstable spectra; hence, converging profiles are spectrally unstable for F sufficiently large.*

1.2.3 Intermediate F

We complete our stability investigation in Sect. 3.3 by carrying out a numerical study for F bounded away from the distinguished values 2 and $+\infty$ of the $L^2(\mathbb{R})$ -spectrum of the linearized operator obtained from linearizing (1.11) about a given periodic traveling wave solution. For F relatively small ($2 < F \leq 4$), we find, unsurprisingly, a smooth continuation of the picture for $F \rightarrow 2^+$, featuring a single band of stable periods between two concave upward curves; see Fig. 4c. However, continuing into the large-but-not-infinite regime ($2.5 \leq F \leq 100$), we find considerable additional structure beyond that described in Numerical Observation 1.

Namely, for $\alpha \in [-2, 0]$ we see that the stability region is enclosed in a lens-shaped region between two smooth concave upward curves corresponding to the lower stability boundary and an upper high-frequency instability boundary, pinching off at a special value $F_*(\alpha)$ after which, consistent with Numerical Observation 1, stable roll waves no longer exist; see Fig. 4a for the case $\alpha = -2$. Examining these curves further for different values of α , we find that they obey a remarkably simple power-law

¹⁶ Here, the Eulerian scaling relation $\Xi = \Xi_0 F^{-\frac{1}{2} - \frac{\alpha}{4}}$ follows by $\Xi = \int_0^X \bar{\tau}(x) dx$, (1.15), and convergence of the profile a .

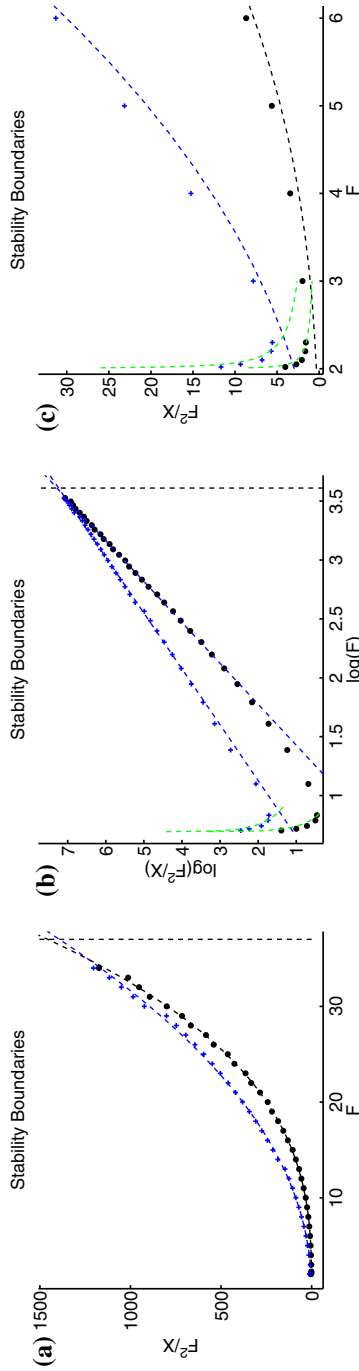


Fig. 4 Lower and upper stability boundaries for $\alpha = -2$, $\nu = 0.1$, and, motivated by (1.15), scaling $q = 0.4F^{-2}$. Solid dots show numerically observed boundaries. Pale dashes indicate approximating curves given by **a** (upper) $F^2/X = e^{0.087 F^{2.88}}$ and (lower) $F^2/X = e^{-2.97 F^{2.83}}$, **b** (upper) $\log(F^2/X) = 2.88 \log(F) + 0.087$ and (lower) $\log(F^2/X) = 2.83 \log(F) - 2.97$. Pale dotted curves (Green in color plates) indicate theoretical boundaries as $F \rightarrow 2^+$. c Small- to large- F transition

description in terms of F , q , α , and X ; see Fig. 4b for an example log–log plot in the case $\alpha = -2$. The general description of this power-law behavior is provided by the following.

Numerical Observation 2 *Both lower and upper stability boundaries appear for $F \gg 1$ to be governed by universal power laws $c_1 \log F + c_2 \log q + c_3 \log X + c_4 \log v = d$, independent of parameters $-2 \leq \alpha \leq 0$, $v > 0$, where for the lower boundary, $c_1 = 0.69$, $c_2 = -3.5$, $c_3 = 1$, $c_4 = 0.18$, and $d = -0.11$, and for the upper boundary, $c_1 = 0.79$, $c_2 = -1.7$, $c_3 = 1$, $c_4 = 0.76$, and $d = 2.2$: see Fig. 7. Values $\alpha > 0$ were not computed.*

Together with the small- F description of Theorem 1.8, these observations give an *essentially complete description* of stability of periodic roll wave solutions of the St. Venant equations (1.1), for $-2 \leq \alpha \leq 0$.

1.3 Discussion and Open Problems

There have been a number of numerical and analytical studies of viscous roll waves in certain small-amplitude limits, in particular for the KdV–KS equations governing formally the weakly unstable limit $F \rightarrow 2^+$ (Frisch et al. 1986; Chang and Demekhin 2002; Chang et al. 1993; Bar and Nepomnyashchy 1995; Ercolani et al. 1993; Pego et al. 2007; Barker et al. 2013; Johnson et al. 2015; Barker 2014). However, to our knowledge, the present study represents the first systematic investigation of the stability of *arbitrary amplitude* roll wave solutions of the viscous St. Venant equations for inclined thin-film flow.

Our main mathematical contribution is the rigorous validation of the formal KdV–KS \rightarrow KdV limit as a description of behavior in the small Froude number/weakly unstable limit $F \rightarrow 2^+$. This, together with the works (Ercolani et al. 1993; Bar and Nepomnyashchy 1995; Johnson et al. 2015; Barker 2014) on KdV–KS \rightarrow KdV, gives a complete classification of existence and stability of viscous St. Venant roll waves in the weakly unstable regime. We note again that KS–KdV \rightarrow KdV is a canonical weakly unstable limit for the type of long-wave instabilities arising in thin-film flow, in the same way that the (real and complex) Ginzburg–Landau equations are canonical models for finite-wavelength “Turing-type” instabilities. However, its analysis, based on singular perturbations of periodic KdV solutions, is essentially different from that of the finite-wavelength case based on regular perturbation of constant solutions (Mielke 1997a, b; Schneider 1996).

From a practical point of view, the main point is perhaps the numerically obtained description of behavior in the passage from small-amplitude to large-amplitude behavior. In particular, the universal scaling law of Numerical Observation 2 gives an unexpected global, simple-to-apply description of stability that seems potentially of use in biological and engineering applications, for which the St. Venant equations appear to be the preferred ones in current use. (Compare with the very complicated behavior in Fig. 2 as δ is varied away from the small- δ limit.) This adds new insight beyond the qualitative picture afforded by the canonical KdV–KS \rightarrow KdV limit. In particular, our numerical results indicate a sharp transition at $F \approx 2.3$ from the

quantitative predictions of the small-amplitude theory to the quite different large- F prediction of Numerical Observation 2. As hydraulic engineering applications typically involve values $2.5 \leq F \leq 20$ (Jeffreys 1925; Brock 1969, 1970; Abd-el Malek. 1991; Richard and Gavriluk 2012, 2013; Freeze et al. 2003), this distinction appears physically quite relevant.

A very interesting open problem, both from the mathematical and engineering point of view, is to rigorously verify this numerically observed rule of thumb. As noted above (see Fig. 4), the upper and lower stability boundaries described in Numerical Observation 2 obey different scalings from those prescribed in (1.15), as $F \rightarrow \infty$, with period growing faster than $X \sim F^{-1/2-5\alpha/4}$ by a factor $F^{1/2-c_1+\alpha(c_2/2+5/4)}$ that is $\gg 1$ for $\alpha \leq \alpha_* \approx 1.54$: in particular, for the two main physical values of interest $\alpha = -2$ and $\alpha = 0$, corresponding to constant (Eulerian) period and constant inflow, respectively. Indeed, given the large values of F to which the stability region extends, this may be deduced by Numerical Observation 1, which implies that all such waves of period $O(F^{-1/2-5\alpha/4})$ are necessarily unstable for $F \gg 1$.

An important consequence is that, rescaling viscosity ν so that the resulting period $X\nu$ after standard invariant scaling remains constant, we find that $\nu \rightarrow 0$. Hence, the limiting behavior of stable waves is described by the joint *inviscid, large Froude number limit* $\nu \rightarrow 0$, $F \rightarrow +\infty$. Figure 5, depicting periodic profiles at the upper and lower stability boundaries for values $F = 5, 10, 15$, clearly indicate convergence as F increases to inviscid Dressler waves (Dressler 1949), alternating smooth portions and shock discontinuities. This agrees with recent observations of (Boudlal and Yu Liapidevskii 2005) that large-amplitude roll waves are experimentally well predicted by a simplified, asymptotic version of the inviscid theory. We conjecture that our lower (low-frequency) stability boundary, corresponding to loss of hyperbolicity of associated Whitham equations, agrees with the inviscid threshold suggested by Noble (2006), Theorem 1.2,¹⁷ while the upper (high-frequency) stability boundary, corresponding to appearance of unstable spectra far from the origin, arises through a homoclinic, or “large- X ,” limit similar to that studied in Gardner (1997), Sandstede and Scheel (2001) for reaction diffusion, KdV and related equations.

We note that both analysis and numerics are complicated in the large- X limit by the appearance, differently from the case treated in Sandstede and Scheel (2001) of essential spectra through the origin of the limiting solitary wave profile at $X = +\infty$, along with the usual zero eigenvalue imposed by translational invariance. Whereas point spectra of a solitary wave are approximated as $X \rightarrow +\infty$ by individual loops of Floquet spectra, curves of continuous spectra are “tiled” by arcs of length $\sim X^{-1}$, leading to the plethora of zero eigenvalues (marked as pale dots, red in color plates) visible in Fig. 8c, d. The large number of roots as $X \rightarrow \infty$ leads to numerical difficulty for both Hill’s method and numerical Evans function techniques, making the resolution of the stability region an extremely delicate computation, requiring 40 days on IU’s 370-node Quarry supercomputer cluster to complete (“Appendix 3”). The asymptotic analysis of this region is thus of considerable practical as well as theoretical interest.

¹⁷ For fixed $4 < F^2 < 90$, this states that waves are stable for fixed velocity/period and inclination angle θ sufficiently small: equivalently (by rescaling), for fixed inclination angle and period X sufficiently large.

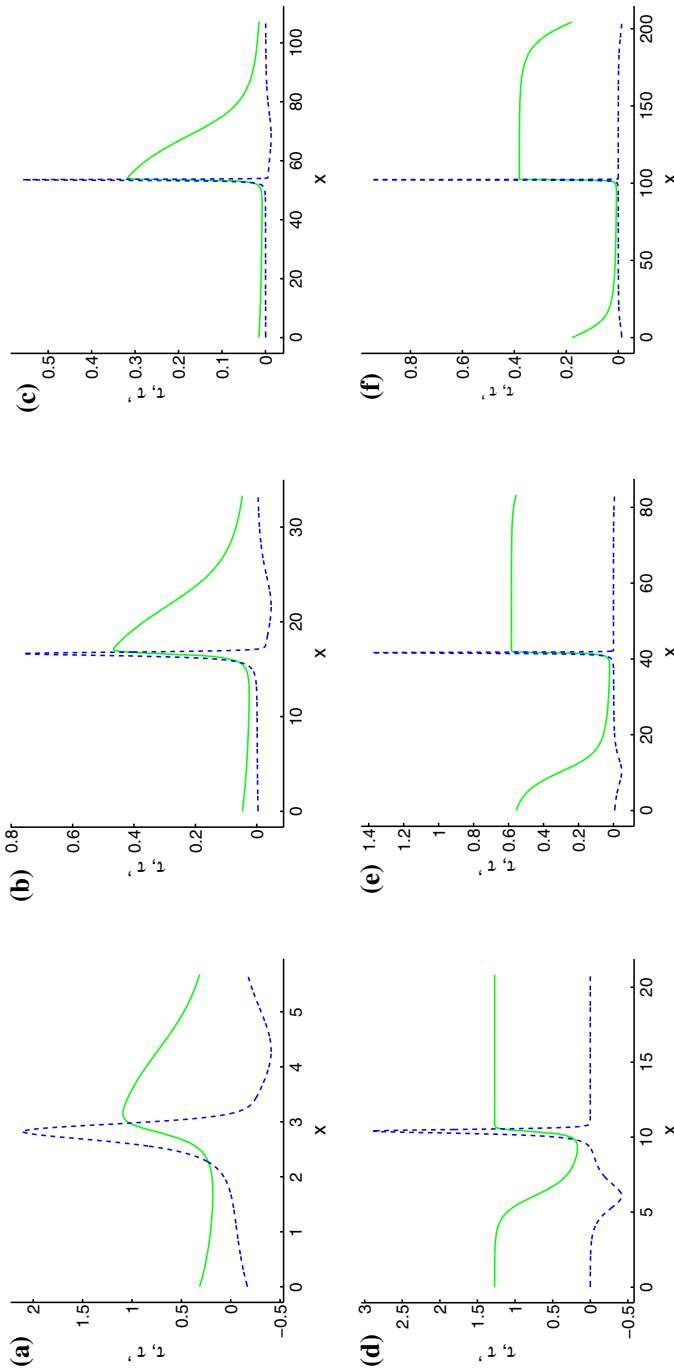


Fig. 5 Convergence to Dressler waves: we plot $\bar{\tau}(x)$ with pale solid curves and $\bar{\tau}'(x)$ with dark dashed curves (green and blue, respectively, in color plates). Here $\alpha = -2$, $\nu = 0.1$, $q = 0.4F^{-2}$, and **a** $F = 5$, $X \approx 6.25$, **b** $F = 10$, $X \approx 33.3$, **c** $F = 15$, $X \approx 107$, **d** $F = 5$, $X \approx 20.8$, **e** $F = 10$, $X \approx 83.3$, **f** $F = 15$, $X \approx 205$

Finally, recall that, just as the KdV–KS \rightarrow KdV limit is derived formally from the viscous St. Venant equations in the weakly unstable limit, the viscous St. Venant equations are derived formally from the more fundamental free-boundary Navier–Stokes equations in the shallow water limit. Alternatively, the KdV–KS \rightarrow KdV limit may be derived directly from the Navier–Stokes equations in a formal weakly unstable/shallow water limit. Rigorous verification of this formal limit, directly from the free-boundary Navier–Stokes equations, is perhaps the fundamental open problem in the theory.

1.4 Plan of the Paper

In Sect. 2.1, we recall the formal derivation of KdV–KS from the viscous St. Venant system and establish Theorem 1.6 concerning the existence of small-amplitude roll waves. These calculations will serve as a guideline for the subsequent analysis: Indeed, we will follow the general strategy for the proof of spectral stability for KdV–KS periodic waves presented in Johnson et al. (2015). In Sect. 2.2, we begin studying the stability of these small-amplitude roll waves by computing a priori estimates on possible unstable eigenvalues for their associated linearized (Bloch) operators: Energy estimates provide natural $O(1)$ bounds (as $\delta = \sqrt{F-2} \rightarrow 0$), whereas an approximate diagonalization process is needed to obtain the sharper bound $O(\delta^3)$. At this stage, we recover, after a suitable rescaling and up to some negligible terms, the spectral problem associated with KdV–KS obtained after the Fenichel’s transformations. In Sect. 2.3, we then follow the proof in Johnson et al. (2015) to complete the spectral stability analysis: For any fixed *nonzero* Bloch number, possible unstable eigenvalues $\lambda(\xi)$ for the linearized St. Venant system as $\delta \rightarrow 0^+$ are expanded as $\lambda(\delta; \xi, \lambda_0) = \delta^3 \lambda_0 + \delta^4 \lambda_1(\xi, \lambda_0) + O(\delta^5)$, where $\lambda_0 \in i\mathbb{R}$ is an explicit eigenvalue associated with the linearized (Bloch) operator for the KdV equation and the corrector $\lambda_1(\xi, \lambda_0)$ is *exactly* the corrector found in the analogous study of the stability of KdV–KS wavetrains in the singular limit $\delta \rightarrow 0^+$: see Barker (2014), Johnson et al. (2015) and Sect. 1.1.3 above. In particular, there it was proven (through numerical evaluation of integrals of certain elliptic functions) that $\text{Ind}(k) < 0$, as defined in (1.9) for all $k \in \mathcal{P}$ corresponding to periods $X = X(k)$ in an open interval (X_m, X_M) with $X_m \approx 8.44$ and $X_M \approx 26.1$. On the other hand, in the regime $0 < |\lambda|/\delta^3 + |\xi| \ll 1$ a further expansion of the Evans function is needed. There, we show that modulo a rescaling of λ by δ^3 this expansion is exactly the one derived in Johnson et al. (2015) for the singular KdV limit of the KdV–KS equation. From the results of Johnson et al. (2015), this concludes the proof of our description of spectral stability in the small Froude number limit $F \rightarrow 2^+$. We then turn our attention to the stability of *large-amplitude* roll waves, far from the distinguished limit $F \rightarrow 2^+$. We then continue our analysis into the large-amplitude regime, far from the weakly unstable limit $F \rightarrow 2^+$. We begin with a study of the distinguished large Froude number limit $F \rightarrow \infty$ in Sect. 3.1, identifying a one-parameter family of limiting systems approachable by various scaling choices in (1.11). An analysis of these limiting systems indicates instability of roll waves for sufficiently large Froude number F . Finally, in Sect. 3.2, we carry out a numerical analysis similar to the one in Barker et al. (2013) where for the KdV–KS equation the full set of model parameters

was explored: here we consider the influence of $2 < F < \infty$ on the range of stability of periodic waves, as parametrized by period X and discharge rate q .

2 Existence and Stability of Roll Waves in the Limit $F \rightarrow 2^+$

In this section, we rigorously analyze in the weakly unstable limit $F \rightarrow 2^+$ the spectral stability of periodic traveling wave solutions of the St. Venant equations (1.11) to small localized (i.e., integrable) perturbations. We begin by studying the existence of such solutions and determining their asymptotic expansions. In particular, we show that such waves exist and, up to leading order, are described by solutions of the KdV–KS equation (1.2) in the singular limit $\delta \rightarrow 0$ (Theorem 1.6).

2.1 Existence of Small-Amplitude Roll Waves: Proof of Theorem 1.6

The goal of this section is to establish the result of Theorem 1.6. To begin, notice that traveling wave solutions of the shallow water equations (1.11) with wave speed c are stationary solutions of the system

$$\partial_t \tau - \partial_x(u + c\tau) = 0, \quad \partial_t u + \partial_x \left(\frac{\tau^{-2}}{2F^2} - cu \right) = 1 - \tau u^2 + v \partial_x \left(\tau^{-2} \partial_x u \right) \tag{2.1}$$

of PDE’s. In particular, from the first PDE it follows that $u = q - c\tau$ for some constant of integration $q \in \mathbb{R}$ and hence τ must satisfy the profile ODE

$$\partial_x \left(\frac{\tau^{-2}}{2F^2} + c^2 \tau \right) = 1 - \tau(q - c\tau)^2 - cv \partial_x \left(\tau^{-2} \partial_x \tau \right). \tag{2.2}$$

Clearly then, we have that $(\tau, u) = (\tau_0, \tau_0^{-1/2})$ is a constant equilibrium solution of (2.1) for any $\tau_0 > 0$. Furthermore, linearizing the profile ODE (2.2) about $\tau = \tau_0$ yields, after rearranging, the ODE

$$cv\tau_0^{-2}\tau'' + (c^2 - c_s^2)\tau' + \left(\frac{\tau_0^{-3/2}/2 - c}{\tau_0^{-1/2}/2} \right)\tau = 0, \quad c_s = \frac{\tau_0^{-3/2}}{F}.$$

Considering the eigenvalues of the above linearized equation as being indexed by the parameters u_0, c , and q it is straightforward to check that a Hopf bifurcation occurs when

$$c = c_s = \frac{\tau_0^{-3/2}}{F} \quad \text{and} \quad F > 2.$$

This verifies that as the Froude number F crosses through $F = 2$, the equilibrium solutions $(\tau, u) = (\tau_0, \tau_0^{-1/2})$, corresponding to a parallel flow, become linearly unstable through a Hopf bifurcation, and hence, nontrivial periodic traveling wave solutions of

(1.11) exist for $F > 2$. Moreover, at the bifurcation point the limiting period of such waves is given by $X = \frac{2\pi}{\omega}$ where $\omega = \tau_0^{5/4} \nu^{-1/2} \sqrt{F - 2}$.

With the above preparation in mind, we want to examine the small-amplitude periodic profiles generated in the weakly nonlinear limit $F \rightarrow 2^+$. To this end, we set $\delta = \sqrt{F - 2}$ and notice that by rescaling space and time in the KdV-like fashion $Y = \delta(x - c_0 t) / \nu^{1/2}$ and $S = \delta^3 t / \nu^{1/2}$, with $c_0 = \tau_0^{-3/2} / 2$, (1.11) become

$$\begin{aligned} \delta^2 \partial_S \tau - \partial_Y (u + c_0 \tau) &= 0, \\ \delta^3 \partial_S u + \delta \partial_Y \left(\frac{\tau^{-2}}{2F^2} - c_0 u \right) &= \nu^{1/2} (1 - \tau u^2) + \nu^{1/2} \delta^2 \partial_Y (\tau^{-2} \partial_Y u). \end{aligned} \tag{2.3}$$

We now search for small-amplitude solutions of this system of the form $(\tau, u) = (\tau_0, \tau_0^{-1/2}) + \delta^2(\tilde{\tau}, \tilde{u})$ with wave speed c_0 in the limit $F \rightarrow 2^+$. The unknowns $\tilde{\tau}$ and \tilde{u} satisfy the system

$$\begin{aligned} \delta^2 \partial_S \tilde{\tau} - \partial_Y (\tilde{u} + c_0 \tilde{\tau}) &= 0 \\ \delta^3 \partial_S \tilde{u} + \delta \partial_Y \left(\frac{(\tau_0 + \delta^2 \tilde{\tau})^{-2}}{2\delta^2 F^2} - c_0 \tilde{u} \right) &= \nu^{1/2} \delta^{-2} (1 - (\tau_0 + \delta^2 \tilde{\tau})(\tau_0^{-1/2} + \delta^2 \tilde{u})^2) + \nu^{1/2} \delta^2 \partial_Y ((\tau_0 + \delta^2 \tilde{\tau})^{-2} \partial_Y \tilde{u}). \end{aligned}$$

Defining the new unknown $\tilde{w} = \delta^{-2} (\tilde{u} + c_0 \tilde{\tau})$ and inserting $\tilde{u} = -c_0 \tilde{\tau} + \delta^2 \tilde{w}$ above yields

$$\begin{aligned} \partial_S \tilde{\tau} - \partial_Y \tilde{w} &= 0 \\ \delta^3 \partial_S \tilde{w} + \delta^{-1} \partial_Y \left(\frac{(\tau_0 + \delta^2 \tilde{\tau})^{-2} - \tau_0^{-2} + 2\tau_0^{-3} \delta^2 \tilde{\tau} - 3\tau_0^4 \delta^4 \tilde{\tau}^2}{2\delta^2 F^2} \right. & \\ \left. + \left(c_0^2 - \frac{\tau_0^{-3}}{F^2} \right) \tilde{\tau} + \frac{3\tau_0^4}{2F^2} \delta^2 \tilde{\tau}^2 - 2c_0 \delta^2 \tilde{w} \right) & \\ = \nu^{1/2} \left((2\tau_0^{-1/2} c_0 - c_0^2 \tau_0) \tilde{\tau}^2 - 2\tau_0^{1/2} \tilde{w} - c_0 \tau_0^{-2} \partial_{YY} \tilde{\tau} + \delta^2 \tilde{g}(\tilde{\tau}, \tilde{w}, \delta) \right) & \\ + \nu^{1/2} \tau_0^{-2} \delta^2 \partial_{YY} \tilde{w} + \nu^{1/2} \delta^2 \partial_Y (\tilde{r}(\tilde{\tau}, \delta) \partial_Y (\delta^2 \tilde{w} - c_0 \tilde{\tau})) & \end{aligned}$$

for some smooth functions \tilde{g}, \tilde{r} . Expanding $F^{-2} = \frac{1}{4} (1 - \delta^2) + O(\delta^4)$ reduces the above system to

$$\begin{aligned} \partial_S \tilde{\tau} - \partial_Y \tilde{w} &= 0 \\ \delta^3 \partial_S \tilde{w} + \delta \partial_Y \left(\frac{\tilde{\tau}}{4\tau_0^3} + \frac{3}{8\tau_0^4} \tilde{\tau}^2 - \tau_0^{-3/2} \tilde{w} + \delta^2 \tilde{f}(\tilde{\tau}, \delta) \right) & \end{aligned}$$

$$= \nu^{1/2} \left(\frac{3}{4\tau_0^2} \tilde{\tau}^2 - 2\tau_0^{1/2} \tilde{w} - \frac{1}{2\tau_0^{7/2}} \partial_{Y Y} \tilde{\tau} + \delta^2 \tilde{g}(\tilde{\tau}, \tilde{w}, \delta) \right) + \nu^{1/2} \tau_0^{-2} \delta^2 \partial_{Y Y} \tilde{w} + \nu^{1/2} \delta^2 \partial_Y \left(\tilde{r}(\tilde{\tau}, \delta) \partial_Y (\delta^2 \tilde{w} - c_0 \tilde{\tau}) \right)$$

for some smooth function \tilde{f} . Rescaling the independent and dependent variables via

$$(Y, S, \tilde{\tau}, \tilde{w}) \mapsto \left(\tau_0^{5/4} Y, \frac{1}{4} \tau_0^{-1/4} S, 3\tau_0^{-1} \tilde{\tau}, 12\tau_0^{1/2} \tilde{w} \right),$$

we arrive at the rescaled system

$$\begin{aligned} \partial_S \tilde{\tau} - \partial_Y \tilde{w} &= 0 \\ \frac{\delta^3}{8\tau_0^{1/4} \nu^{1/2}} \partial_S \tilde{w} + \frac{\delta}{2\tau_0^{1/4} \nu^{1/2}} \partial_Y \left(\tilde{\tau} + \frac{1}{2} \tilde{\tau}^2 - \tilde{w} + \delta^2 f(\tilde{\tau}, \delta) \right) \\ &= \frac{1}{2} \tilde{\tau}^2 - \tilde{w} - \partial_{Y Y} \tilde{\tau} + \delta^2 g(\tilde{\tau}, \tilde{w}, \delta) + \frac{1}{2} \delta^2 \partial_{Y Y} \tilde{w} + \delta^2 \partial_Y \left(r(\tilde{\tau}, \delta) \partial_Y (\delta^2 \tilde{w} - c_0 \tilde{\tau}) \right) \end{aligned} \tag{2.4}$$

for some smooth functions f, g , and r .

We now search for periodic traveling waves of the form $(\tilde{\tau}, \tilde{w})(Y - \tilde{c}S)$ in the rescaled system (2.4). Changing to the moving coordinate frame $(Y - \tilde{c}S, S)$, in which the S -derivative becomes zero, and integrating the first equation with respect to the new spatial variable $Y - \tilde{c}S$, we find that $\tilde{w} = \tilde{q} - \tilde{c}\tilde{\tau}$ for some constant \tilde{q} . Substituting this identity into the second equation in (2.4), also expressed in the moving coordinate frame $(Y - \tilde{c}S, S)$, gives

$$\begin{aligned} \frac{\delta^3}{8\tau_0^{1/4} \nu^{1/2}} \tilde{c}^2 \tilde{\tau}' + \frac{\delta}{2\tau_0^{1/4} \nu^{1/2}} \left((1 + \tilde{c}) \tilde{\tau} + \frac{1}{2} \tilde{\tau}^2 + \delta^2 f(\tilde{\tau}, \delta) \right)' \\ = -\tilde{q} + \frac{1}{2} \tilde{\tau}^2 + \tilde{c}\tilde{\tau} + \delta^2 G(\tilde{\tau}, \delta) - \left((1 + \delta^2 B(\tilde{\tau}, \delta)) \tilde{\tau}' \right)' \end{aligned}$$

for some smooth functions G and B . Next, introducing the near-identity change in dependent variables

$$\tilde{T} = - \left(\tilde{\tau} + \delta^2 \int_0^{\tilde{\tau}} B(x, \delta) dx \right) \tag{2.5}$$

gives, finally, the reduced, nondimensionalized profile equation

$$\tilde{T}'' + \frac{1}{2} \tilde{T}^2 - \tilde{c}\tilde{T} - \tilde{q} = -\tilde{\delta} \left((\tilde{c} + 1)\tilde{T} - \frac{1}{2} \tilde{T}^2 \right)' + \tilde{\delta}^2 m(\tilde{T}, \tilde{T}', \tilde{\delta}), \quad \tilde{\delta} := \frac{\delta}{2\tau_0^{1/4} \nu^{1/2}} \tag{2.6}$$

for some smooth function m .

It is well known (see [Bottman and Deconinck 2009](#) for instance) that the limiting $\tilde{\delta} = 0$ profile equation

$$T_0'' + \frac{1}{2}T_0^2 - \tilde{c}T_0 = \tilde{q} \tag{2.7}$$

selects for a given (\tilde{c}, \tilde{q}) , up to translation, a one-parameter subfamily of the cnoidal waves of the KdV equation $u_t + uu_x + u_{xxx} = 0$, which are given explicitly as a three-parameter family by

$$T_0(x; a_0, k, \kappa) = a_0 + 12k^2\kappa^2 \operatorname{cn}^2(\kappa x, k),$$

where $\operatorname{cn}(\cdot, k)$ is the Jacobi elliptic cosine function with elliptic modulus $k \in (0, 1)$, $\kappa > 0$ is a scaling parameter, and a_0 is an arbitrary real constant related to the Galilean invariance of the KdV equation, with the parameters (a_0, k, κ) being constrained by (\tilde{c}, \tilde{q}) through the relations

$$\begin{aligned} \tilde{c} &= a_0 + 4\kappa^2(2k^2 - 1), \\ \tilde{q} &= 24k^2(1 - k^2)\kappa^4 - a_0\left(\frac{1}{2}a_0 + 4\kappa^2(2k^2 - 1)\right). \end{aligned}$$

Note that these cnoidal profiles are $2K(k)/\kappa$ periodic, where $K(k)$ is the complete elliptic integral of the first kind.

Now, noting that (2.6) can be written as

$$\frac{1}{\tilde{\delta}} \left(\frac{1}{2}(\tilde{T}')^2 + \frac{1}{6}\tilde{T}^3 - \frac{\tilde{c}}{2}\tilde{T}^2 - \tilde{q}\tilde{T} \right)' = \tilde{T}' \left(-\left(\tilde{c} + 1\right)\tilde{T} - \frac{1}{2}\tilde{T}^2 \right)' + \tilde{\delta} m(\tilde{T}, \tilde{T}', \tilde{\delta}),$$

standard arguments in the study of *regular perturbations of planar Hamiltonian systems* (see, for example, [Guckenheimer and Holmes 1990](#), Chapter 4) imply that, among the above-mentioned one-dimensional family of KdV cnoidal waves T_0 , only those satisfying

$$\int_0^{2K(k)/\kappa} T_0' \left((\tilde{c} + 1)T_0 - \frac{1}{2}T_0^2 \right)' dx = 0 \tag{2.8}$$

can continue for $0 < \tilde{\delta} \ll 1$ into a family of periodic solutions of (2.6) and that, further, simple zeros of (2.8) do indeed continue for small $\tilde{\delta}$ into a unique, up to translations, three-parameter family of periodic solutions of (2.6); that is, for each fixed $0 < \tilde{\delta} \ll 1$ we find, up to translations, a two-parameter family of periodic solutions of (2.6) that may be parametrized by a_0 and k . The observation that, in the present case, the selection principle (2.8) indeed determines a unique wave that is a simple zero, follows directly from the proof of Proposition 1.1 (see Remark 1.2) since Eq. (2.7) implies

$$\begin{aligned} \int_0^{2K(k)/\kappa} T_0' \left((\tilde{c} + 1)T_0 - \frac{1}{2}T_0^2 \right)' dx &= \int_0^{2K(k)/\kappa} T_0' (T_0 + T_0'')' dx \\ &= - \int_0^{2K(k)/\kappa} T_0 (T_0'' + T_0''') dx, \end{aligned}$$

in agreement with the KdV–KS case. This shows that the profile expansion agrees to order $O(\delta)$ with the KdV–KS expansion. Indeed, further computations show that the expansion of the profile coincides with the KdV–KS expansion up to order $O(\delta^2)$. To complete the proof of Theorem 1.6 we need to only observe that, instead of fixing the speed as above and letting the period vary, one may alternatively fix the period and vary the velocity.

Remark 2.1 Viewed from a standard dynamical systems point of view, the $F \rightarrow 2^+$ limit may be recognized as a *Bogdanov–Takens*, or saddle-node bifurcation; see, for example, the corresponding bifurcation analysis carried out for an artificial viscosity version of Saint Venant in [Hong Hwang and Chang \(1987\)](#). The unfolding of a Bogdanov–Takens point proceeds, similarly as above, by rescaling/reduction to a perturbed Hamiltonian system ([Guckenheimer and Holmes 1990](#), Section 7.3).

2.2 Estimate on Possible Unstable Eigenvalues

Next, we turn to analyzing the spectral stability (to localized perturbations)¹⁸ of the asymptotic profiles of the St. Venant equation constructed in Theorem 1.6. To begin, let $(\bar{\tau}_\delta, \bar{u}_\delta)(x - \bar{c}_\delta t)$ denote a periodic traveling wave solution of the viscous St. Venant equation (1.11), as given by Theorem 1.6 for $\delta = \sqrt{F - 2} \in (0, \delta_0)$. More explicitly, in terms of the expressions given in Theorem 1.6, the periodic profiles are

$$\bar{\tau}_\delta(\theta) = \tau_0 + \delta^2 \frac{\tau_0}{3} \tilde{\tau}_\delta \left(\frac{\tau_0^{5/4} \delta}{\nu^{1/2}} \theta \right), \quad \bar{u}_\delta(\theta) = u_0 + \delta^2 \frac{u_0}{6} \tilde{u}_\delta \left(\frac{\tau_0^{5/4} \delta}{\nu^{1/2}} \theta \right) \quad (2.9)$$

and the period X_δ , wave speed \bar{c}_δ , and constant of integration $q_\delta \equiv \bar{u}_\delta + \bar{c}_\delta \bar{\tau}_\delta$ are expressible via

$$X_\delta = \frac{\nu^{1/2}}{\tau_0^{5/4} \delta} X, \quad \bar{c}_\delta = c_0 + \frac{\delta^2}{4\tau_0^{3/2}} \tilde{c}_\delta, \quad q_\delta = u_0 + \bar{c}_\delta \tau_0 + \frac{\delta^2}{12\tau_0^{1/2}} \tilde{q}, \quad (2.10)$$

¹⁸ The strongest kind of spectral stability, in the sense that it implies spectral stability to co-periodic perturbations, subharmonic perturbations, side-band perturbations, etc.

with τ_0, u_0 constant, $c_0 = \tau_0^{-3/2}/F$, and $\theta = x - \bar{c}_\delta t$. Linearizing (1.11) about $(\bar{\tau}_\delta, \bar{u}_\delta)$ in the co-moving coordinate frame¹⁹ $(x - \bar{c}t, t)$ leads to the linear evolution system

$$\begin{aligned} \partial_t \tau - \partial_x(u + \bar{c}\tau) &= 0, \\ \partial_t u - \partial_x \left(\bar{c}u + \left(\frac{\bar{\tau}^{-3}}{F^2} - 2\bar{\tau}^{-3}\bar{u}' \right) \tau \right) &= -\bar{u}^2\tau - 2\bar{u}\bar{\tau} + v\partial_x(\bar{\tau}^{-2}\partial_x u) \end{aligned} \quad (2.11)$$

governing the perturbation (τ, u) of $(\bar{\tau}, \bar{u})$. Seeking time-exponentially dependent modes leads to the spectral problem

$$\begin{aligned} (u + \bar{c}\tau)' &= \lambda \tau, \\ v(\bar{\tau}^{-2}u')' &= (\lambda + 2\bar{u}\bar{\tau})u - \left(\left(\frac{\bar{\tau}^{-3}}{F^2} - 2\bar{\tau}^{-3}\bar{u}' \right) \tau' + \bar{c}u' \right) \\ &\quad + \left(\bar{u}^2 - \left(\frac{\bar{\tau}^{-3}}{F^2} - 2\bar{\tau}^{-3}\bar{u}' \right)' \right) \tau, \end{aligned} \quad (2.12)$$

where primes denote differentiation with respect to x . In particular, notice that (2.12) is an ODE spectral problem with X_δ -periodic coefficients. As described in Sect. 1.1 above, Floquet theory implies that the $L^2(\mathbb{R})$ spectrum associated with (2.11) is comprised entirely of essential spectrum and can be smoothly parametrized by the discrete eigenvalues of the spectral problem (2.12) considered with the quasi-periodic boundary conditions $(\tau, u)(x + X_\delta) = e^{i\xi}(\tau, u)(x)$ for some value of the Bloch parameter $\xi \in [-\pi/X_\delta, \pi/X_\delta)$. The underlying periodic solution $(\bar{\tau}, \bar{u})$ is said to be (diffusively) spectrally stable provided conditions (D1)–(D3) introduced in the introduction hold. Reciprocally, the solution will be spectrally unstable if there exists a $\xi \in [-\pi/X_\delta, \pi/X_\delta)$ such that the associated Bloch operator has an eigenvalue in the open right half plane.

In this section, we provide a priori estimates on the possible unstable Bloch eigenvalues of the above eigenvalue problem (2.12). As a first step, we carefully examine the hyperbolic–parabolic structure of the eigenvalue problem and demonstrate that, as $F \rightarrow 2^+$ or, equivalently, as $\delta \rightarrow 0^+$, the unstable Bloch eigenvalues of this system are $O(1)$. Next, we prove a simple consistent splitting result that establishes all unstable Bloch eigenvalues of (2.12) converge to zero as $\delta \rightarrow 0^+$. We can then bootstrap these estimates to perform a more refined analysis of the eigenvalue problem demonstrating that such unstable eigenvalues are necessarily $O(\delta^3)$ as $\delta \rightarrow 0^+$.

2.2.1 Unstable Eigenvalues Converge to Zero as $\delta \rightarrow 0^+$

We begin by ruling out the existence of sufficiently large unstable eigenvalues for (2.12). Setting $Z := (\tau, u, \bar{\tau}^{-2}u')^T$, and recalling that $\bar{u} = q - \bar{c}\bar{\tau}$ for some constant $q \in \mathbb{R}$, we first write (2.12) as a first-order system

$$Z'(x) = A(x, \lambda)Z(x), \quad (2.13)$$

¹⁹ Henceforth, we suppress the dependence of $\bar{\tau}, \bar{u}, q$, and \bar{c} on δ .

where

$$A(x, \lambda) := \begin{pmatrix} \lambda/\bar{c} & 0 & -\bar{\tau}^2/\bar{c} \\ 0 & 0 & \bar{\tau}^2 \\ \frac{(q-\bar{c}\bar{\tau})^2-\bar{\alpha}_x-\bar{\alpha}\lambda/\bar{c}}{\nu} & \frac{\lambda+2\bar{\tau}(q-\bar{c}\bar{\tau})}{\nu} & \frac{-\bar{c}\bar{\tau}^2+\bar{\alpha}\tau^2/\bar{c}}{\nu} \end{pmatrix}, \quad \bar{\alpha} := \bar{\tau}^{-3}(F^{-2} + 2\bar{c}\nu\bar{\tau}'). \tag{2.14}$$

Setting $B(x, \lambda) := \begin{pmatrix} \lambda/\bar{c} & 0 & 0 \\ 0 & 0 & \bar{\tau}^2 \\ -\frac{\bar{\alpha}\lambda/\bar{c}}{\nu} & \frac{\lambda}{\nu} & 0 \end{pmatrix}$ and noting that $A - B$ is $O(1)$ as $|\lambda| \rightarrow \infty$, we expect that the spectral problem (2.13) is governed by the principal part $B(x, \lambda)$ for $|\lambda|$ sufficiently large. A direct inspection shows that the eigenvalues of B are given by $\frac{\lambda}{\bar{c}}$ and $\pm\bar{\tau}\sqrt{\frac{\lambda}{\nu}}$, so that the eigenvalues of B have two principal growth rates as $|\lambda| \rightarrow \infty$. In the following, we keep track of both of these spectral scales by a series of carefully chosen coordinate transformations preserving periodicity; for details of these transformations, see Section 4.1 of Barker et al. (2011).

With the above preliminaries, we begin by verifying that the unstable spectra for the system (2.12) are $O(1)$ for δ sufficiently small. Throughout, we use the notation $\|u\|^2 = \int_0^{X_\delta} |u(x)|^2 dx$. Note that although we focus on uniformity in δ in the forthcoming estimates of the unstable spectra, the norms $\|\cdot\|$ do depend on δ through the period X_δ .

Lemma 2.2 *Let $(\bar{\tau}_\delta, \bar{u}_\delta)$ be a family of periodic traveling wave solution of (1.11) defined as in Theorem 1.6 for all $\delta = \sqrt{F-2} \in (0, \delta_0)$ for some $\delta_0 > 0$ sufficiently small. Then, there exist constants $R_0, \eta > 0$ and $0 < \delta_1 < \delta_0$ such that, for all $\delta \in (0, \delta_1)$, the spectral problem (2.12) has no $L^\infty(\mathbb{R})$ eigenvalues with $\Re(\lambda) \geq -\eta$ and $|\lambda| \geq R_0$.*

Proof Suppose that λ is an $L^\infty(\mathbb{R})$ eigenvalue for the spectral problem (2.12) and let (τ, u) be a corresponding eigenfunction satisfying $(u, \tau, \tau')(X_\delta) = e^{i\xi}(u, \tau, \tau')(0)$ for some $\xi \in [-\pi/X_\delta, \pi/X_\delta]$. As described above, setting $Z := (\tau, u, \bar{\tau}^{-2}u')^T$ allows us to write (2.12) as the first-order system (2.13), where the coefficient matrix $A(x, \lambda)$ is given explicitly in (2.14). By performing a series of X_δ -periodic change in variables, carried out in detail in (Barker et al. 2011, Section 4.1), we find there exists a X_δ -periodic change in variables $W(\cdot) = P(\cdot; \lambda, \delta)Z(\cdot)$ that transforms the above spectral problem into

$$W'(x) = (D_\lambda + N)(x, \lambda)W(x), \tag{2.15}$$

supplemented with the boundary condition $W(X_\delta) = e^{i\xi} W(0)$, where the matrices D_λ, N are defined as

$$D_\lambda(\cdot, \lambda) = \text{diag} \left(\frac{\lambda}{\bar{c}} + \theta_0 + \frac{\theta_1}{\lambda}, \quad \bar{\tau}\sqrt{\frac{\lambda}{\nu}}, \quad -\bar{\tau}\sqrt{\frac{\lambda}{\nu}} \right), \quad \theta_0 = \frac{\bar{\alpha}\bar{\tau}^2}{\bar{c}\nu}, \tag{2.16}$$

$\bar{\alpha}$ as in (2.14), and $N := \begin{pmatrix} 0 & N_{H,D} \\ N_{D,H} & N_{D,D} \end{pmatrix}$ with $N_{D,D}$ a 2×2 matrix. Here, $N(\cdot, \lambda)$ is an X_δ -periodic matrix, and moreover, the individual blocks of the matrix $N(\cdot, \lambda)$ expand as

$$\begin{aligned} N_{D,D}(\cdot, \lambda) &= N_{D,D}^0 + \lambda^{-\frac{1}{2}} N_{D,D}^1 + \lambda^{-1} N_{D,D}^2, \\ N_{D,H}(\cdot, \lambda) &= N_{D,H}^0 + \lambda^{-\frac{1}{2}} N_{D,H}^1, \\ N_{H,D}(\cdot, \lambda) &= N_{H,D}^0 + \lambda^{-\frac{1}{2}} N_{H,D}^1 + \lambda^{-1} N_{H,D}^2 + \lambda^{-\frac{3}{2}} N_{H,D}^3, \end{aligned} \tag{2.17}$$

with $|N_{*,*}^j|$ bounded uniformly in $\delta \ll 1$. Explicit formulae for $N_{k,l}^j$ and θ_1 are given in ‘‘Appendix 1.’’

Now, a crucial observation is that, by Theorem 1.6, together with the scalings (2.9)–(2.10), we have

$$\lim_{\delta \rightarrow 0^+} \theta_0(x) = \frac{\tau_0^{1/2}}{2\nu} > 0.$$

It follows that θ_0 is strictly positive and uniformly bounded away from zero, for all $\delta > 0$ sufficiently small. Thus, there exists $\eta, \delta_1 > 0$ sufficiently small and $R_0 > 0$ sufficiently large such that if $|\lambda| \geq R_0$ and $\Re(\lambda) \geq -\eta$, then the quantity $\Re(\frac{\lambda}{c} + \theta_0 + \frac{\theta_1}{\lambda})$ is strictly positive and bounded away from zero, uniformly in δ for $0 < \delta < \delta_1$. Likewise, by choosing δ_1 smaller if necessary, the quantity $|\lambda|^{1/2} \Re(\bar{\tau} \sqrt{\frac{\lambda}{\nu}})$ may be taken to be strictly positive and bounded away from 0, uniformly in δ in the same set of parameters.

Finally, under the same conditions, taking R_0 possibly larger and decomposing

$$W := (W_H, W_{D,+}, W_{D,-})^T,$$

observing that $|W_H|, |W_{D,+}|$ and $|W_{D,-}|$ are X_δ -periodic functions, it follows by standard energy estimates, taking the real part of the complex $L^2[0, X_\delta]$ -inner product of each W_j against the W_j -coordinate of (2.15)–(2.17), using the above-demonstrated coercivity (nonvanishing real part) of the entries of the leading-order diagonal term D_λ , and rearranging, that there exists a constant $C > 0$ independent of R_0 such that, for all $0 < \delta < \delta_1, \Re(\lambda) \geq -\eta$ and $|\lambda| \geq R_0$, we have

$$\begin{aligned} \|W_H\|^2 &\leq C (\|W_{D,+}\| + \|W_{D,-}\|) \|W_H\| \text{ and } \|W_{D,+}\|^2 + \|W_{D,-}\|^2 \\ &\leq C R_0^{-1/2} (\|W_{D,+}\| + \|W_{D,-}\|) \|W_H\|. \end{aligned}$$

Thus, $\|W_H\| \leq C (\|W_{D,+}\| + \|W_{D,-}\|) \leq C^2 R_0^{-1/2} \|W_H\|$, yielding a contradiction for R_0 sufficiently large.

Next, we rescale the spatial variable x as $y = \delta x$, noting that, since $\delta X_\delta = \nu^{1/2} \tau_0^{-5/4} X$, the period is then independent of δ . Then, the first-order system (2.13) can be rewritten as

$$\delta Z'(y) = \left(A_0(\lambda) + \delta^2 A_1(y; \lambda, \delta) \right) Z(y) \tag{2.18}$$

coupled with the boundary condition $Z(\delta X_\delta) = e^{i\xi} Z(0)$ for some $\xi \in [-\pi/\delta X_\delta, \pi/\delta X_\delta]$, where

$$A_0(\lambda) = \begin{pmatrix} 2\lambda\tau_0^{3/2} & -2\lambda\tau_0^{3/2} & 0 \\ 0 & 0 & \tau_0^2 v^{-1} \\ \lambda - 2\sqrt{\tau_0} & 2\lambda & 0 \end{pmatrix}$$

is constant and $A_1(\cdot; \lambda, \delta)$ is uniformly bounded (for λ and δ in any compact set). More precisely, for any δ in a compact subset of $[0, \delta_0)$, we have

$$A_1(\cdot; \lambda, \delta) = \begin{pmatrix} \mathcal{O}(\lambda) & \mathcal{O}(\lambda) & 0 \\ 0 & 0 & \mathcal{O}(1) \\ \mathcal{O}(1) & \mathcal{O}(1) & \mathcal{O}(1) \end{pmatrix}.$$

By analyzing the eigenvalues of $A_0(\lambda)$, we now show that the possible unstable eigenvalues for (2.12) converge to the origin as $\delta \rightarrow 0^+$.

Lemma 2.3 *Let $(\bar{\tau}_\delta, \bar{u}_\delta)$ be a family of periodic traveling wave solution of (1.11) defined as in Theorem 1.6 for all $\delta = \sqrt{F - 2} \in (0, \delta_0)$ for some $\delta_0 > 0$ sufficiently small. Then, for every $\varepsilon > 0$, there exists a $\delta_1 \in (0, \delta_0)$ such that for all $\delta \in (0, \delta_1)$, the spectral problem (2.12) has no $L^\infty(\mathbb{R})$ eigenvalues with $\Re(\lambda) \geq 0$ and $|\lambda| \geq \varepsilon$.*

Proof By Lemma 2.2, it is sufficient to consider λ on a compact set $\varepsilon \leq |\lambda| \leq R_0$, $\Re \lambda \geq 0$, whence (2.18), $\delta \rightarrow 0^+$ represents a uniform family of semiclassical limit problems, with A_0, A_1 varying in compact sets. By standard WKB-type estimates [see, for example, the ‘‘Tracking Lemma’’ of Gardner and Zumbrun (1998); Zumbrun and Howard (1998); Plaza and Zumbrun (2004), these have no bounded solutions for $0 < \delta \leq \delta_0$ sufficiently small, so long as A_0 satisfies *consistent splitting*, meaning that its eigenvalues have nowhere-vanishing real parts: equivalently, $A_0(\lambda)$ has no purely imaginary eigenvalue for $\Re \lambda > 0$ and $\varepsilon \leq |\lambda| \leq R_0$. Indeed, it is easy to see using convergence as $\delta \rightarrow 0$ of the associated periodic Evans function of Gardner (1993) (following from continuous dependence on parameters of solutions of ODE), the correspondence between bounded solutions and zeros of the Evans function, and analyticity of the Evans function together with properties of limits of analytic functions, that $A_0(\lambda)$ has a pure imaginary eigenvalue, i.e., the $\delta = 0$ version of (2.18) has a bounded solution, if and only if there are bounded solutions of (2.18) for a sequence $\lambda_\delta \rightarrow \lambda$ as $\delta \rightarrow 0$.

To prove the lemma therefore, we establish consistent splitting of A_0 for $\lambda \in \Lambda := \{\lambda : \varepsilon \leq |\lambda|, \Re \lambda > 0\}$. The eigenvalues $\gamma(\lambda)$ of the matrix $A_0(\lambda)$ are the solutions of the equation

$$\gamma^3 - 2\lambda\tau_0^{3/2}\gamma^2 - 2\lambda\tau_0^2v^{-1}\gamma + 2\lambda^2\tau_0^{7/2}v^{-1} + 4\lambda\tau_0^4v^{-1} = 0. \tag{2.19}$$

Suppose that $\gamma = i\Omega \in \mathbb{R}i$ is an eigenvalue of $A_0(\lambda)$ for some $\lambda \in \Lambda$. From (2.19), it follows that λ must be a root of the quadratic equation

$$2\lambda^2 \tau_0^{7/2} v^{-1} + 2\lambda \left(2\tau_0^4 v^{-1} + \Omega^2 \tau_0^{3/2} - 2i\Omega \tau_0^2 v^{-1} \right) - i\Omega^3 = 0. \tag{2.20}$$

By Lemma 2.2 above, if Ω is sufficiently large, then the roots of (2.20) satisfy $\Re(\lambda) \leq 0$, else, by the discussion surrounding the Evans function, above, there would be bounded solutions of (2.18) for $\Re\lambda > 0$, $|\lambda|$ large, and δ arbitrarily small, a contradiction. (Alternatively, one may repeat the steps of the proof of Lemma 2.2 for (2.18) with $\delta = 0$.) Increasing Ω then from the supposed value corresponding to an eigenvalue of A_λ , and tracking the corresponding root λ of (2.20), we see that eventually this root must cross the imaginary axis in moving from $\Re\lambda \geq 0$ to $\Re\lambda \leq 0$. Thus, it is sufficient to search for roots of (2.20) of the form $\lambda = i\Theta$ for some $\Theta \in \mathbb{R}$. Substituting this ansatz into (2.20) and grouping real and imaginary parts implies that Ω and Θ satisfy the system of equations $\Theta (\tau_0^{3/2} \Theta - \Omega) = 0$ and $2\tau_0^{3/2} \Theta = \Omega \times \Omega^2 / [\Omega^2 + 2v^{-1} \tau_0^{3/2}]$, from which it easily follows that $\Omega = \Theta = 0$. It follows that for all $\Omega \neq 0$, the real parts of the roots $\lambda_j(\Omega)$ of (2.20) have constant signs, so that, for each $\varepsilon > 0$, $A_0(\lambda)$ indeed has consistent splitting in the region Λ , and the lemma immediately follows. \square

2.2.2 Unstable Eigenvalues are $O(\delta^3)$

Next, we bootstrap the estimates of Lemmas 2.2 and 2.3 to provide a second energy estimate on the reduced “slow”, or KdV, block of the spectral problem (2.12) in the limit $\delta \rightarrow 0^+$. Notice that *this result relies heavily on the fact that the corresponding spectral problem for the linearized KdV equation about a cnoidal wave $T_0(\cdot; a_0, k, \mathcal{G}(k))$ described in Theorem 1.8 has been explicitly solved in Bottman and Deconinck (2009); Spektor (1988) using the associated completely integrable structure, and in particular has been found to be spectrally stable²⁰ for all $k \in (0, 1)$.*

Proposition 2.4 *Let $(\bar{\tau}_\delta, \bar{u}_\delta)$ be a family of periodic traveling wave solution of (1.11) defined as in Theorem 1.6 for all $\delta = \sqrt{F - 2} \in (0, \delta_0)$ for some $\delta_0 > 0$ sufficiently small.*

Then, there exist positive constants C_1, C_2 and $\delta_1 \in (0, \delta_0)$ such that for all $\delta \in (0, \delta_1)$ the spectral problem (2.12) has no $L^\infty(\mathbb{R})$ eigenvalues with $\Re(\lambda) \geq C_1 \delta^4$ or $(\Re(\lambda) \geq 0$ and $|\lambda| \geq C_2 \delta^3)$.

Proof By Lemmas 2.2 and 2.3, the possible unstable eigenvalues for the spectral problem (2.12) converge to the origin as $\delta \rightarrow 0^+$. To analyze the behavior of these possible unstable eigenvalues further, we rescale the unknown Z in (2.18) to $W = (Z_1, \lambda^{2/3} Z_2, \lambda^{1/3} Z_3)^T, \lambda^{1/3}$ denoting the principle third root, yielding the system

$$\delta W'(y) = \left(B_0(\lambda) + \delta^2 \lambda^{-1/3} B_1(y; \lambda, \delta) \right) W(y)$$

²⁰ In the Hamiltonian sense, meaning the linearization about T_0 of the KdV equation has purely imaginary spectrum.

with boundary conditions $W(\delta X_\delta) = e^{i\xi} W(0)$ for some $\xi \in [-\pi/\delta X_\delta, \pi/\delta X_\delta]$, where

$$B_0(\lambda) = \lambda^{1/3} \begin{pmatrix} 2\lambda^{2/3}\tau_0^{3/2} & -2\tau_0^{3/2} & 0 \\ 0 & 0 & \tau_0^2 v^{-1} \\ \lambda - 2\sqrt{\tau_0} & 2\lambda^{1/3} & 0 \end{pmatrix}$$

and $B_1(\cdot; \lambda, \delta)$ is uniformly bounded for (λ, δ) in any compact subset of $\mathbb{C} \times [0, \delta_0)$. More precisely, for any δ in a compact subset of $[0, \delta_0)$, we have

$$B_1(\cdot; \lambda, \delta) = \begin{pmatrix} O(\lambda^{2/3}) & O(\lambda^{2/3}) & 0 \\ 0 & 0 & O(\lambda^{2/3}) \\ O(\lambda^{2/3}) & O(1) & O(\lambda^{1/3}) \end{pmatrix}.$$

To track the most dangerous terms, we write the above system as

$$\delta W'(y) = \left(\lambda^{1/3} M_0 + (2\lambda^{2/3} + \delta^2 \lambda^{-1/3} \beta(y)) M_1 + \lambda R_0(\lambda) + \delta^2 R_1(y; \lambda, \delta) \right) W(y), \tag{2.21}$$

where

$$M_0 = \begin{pmatrix} 0 & -2\tau_0^{3/2} & 0 \\ 0 & 0 & \tau_0^2 v^{-1} \\ -2\sqrt{\tau_0} & 0 & 0 \end{pmatrix}, \quad M_1 = \begin{pmatrix} 0 & 0 & 0 \\ 0 & 0 & 0 \\ 0 & 1 & 0 \end{pmatrix},$$

and the function $\beta(\cdot)$ is some explicit periodic function expressed in terms of τ_0, v and asymptotic KdV profiles, while the R_j matrices are uniformly bounded functions of λ and δ on compact subsets of $\mathbb{C} \times [0, \delta_0)$. The goal is to now reduce the first-order problem (2.21) to a constant-coefficient problem at a sufficiently high order in λ and δ .

To begin, we diagonalize M_0 by defining the matrices

$$P_0 = \begin{pmatrix} 1 & 0 & 0 \\ 0 & \frac{K_0}{2\tau_0^{3/2}} & 0 \\ 0 & 0 & -\frac{v K_0^2}{2\tau_0^{7/2}} \end{pmatrix} \begin{pmatrix} 1 & 1 & 1 \\ 1 & \omega & \omega^2 \\ 1 & \omega^2 & \omega \end{pmatrix}, \quad P_0^{-1} = \frac{1}{3} \begin{pmatrix} 1 & 1 & 1 \\ 1 & \omega^2 & \omega \\ 1 & \omega & \omega^2 \end{pmatrix} \begin{pmatrix} 1 & 0 & 0 \\ 0 & \frac{2\tau_0^{3/2}}{K_0} & 0 \\ 0 & 0 & -\frac{2\tau_0^{7/2}}{v K_0^2} \end{pmatrix},$$

where $K_0 = 4^{1/3} \tau_0^{4/3} v^{-1/3}$ and $\omega = e^{2i\pi/3}$. Setting $Y(\cdot) = P_0^{-1} W(\cdot)$, the system (2.21) can be written in equivalent form

$$\delta Y'(y) = \left(\lambda^{1/3} D_0 - \frac{\tau_0^2}{3vK_0} (2\lambda^{2/3} + \delta^2 \lambda^{-1/3} \beta(y)) Q_1 + \lambda \tilde{R}_0(\lambda) + \delta^2 \tilde{R}_1(y; \lambda, \delta) \right) Y(y) \tag{2.22}$$

where

$$D_0 = \begin{pmatrix} -K_0 & 0 & 0 \\ 0 & -K_0\omega & \\ 0 & 0 & -K_0\omega^2 \end{pmatrix} \quad Q_1 = \begin{pmatrix} 1 & \omega & \omega^2 \\ \omega & \omega^2 & 1 \\ \omega^2 & 1 & \omega \end{pmatrix},$$

and \tilde{R}_j are uniformly bounded in (λ, δ) on compact subsets of $\mathbb{C} \times [0, \delta_0)$. This effectively diagonalizes system (2.21) to leading order.

Aiming at reducing (2.22) to a constant-coefficient problem at a higher order, we choose $q(\cdot)$ satisfying

$$q'(\cdot) = \frac{\tau_0^2}{3\nu K_0} (\beta(\cdot) - \langle \beta(\cdot) \rangle),$$

where $\langle \cdot \rangle$ denotes average over one period. Notice that the periodicity of $\beta(\cdot)$ implies that q is (δX_δ) -periodic. Now, since the matrix $(I_3 + \delta^2 \lambda^{-1/3} q(\cdot) Q_1)$ is invertible for $\delta^2 \lambda^{-1/3}$ sufficiently small, for such parameters we can make the change in variables

$$U(\cdot) = (I_3 + \delta^2 \lambda^{-1/3} q(\cdot) Q_1) Y(\cdot),$$

with $U(\cdot)$ satisfying the first-order system

$$\begin{aligned} \delta U'(y) = & (\lambda^{1/3} D_0 - \frac{\tau_0^2}{3\nu K_0} (2\lambda^{2/3} + \delta^2 \lambda^{-1/3} \langle \beta(\cdot) \rangle) Q_1 \\ & + \lambda \bar{R}_0(y; \lambda, \delta) + \delta^2 \bar{R}_1(y; \lambda, \delta) + \delta^4 \lambda^{-2/3} \bar{R}_2(y; \lambda, \delta)) U(y), \end{aligned}$$

with \bar{R}_j uniformly bounded in (λ, δ) on compact subsets of $\mathbb{C} \times [0, \delta_0)$.

Next, we diagonalize the system at a higher order. Since D_0 has distinct eigenvalues, we may choose a constant matrix P_1 such that the commutator $[P_1, D_0]$ equals the off-diagonal part of Q_1 . Then, provided that λ and $\delta^2 \lambda^{-2/3}$ are small enough, we may change the unknown to

$$S(\cdot) = \left(I_3 + \frac{\tau_0^2}{3\nu K_0} (2\lambda^{1/3} + \delta^2 \lambda^{-2/3} \langle \beta(\cdot) \rangle) P_1 \right) U(\cdot)$$

with $S(\cdot)$ satisfying the first-order system

$$\delta S'(y) = \left(D_1(\lambda, \delta) + \lambda \hat{R}_0(y; \lambda, \delta) + \delta^2 \hat{R}_1(y; \lambda, \delta) + \delta^4 \lambda^{-1} \hat{R}_2(y; \lambda, \delta) \right) S(y) \tag{2.23}$$

where \hat{R}_j are uniformly bounded in (λ, δ) on compact subsets of $\mathbb{C} \times [0, \delta_0)$ and $D_1(\lambda, \delta)$ is a constant-coefficient diagonal matrix whose diagonal entries are

$$\begin{aligned} \mu_0(\lambda, \delta) &= -K_0 \lambda^{1/3} - \frac{\tau_0^2}{3\nu K_0} (2\lambda^{2/3} + \delta^2 \lambda^{-1/3} \langle \beta(\cdot) \rangle) \\ \mu_+(\lambda, \delta) &= -K_0 \omega \lambda^{1/3} - \frac{\tau_0^2 \omega^2}{3\nu K_0} (2\lambda^{2/3} + \delta^2 \lambda^{-1/3} \langle \beta(\cdot) \rangle) \\ \mu_-(\lambda, \delta) &= -K_0 \omega^2 \lambda^{1/3} - \frac{\tau_0^2 \omega}{3\nu K_0} (2\lambda^{2/3} + \delta^2 \lambda^{-1/3} \langle \beta(\cdot) \rangle). \end{aligned}$$

In particular, we find

$$\begin{aligned} \Re(\mu_0(\lambda, \delta)) &= -\left(K_0 + \frac{\tau_0^2}{3\nu K_0} \delta^2 |\lambda|^{-2/3} \langle \beta(\cdot) \rangle \right) \Re(\lambda^{1/3}) - \frac{\tau_0^2}{3\nu K_0} \frac{2\Re(\bar{\lambda} \lambda^{1/3})}{|\lambda|^{2/3}}, \\ \Re(\mu_+(\lambda, \delta)) &= -\left(K_0 + \frac{\tau_0^2}{3\nu K_0} \delta^2 |\lambda|^{-2/3} \langle \beta(\cdot) \rangle \right) \Re(\omega \lambda^{1/3}) - \frac{\tau_0^2}{3\nu K_0} \frac{2\Re(\bar{\lambda} \omega \lambda^{1/3})}{|\lambda|^{2/3}}, \\ \Re(\mu_-(\lambda, \delta)) &= -\left(K_0 + \frac{\tau_0^2}{3\nu K_0} \delta^2 |\lambda|^{-2/3} \langle \beta(\cdot) \rangle \right) \Re(\omega^2 \lambda^{1/3}) - \frac{\tau_0^2}{3\nu K_0} \frac{2\Re(\bar{\lambda} \omega^2 \lambda^{1/3})}{|\lambda|^{2/3}}, \end{aligned}$$

so that, when $\Re(\lambda) \geq 0$ and λ and $\delta^2 |\lambda|^{-2/3}$ are sufficiently small,

$$\begin{aligned} \Re(\mu_0(\lambda, \delta)) &\leq -C|\lambda|^{1/3}, \\ \Re(\mu_+(\lambda, \delta)) &\geq \begin{cases} C|\lambda|^{1/3}, & \text{if } \Im(\lambda) \geq 0 \\ C \left(\frac{\Re(\lambda)}{|\lambda|^{2/3}} + \frac{|\Im(\lambda)|}{|\lambda|^{1/3}} \right), & \text{if } \Im(\lambda) \leq 0 \end{cases}, \\ \Re(\mu_-(\lambda, \delta)) &\geq \begin{cases} C|\lambda|^{1/3}, & \text{if } \Im(\lambda) \leq 0 \\ C \left(\frac{\Re(\lambda)}{|\lambda|^{2/3}} + \frac{|\Im(\lambda)|}{|\lambda|^{1/3}} \right), & \text{if } \Im(\lambda) \geq 0 \end{cases}. \end{aligned}$$

Using an energy estimate as in the proof of Lemma 2.2 above, it follows for $\epsilon, \delta_1 > 0$ sufficiently small and $R > 0$ sufficiently large that for $0 < \delta < \delta_1$ system (2.23) has no bounded solutions provided that

$$\Re(\lambda) \geq 0, \quad |\lambda| \leq \epsilon, \quad \Re(\lambda) |\lambda|^{1/3} + |\Im(\lambda)| |\lambda|^{2/3} \geq R \delta^4. \tag{2.24}$$

In particular, this shows that as $\delta \rightarrow 0^+$ the unstable eigenvalues satisfy $|\lambda| = O(\delta^{12/5})$.

Next, we refine the above bound by using spectral stability of the limiting cnoidal wave. To do so, we scale unknowns of the system (2.12) according to

$$\tau(\theta) = \delta^2 \frac{\tau_0}{3} a \left(\frac{\tau_0^{5/4} \delta}{\nu^{1/2}} \theta \right), \quad u(\theta) = \delta^2 \frac{u_0}{6} b \left(\frac{\tau_0^{5/4} \delta}{\nu^{1/2}} \theta \right), \quad \lambda = \frac{\delta^3}{4\tau_0^{1/4} \nu^{1/2}} \Lambda. \tag{2.25}$$

Our goal is to prove that the rescaled system obtained from (2.12) has no unstable eigenvalues Λ with $|\Lambda|$ sufficiently large. To this end, notice that by (2.24) the possible

unstable eigenvalues Λ must satisfy the estimate

$$\Re(\Lambda) \geq 0, \quad \Re(\Lambda) |\Lambda|^{1/3} + \delta |\Im(\Lambda)| |\Lambda|^{2/3} = O(1), \tag{2.26}$$

so that, in particular, we already know that $\Lambda = O(\delta^{-3/5})$. Rewriting the eigenvalue system (2.12) in terms of the unknown $V(Y) = (\delta^{-2}(b(Y) + \bar{c} a(Y)), a(Y), a'(Y))$ results in the system

$$V'(Y) = (A_{\text{KdV}}(Y; \Lambda) + \Lambda \delta B + \delta C(Y) + R(Y; \Lambda, \delta)) V(Y) \tag{2.27}$$

with²¹

$$\begin{aligned} A_{\text{KdV}}(\cdot; \Lambda) &= \begin{pmatrix} 0 & \Lambda & 0 \\ 0 & 0 & 1 \\ -1 & \sigma_0 - T_0(\cdot) & 0 \end{pmatrix}, \\ B &= \frac{1}{2\tau_0^{1/4} \nu^{1/2}} \begin{pmatrix} 0 & 0 & 0 \\ 0 & 0 & 0 \\ 0 & 1 & 0 \end{pmatrix} \\ C(\cdot) &= \frac{1}{2\tau_0^{1/4} \nu^{1/2}} \begin{pmatrix} 0 & 0 & 0 \\ 0 & 0 & 0 \\ 0 & T_0'(\cdot) - T_1(\cdot) - 1 + T_0(\cdot) - \sigma_0 \end{pmatrix}, \end{aligned}$$

and

$$R(\cdot; \Lambda, \delta) = \begin{pmatrix} 0 & 0 & 0 \\ 0 & 0 & 0 \\ O(\Lambda \delta^3) + O(\delta^2) & O(\Lambda \delta^3) + O(\delta^2) & O(\Lambda \delta^2) + O(\delta^2) \end{pmatrix}.$$

To make use of known results about KdV, we rewrite the above spectral problem in a more standard way by introducing the unknown $W(\cdot) = (V_2(\cdot), V_3(\cdot), -V_1(\cdot) + (\sigma_0 - T_0(\cdot)) V_2(\cdot))^T$. This leads to

$$W'(Y) = (H_0(Y; \Lambda) + \Lambda \delta H_1 + \delta H_2(Y) + R(Y; \Lambda, \delta)) W(Y) \tag{2.28}$$

with

$$H_0(\cdot; \Lambda) = \begin{pmatrix} 0 & 1 & 0 \\ 0 & 0 & 1 \\ -\Lambda - T_0'(\cdot) & \sigma_0 - T_0(\cdot) & 0 \end{pmatrix}, \tag{2.29}$$

²¹ We don't need here the exact form of C but we specify it for latter use.

$$\begin{aligned}
 H_1 &= \frac{1}{2\tau_0^{1/4} \nu^{1/2}} \begin{pmatrix} 0 & 0 & 0 \\ 1 & 0 & 0 \\ 0 & 0 & 0 \end{pmatrix}, \\
 H_2(\cdot) &= \frac{1}{2\tau_0^{1/4} \nu^{1/2}} \begin{pmatrix} 0 & 0 & 0 \\ T_0'(\cdot) - T_1(\cdot) - 1 + T_0(\cdot) - \sigma_0 & 0 & 0 \\ 0 & 0 & 0 \end{pmatrix}, \tag{2.30}
 \end{aligned}$$

and

$$R(\cdot; \Lambda, \delta) = \begin{pmatrix} 0 & 0 & 0 \\ O(\Lambda \delta^3) + O(\delta^2) & O(\Lambda \delta^2) + O(\delta^2) & O(\Lambda \delta^3) + O(\delta^2) \\ 0 & 0 & 0 \end{pmatrix}.$$

The leading-order “KdV” part may now be changed to a diagonal constant-coefficient matrix through an explicit periodic Floquet change in variable $P(\cdot; \Lambda)$ such that

$$P(\cdot; \Lambda) = \begin{pmatrix} 1 & 0 & 0 \\ 0 & \Lambda^{1/3} & 0 \\ 0 & 0 & \Lambda^{2/3} \end{pmatrix} \left(\begin{pmatrix} 1 & 1 & 1 \\ 1 & \omega & \omega^2 \\ 1 & \omega^2 & \omega \end{pmatrix} + O(\Lambda^{-2/3}) \right),$$

with inverse

$$\left(\frac{1}{3} \begin{pmatrix} 1 & 1 & 1 \\ 1 & \omega^2 & \omega \\ 1 & \omega & \omega^2 \end{pmatrix} + O(\Lambda^{-2/3}) \right) \begin{pmatrix} 1 & 0 & 0 \\ 0 & \Lambda^{-1/3} & 0 \\ 0 & 0 & \Lambda^{-2/3} \end{pmatrix}.$$

Indeed, using that $\Lambda = O(\delta^{-3/5})$, replacing W with $Y(\cdot) = P(\cdot; \Lambda)^{-1}W(\cdot)$ leads to the system

$$Y' = \left(D(\Lambda) + \Lambda^{2/3} \delta Q_1 + R(\cdot; \Lambda, \delta) \right) Y \tag{2.31}$$

with

$$D(\Lambda) = \begin{pmatrix} \mu_0(\Lambda) & 0 & 0 \\ 0 & \mu_+(\Lambda) & 0 \\ 0 & 0 & \mu_-(\Lambda) \end{pmatrix} \quad Q_1 = \frac{1}{6\tau_0^{1/4} \nu^{1/2}} \begin{pmatrix} 1 & 1 & 1 \\ \omega^2 & \omega^2 & \omega^2 \\ \omega & \omega & \omega \end{pmatrix},$$

and $R(\cdot; \Lambda, \delta) = O(\delta)$, where the μ_0 and μ_{\pm} are smooth functions of Λ . In particular, we know that when $\Re(\Lambda) \geq 0$, we have

$$\Re(\mu_0(\Lambda)) \geq 0, \quad \Re(\mu_+(\Lambda)) \leq 0, \quad \Re(\mu_-(\Lambda)) \leq 0,$$

and

$$\begin{aligned}
 \mu_0(\Lambda) &= \Lambda^{1/3}(1 + O(\Lambda^{-2/3})) \\
 \mu_+(\Lambda) &= \Lambda^{1/3}(\omega + O(\Lambda^{-2/3})) \quad . \\
 \mu_-(\Lambda) &= \Lambda^{1/3}(\omega^2 + O(\Lambda^{-2/3}))
 \end{aligned}$$

Next, provided that $\Lambda^{1/3}\delta$ is sufficiently small, which is guaranteed for δ sufficiently small since $\Lambda = O(\delta^{-3/5})$, we can use a near-identity change in variables to diagonalize the system (2.31) to order $O(\Lambda^{2/3}\delta)$, resulting in the system

$$Z'(Y) = \left(D_1(\Lambda, \delta) + O(\Lambda^{5/3} \delta^4) + O(\delta) \right) Z(Y),$$

where $D_1(\Lambda, \delta)$ is a constant-coefficient diagonal matrix whose diagonal entries are

$$\begin{aligned} \mu_0(\Lambda, \delta) &= \mu_0(\Lambda) + \frac{1}{6\tau_0^{1/4} \nu^{1/2}} \Lambda^{2/3} \delta, \\ \mu_+(\Lambda, \delta) &= \mu_+(\Lambda) + \frac{\omega^2}{6\tau_0^{1/4} \nu^{1/2}} \Lambda^{2/3} \delta, \\ \mu_-(\Lambda, \delta) &= \mu_+(\Lambda) + \frac{\omega}{6\tau_0^{1/4} \nu^{1/2}} \Lambda^{2/3} \delta. \end{aligned}$$

Hence, when $\Re(\Lambda) \geq 0$, Λ is large, and $\delta |\Lambda|^{1/3}$ is small,

$$\begin{aligned} \Re(\mu_0(\Lambda, \delta)) &\geq C|\Lambda|^{1/3} \\ \Re(\mu_+(\Lambda, \delta)) &\leq -C \left(\Re(\Lambda)|\Lambda|^{-2/3} + \delta |\Lambda|^{2/3} \right) \\ \Re(\mu_-(\Lambda, \delta)) &\leq -C \left(\Re(\Lambda)|\Lambda|^{-2/3} + \delta |\Lambda|^{2/3} \right), \end{aligned}$$

which, when combined with previous exclusions, is sufficient to prove by an energy argument similar to that in Lemma 2.2 above that if $\delta_1 \in (0, \delta_0)$ is sufficiently small and $R > 0$ is sufficiently large, there are no eigenvalues of (2.31) when $0 < \delta < \delta_1$ and

$$\Re(\Lambda) \geq 0, \quad \frac{\Re(\Lambda)}{\delta |\Lambda|^{2/3}} + |\Lambda|^{2/3} \geq R.$$

In particular, it follows that any unstable eigenvalue λ of the original spectral problem (2.12) must satisfy the estimates $|\lambda| = O(\delta^3)$ and $\Re(\lambda) = O(\delta^4)$ as $\delta \rightarrow 0^+$, by $|\Lambda| \leq R^{3/2}$ and $\Re(\Lambda) \leq R\delta|\Lambda|^{2/3} \leq R\delta$, together with the scaling $\lambda = c\delta^3\Lambda$, with $c > 0$ a real constant. □

2.3 Connection to the KdV–KS Index: Proof of Theorem 1.8

It follows from Proposition 2.4 that, in order to complete the proof of Theorem 1.8, it remains to study the eigenvalues of (2.12), supplemented with the appropriate Bloch quasi-periodic boundary conditions, of the form $\lambda = \Lambda\delta^3$ with Λ confined to a compact subset of \mathbb{C} and $0 < \delta \ll 1$. More precisely, using the rescaling (2.25) from the proof of Proposition 2.4 and setting $(\alpha, \beta) = (\delta^{-2}(b + \bar{c}a), a)$, we must study the spectral problem

$$\begin{aligned} \Lambda\beta - \alpha' &= 0 \\ \tilde{\delta}(\beta + \tilde{\tau}\beta + \tilde{c}\beta - \alpha)' &= \tilde{\tau}\beta + \tilde{c}\beta - \alpha - \beta'' + O(\tilde{\delta}^2)f(\alpha, \beta, \beta'), \end{aligned} \tag{2.32}$$

for some smooth function f , supplemented with the boundary condition $(\alpha, \beta, \beta')(X) = e^{i\xi}(\alpha, \beta, \beta')(0)$ for some $\xi \in [-\pi/X, \pi/X)$. Here, $\tilde{\delta} = \frac{1}{2}\tau_0^{-1/4}v^{-1/2}\delta$ is as in Theorem 1.6, and the bounds in $O(\dots)$ are uniform as Λ varies on compact subsets of \mathbb{C} .

To study the above one-parameter family of eigenvalue problems, parametrized by the Bloch frequency ξ , we can define a periodic Evans function, a complex analytic function whose zeros, for each fixed ξ , agree in location and algebraic multiplicity with the eigenvalues of the boundary value problem (2.32). To proceed, we first recall, from the proof of Proposition 2.4, that the spectral problem under scaling (2.25) may be written as the dynamical system [Eq. (2.28)]

$$W'(Y) = \left(H_0(Y; \Lambda) + \Lambda \delta H_1 + \delta H_2(Y) + O(\tilde{\delta}^2) \right) W(Y)$$

for $W = (\beta, \beta', -\alpha + (\sigma_0 - T_0)\beta)^T$, where H_0, H_1, H_2 are given by (2.29) and (2.30). Introducing the new dependent variables $Z = (W_1, W_2, W_3 + \tilde{\delta}((\Lambda - T'_0 - T_1)W_1 + (-1 + T_0 + \sigma_0)W_2))^T$, the differential system becomes

$$Z' = \left(\begin{pmatrix} 0 & 1 & 0 \\ 0 & 0 & 1 \\ -\Lambda - T'_0 & \sigma_0 - T_0 & 0 \end{pmatrix} + \tilde{\delta} \begin{pmatrix} 0 & 0 & 0 \\ 0 & 0 & 0 \\ T''_0 - T'_1 & 2T'_0 - T_1 + \Lambda & T_0 - 1 + \sigma_0 \end{pmatrix} + O(\tilde{\delta}^2) \right) Z. \tag{2.33}$$

Let $\Phi(\cdot, \Lambda, \tilde{\delta})$ denote the associated 3×3 fundamental solution matrix²² associated with (2.33). It is an easy consequence of the regularity with respect to parameters of the flow associated with the differential system (2.33) that $\Phi(\cdot, \Lambda, \tilde{\delta})$ is analytic with respect to $\Lambda \in \mathbb{C}$ and $\tilde{\delta}$. Moreover, for any fixed $(\xi, \tilde{\delta})$, eigenvalues Λ of (2.32) agree in location and algebraic multiplicity with roots of the Evans function

$$E_{SV}(\Lambda, \xi, \tilde{\delta}) := \det \left(\Phi(X, \Lambda, \tilde{\delta}) - e^{i\xi X} \text{Id} \right); \tag{2.34}$$

see Gardner (1993) for details. To complete the proof of Theorem 1.8, we must study the roots of the function $E_{SV}(\cdot, \xi, \tilde{\delta})$ on compact subsets of \mathbb{C} for all $\xi \in [-\pi/X, \pi/X)$ and $0 < \tilde{\delta} \ll 1$.

In order to connect the stability properties of the small-amplitude roll waves described by Theorem 1.6 to those of the associated leading order approximating KdV–KS waves given in Proposition 1.1, we also define an Evans function $E_{KdV-KS}(\Lambda, \xi, \delta)$ for the eigenvalue boundary value problem

$$\Lambda z + ((T_\delta - \sigma_\delta)z)' + z''' + \delta(z'' + z''') = 0 \tag{2.35}$$

²² In particular, this guarantees that $\Phi(0, \Lambda, \tilde{\delta}) = \text{Id}$.

with $(z, z', z'', z''')(X) = e^{i\xi X}(z, z', z'', z''')(0)$. The next result shows that the Evans function $E_{\text{KdV-KS}}$ is faithfully described, to leading order, by the St. Venant Evans function E_{SV} for $0 < \tilde{\delta} \ll 1$.

Proposition 2.5 *Uniformly on compact sets of $\Lambda \in \mathbb{C}$, the Evans function $E_{\text{KdV-KS}}$ can be expanded for $0 < \delta \ll 1$ as*

$$E_{\text{KdV-KS}}(\Lambda, \xi, \tilde{\delta}) = -e^{i\xi X}(1 + O(\tilde{\delta})) \exp\left(\frac{X}{\tilde{\delta}}\right) \times \left(E_{\text{SV}}(\Lambda, \xi, \tilde{\delta}) + O(\tilde{\delta}^2(|\Lambda|^2 + |\xi|^2) + O(\tilde{\delta}^3(|\Lambda| + |\xi|)))\right). \tag{2.36}$$

Proof A similar expansion has been obtained for $E_{\text{KdV-KS}}$ in Johnson et al. (2015, Propositions 3.7 and 4.1). Our proof parallels the arguments there but in a slightly more precise way in order to equate leading-order terms with those of E_{SV} .

The starting point is, as in the proof of Johnson et al. (2015, Propositions 3.7), that the spectral problem (2.35) may be equivalently written, through a series of variables transformations with Jacobian of size $1 + \mathcal{O}(\delta)$, as

$$Z' = \left(\begin{pmatrix} 0 & 1 & 0 \\ 0 & 0 & 1 \\ -\Lambda - T'_0 & \sigma_0 - T_0 & 0 \end{pmatrix} + \delta \begin{pmatrix} 0 & 0 & 0 \\ 0 & 0 & 0 \\ T''_0 - T'_1 & 2T'_0 - T_1 + \Lambda & T_0 - 1 + \sigma_0 \end{pmatrix} \right) Z + O(\delta^2)g_1(Z, w)$$

$$w' = -\frac{1}{\delta}w + O(\delta)g_2(Z, w)$$

for some smooth functions g_1, g_2 ; see Johnson et al. (2015, Propositions 3.7) for details. To obtain the expected homogeneity in (Λ, ξ) we also use that the above system supports a conservation law

$$\Lambda Z_1 = \left[(T_0 - \sigma_0 - 1 + T'_0 + \Lambda + \delta(T_1 + T'_1 + T''_0 - T_0 + \sigma_0 + 1)) Z_1 + (T_0 - \sigma_0 - 1 + \delta(T_1 + 2T'_0 + \Lambda)) Z_2 + (-1 - \delta(T_0 - \sigma_0 - 1)) Z_3 + O(\delta^2)[Z, w] \right]' \tag{2.37}$$

and that the derivative v'_δ of the profile built in Proposition 1.1 provides a special solution of the system when $\Lambda = 0$. Elaborating on this, manipulations on lines and columns of the determinant usually performed to validate at the spectral level averaged (or ‘‘Whitham’’) equations (Serre 2005) then yield that the Evans function $E_{\text{KdV-KS}}(\Lambda, \xi, \tilde{\delta})$ may be written as

$$E_{\text{KdV-KS}}(\Lambda, \xi, \tilde{\delta}) = -e^{i\xi X}(1 + O(\tilde{\delta})) \exp\left(\frac{X}{\tilde{\delta}}\right) \det\left(M(\Lambda, \xi, \tilde{\delta}) + \tilde{M}(\Lambda, \xi, \tilde{\delta})\right), \tag{2.38}$$

where

$$M(\Lambda, \xi, \tilde{\delta}) = \begin{pmatrix} 0 \\ N & 0 \\ 0 & 0 & 1 \end{pmatrix},$$

$$N(\Lambda, \xi, \tilde{\delta}) = \begin{pmatrix} O(|\Lambda| + |\xi|) & O(1) & O(1) \\ O(|\Lambda| + |\xi|) & O(1) & O(1) \\ O(|\Lambda|^2 + |\Lambda||\xi|) & O(|\Lambda| + |\xi|) & O(|\Lambda| + |\xi|) \end{pmatrix},$$

and

$$\tilde{M}(\Lambda, \xi, \tilde{\delta}) = \begin{pmatrix} O(\tilde{\delta}^2(|\Lambda| + |\xi|)) & O(\tilde{\delta}^2) & O(\tilde{\delta}^2) & O(\tilde{\delta}^2) \\ O(\tilde{\delta}^2(|\Lambda| + |\xi|)) & O(\tilde{\delta}^2) & O(\tilde{\delta}^2) & O(\tilde{\delta}^2) \\ O(\tilde{\delta}^2|\Lambda|(|\Lambda| + |\xi|)) & O(\tilde{\delta}^2(|\Lambda| + |\xi|)) & O(\tilde{\delta}^2(|\Lambda| + |\xi|)) & O(\tilde{\delta}^2) \\ O(\tilde{\delta}|\Lambda|) & O(\tilde{\delta}) & O(\tilde{\delta}) & O(\tilde{\delta}) \end{pmatrix}.$$

Again, see Johnson et al. (2015, Propositions 3.7) for details.

Now, returning to the St. Venant spectral problem (2.33), we notice that (2.33) also supports a conservation law in form (2.37) and, furthermore, the space derivative of the traveling wave profile provides a special solution when $\Lambda = 0$. Using calculations completely analogous to those described above for the KdV–KS spectral problem (2.35), it follows that we can write

$$E_{SV}(\Lambda, \xi, \tilde{\delta}) = (1 + O(\delta)) \det \left(N(\Lambda, \xi, \tilde{\delta}) + \tilde{N}(\Lambda, \xi, \tilde{\delta}) \right),$$

where N is exactly the same matrix as above²³ and

$$\tilde{N}(\Lambda, \xi, \tilde{\delta}) = \begin{pmatrix} O(\tilde{\delta}^2(|\Lambda| + |\xi|)) & O(\tilde{\delta}^2) & O(\tilde{\delta}^2) \\ O(\tilde{\delta}^2(|\Lambda| + |\xi|)) & O(\tilde{\delta}^2) & O(\tilde{\delta}^2) \\ O(\tilde{\delta}^2|\Lambda|(|\Lambda| + |\xi|)) & O(\tilde{\delta}^2(|\Lambda| + |\xi|)) & O(\tilde{\delta}^2(|\Lambda| + |\xi|)) \end{pmatrix}.$$

The expansion (2.36) follows conveniently by expanding the determinant $\det(M + \tilde{M})$ in (2.38). □

The proof of Theorem 1.8 now follows immediately from the proof of Proposition 1.3 in Johnson et al. (2015) for the stability of KdV–KS waves in the KdV limit $\delta \rightarrow 0^+$. Indeed, the proof in Johnson et al. (2015) followed by studying the renormalized KdV–KS Evans function

$$\bar{E}_{KdV-KS}(\Lambda, \xi, \tilde{\delta}) = e^{-i\xi X} (1 + O(\tilde{\delta})) \exp\left(-\frac{X}{\tilde{\delta}}\right) E_{KdV-KS}(\Lambda, \xi, \tilde{\delta}),$$

²³ Not just in order of magnitude, but by component-wise identification of the coefficients.

and using the asymptotic description of $\overline{E}_{\text{KdV-KS}}(\Lambda, \xi, \tilde{\delta})$ up to $O(\tilde{\delta}^2(|\Lambda|^2 + |\xi|^2)) + O(\tilde{\delta}^3(|\Lambda| + |\xi|))$. Since Proposition 2.5 implies that

$$E_{\text{SV}}(\Lambda, \xi, \tilde{\delta}) = \overline{E}_{\text{KdV-KS}}(\Lambda, \xi, \tilde{\delta}) + O(\tilde{\delta}^2(|\Lambda|^2 + |\xi|^2)) + O(\tilde{\delta}^3(|\Lambda| + |\xi|))$$

it follows that the same arguments can be applied *without modification* to the Evans function $E_{\text{SV}}(\Lambda, \xi, \tilde{\delta})$. For completeness, we briefly sketch the details.

For $k \in (0, 1)$ such that condition (A) holds, all the nonzero Bloch eigenvalues of the St. Venant linearized operator admit a smooth expansion in $\tilde{\delta}$ for $0 < \tilde{\delta} \ll 1$. In particular, to each pair (ξ, Λ_0) such that $\Lambda_0 \in \mathbb{R}i$ is a nonzero eigenvalue of the KdV Bloch operator $\mathcal{L}_\xi[T_0]$, there is a unique root of $E_{\text{SV}}(\Lambda, \xi, \tilde{\delta})$ for $0 < \tilde{\delta} \ll 1$ that can be expanded in $\tilde{\delta}$ as

$$\Lambda(\tilde{\delta}; \xi, \Lambda_0) = \Lambda_0 + \tilde{\delta}\lambda_1(\xi, \Lambda_0) + \mathcal{O}(\tilde{\delta}^2)$$

where $\lambda_1(\cdot, \cdot)$ is the function already involved in definition (1.9); see (Johnson et al. 2015, Corollary 3.8). As this expansion is uniform in (ξ, Λ_0) when (ξ, Λ_0) varies in a compact set that does not contain $(0, 0)$, it follows that for any neighborhood \mathcal{U} of 0 in the spectral plane, the condition $k \in \mathcal{P}$ provides when $\tilde{\delta}$ is sufficiently small a negative upper bound on the real part of the spectrum in $\mathbb{C} \setminus \{0\}$; see (Johnson et al. 2015, Corollary 3.10) for details.

On the other hand, when $\xi = 0$ the origin is an eigenvalue of the KdV Bloch operator $\mathcal{L}_0[T_0]$ of algebraic multiplicity three and geometric multiplicity two. To unfold the degeneracy for $0 < \tilde{\delta} \ll 1$, we directly apply the arguments in Johnson et al. (2015, Section 4). By studying the three asymptotic regions $0 < \tilde{\delta} \lesssim |\xi|$ (Johnson et al. 2015, Lemma 4.4), $\tilde{\delta} \sim |\xi|$ (Johnson et al. 2015, Lemma 4.6), and $0 \leq |\xi| \lesssim \tilde{\delta}$ (Johnson et al. 2015, Lemma 4.7) separately, it follows that the condition $k \in \mathcal{P}$ implies that a set of “subcharacteristic conditions” hold which, in turn, are shown to imply that all the roots of $E_{\text{SV}}(\Lambda, \xi, \tilde{\delta})$, with $0 < |(\Lambda, \xi)| \ll 1$ and $0 < \tilde{\delta} \ll 1$ all have negative real parts. More precisely, under these conditions it is shown that the (diffusive) spectral stability conditions (D1)-(D3) and the nondegeneracy hypothesis (H1) are satisfied when δ is sufficiently small. This completes the proof of Theorem 1.8.

3 Stability of Large-Amplitude Roll Waves

In the previous section, we rigorously justified the KdV–KS equation (1.2) as a correct description for the weak hydrodynamic instability in inclined thin-film flow. In particular, in the weakly nonlinear regime $F \rightarrow 2^+$ we saw that the KdV–KS equation accurately predicts the stability of the associated small-amplitude roll wave solutions of the shallow water equations (1.1). We now complement this study by continuing our analysis into the large-amplitude regime, far from the weakly unstable limit $F \rightarrow 2^+$, performing a systematic stability analysis for roll waves with Froude number on the entire range of existence $F > 2$, including the distinguished limit $F \rightarrow \infty$. We begin by considering the limit $F \rightarrow \infty$, identifying a one-parameter family of limiting systems approachable by various scaling choices in the shallow water equations. We will

then numerically study the influence of intermediate Froude numbers $2 < F < \infty$ on the range of stability of periodic waves.

3.1 Scaling as $F \rightarrow \infty$

In our $F \rightarrow \infty$ studies, we investigate the stability of periodic traveling wave solutions of some asymptotic systems obtained from (1.11) via scaling arguments. To begin, performing the change in variables $(x, t) \mapsto (\tilde{x}, \tilde{t}) = (k(x - ct), t)$ in (1.11) and erasing tildes yields the equivalent system

$$\partial_t \tau - k c \partial_x \tau - k \partial_x u = 0, \quad \partial_t u - k c \partial_x u + k \partial_x \left(\frac{\tau^{-2}}{2F^2} \right) = 1 - \tau u^2 + \nu k^2 \partial_x (\tau^{-2} \partial_x u).$$

To prepare for sending $F \rightarrow \infty$ above, we first scale the dependent quantities independently via $\tau = F^{\alpha_\tau} a, u = F^{\alpha_u} b, k = F^{\alpha_k} k_0$ and $c = F^{\alpha_c} c_0$. This transforms the above shallow water system to

$$\begin{aligned} F^{\alpha_\tau} \partial_t a - k_0 c_0 F^{\alpha_\tau + \alpha_k + \alpha_c} \partial_x a - k_0 F^{\alpha_u + \alpha_k} \partial_x b &= 0, \\ F^{\alpha_u} \partial_t b - k_0 c_0 F^{\alpha_u + \alpha_k + \alpha_c} \partial_x b + k_0 F^{\alpha_k - 2 - 2\alpha_\tau} \partial_x \left(\frac{a^{-2}}{2} \right) \\ &= 1 - F^{\alpha_\tau + 2\alpha_u} a b^2 + \nu k_0^2 F^{\alpha_u + 2\alpha_k - 2\alpha_\tau} \partial_x (a^{-2} \partial_x b). \end{aligned} \tag{3.1}$$

Seeking stationary 1-periodic solutions of (3.2) leads to an ODE system

$$\begin{aligned} -c_0 F^{\alpha_\tau + \alpha_c} a' - F^{\alpha_u} b' &= 0, \\ k_0 c_0^2 F^{\alpha_\tau + \alpha_k + 2\alpha_c} a' + k_0 F^{\alpha_k - 2 - 2\alpha_\tau} \left(\frac{a^{-2}}{2} \right)' \\ &= 1 - F^{\alpha_\tau + 2\alpha_u} a b^2 - \nu k_0^2 c_0 F^{\alpha_c + 2\alpha_k - \alpha_\tau} (a^{-2} a')', \end{aligned}$$

governing the traveling wave solutions of (1.11) in the appropriate moving frame. Note that, by its expression as $\int_0^X \bar{\tau}(x) dx$, the period in the physical Eulerian variables scales as $F^{\alpha_\tau - \alpha_k}$ under the above transformations. To balance the terms of the “elliptic-constant” right-hand side above, we choose now to impose $\alpha_\tau + 2\alpha_u = 0$ and $\alpha_c + 2\alpha_k - \alpha_\tau = 0$. This effectively leaves two free parameters, say $\alpha = \alpha_\tau$ and $\beta = \alpha_k$, with $\alpha_u = -\alpha/2$ and $\alpha_c = \alpha - 2\beta$. Under this choice, the above profile system now reads

$$\begin{aligned} -c_0 F^{\frac{5}{2}\alpha - 2\beta} a' - b' &= 0, \\ k_0 c_0^2 F^{3\alpha - 3\beta} a' + k_0 F^{-2 - 2\alpha + \beta} \left(\frac{a^{-2}}{2} \right)' &= 1 - a b^2 - \nu k_0^2 c_0 (a^{-2} a')'. \end{aligned} \tag{3.2}$$

The first equation may be integrated to yield $b = q_0 - F^{\frac{5}{2}\alpha - 2\beta} c_0 a$ where q_0 is a constant of integration. Substituting this into the second equation above, the rescaled profile system is reduced to the scalar equation

$$\begin{aligned}
 &k_0 c_0^2 F^{3\alpha-3\beta} a' + k_0 F^{-2-2\alpha+\beta} \left(\frac{a^{-2}}{2}\right)' \\
 &= 1 - a (q_0 - F^{\frac{5}{2}\alpha-2\beta} c_0 a)^2 - \nu k_0^2 c_0 (a^{-2} a')'. \tag{3.3}
 \end{aligned}$$

In order to ensure that the “elliptic part” $(a^{-2} a')'$ is not asymptotically negligible as $F \rightarrow \infty$, we restrict ourselves to the parameter regimes where $\frac{5}{4}\alpha \leq \beta \leq 2\alpha + 2$, $\beta \geq \alpha$. In particular, this latter choice requires $\alpha \geq -2$. With the above choices, the full rescaled shallow water equations (3.1) now read as

$$\begin{aligned}
 &F^\alpha \partial_t a - k_0 c_0 F^{2\alpha-\beta} \partial_x a - k_0 F^{\beta-\alpha/2} \partial_x b = 0, \\
 &F^{-\alpha/2} \partial_t b - k_0 c_0 F^{\alpha/2-\beta} \partial_x b + k_0 F^{-2-2\alpha+\beta} \partial_x \left(\frac{a^{-2}}{2}\right) \\
 &= 1 - a b^2 + \nu k_0^2 F^{2\beta-5\alpha/2} \partial_x (a^{-2} \partial_x b), \tag{3.4}
 \end{aligned}$$

which is a two-parameter family of systems, parametrized by $\alpha \geq -2$ and $\frac{5}{4}\alpha \leq \beta \leq 2\alpha + 2$.

Finally, when sending $F \rightarrow \infty$ in (3.4), we balance the first-order terms of the reduced profile Eq. (3.2) by requiring $3\alpha - 3\beta = -2 - 2\alpha + \beta$, i.e., that $\beta = \frac{1}{2} + 5\alpha/4$, effectively reducing our scalings to a one-parameter family indexed by $\alpha \geq -2$. In particular, under this choice the full one-parameter family of rescaled shallow water systems reads as

$$\begin{aligned}
 &F^\alpha \partial_t a - k_0 c_0 F^{3\alpha/4-1/2} \partial_x a - k_0 F^{1/2+3\alpha/4} \partial_x b = 0, \\
 &F^{-\alpha/2} \partial_t b - k_0 c_0 F^{-3\alpha/4-1/2} \partial_x b + k_0 F^{-3/2-3\alpha/4} \partial_x \left(\frac{a^{-2}}{2}\right) \\
 &= 1 - a b^2 + \nu k_0^2 F \partial_x (a^{-2} \partial_x b), \tag{3.5}
 \end{aligned}$$

and the associated rescaled profile system is equivalent to $b = q_0 - F^{-1} c_0 a$, q_0 constant and

$$F^{-3/2-3\alpha/4} \left(k_0 c_0^2 a' + k_0 \left(\frac{a^{-2}}{2}\right)' \right) = 1 - a (q_0 - F^{-1} c_0 a)^2 - \nu k_0^2 c_0 (a^{-2} a')'. \tag{3.6}$$

By the discussion above Eq. (3.2), the Eulerian period of the periodic profiles satisfying (3.6) scale as $F^{-\alpha/4-1/2}$. Notice that (3.6) is equivalent to the profile Eq. (1.16) claimed in the introduction.

As mentioned in the introduction, taking $F \rightarrow \infty$ in (3.6) produces different limiting profile equations depending on whether $\alpha = -2$ or if $\alpha > -2$. Next, we discuss both limiting profile equations and the spectral problems governing the stability of the profiles.

3.1.1 Case $\alpha = -2$

Taking $\alpha = -2$ in the above discussion corresponds to rescaling (3.2) via

$$\tau = F^{-2} a, \quad u = F b, \quad k = k_0 F^{-2}, \quad c = c_0 F^2$$

Note that in this case, the Eulerian period of the profile is held constant as $F \rightarrow \infty$. With this choice, the profile Eq. (3.6) reads as

$$\left(k_0 c_0^2 a' + k_0 \left(\frac{a^{-2}}{2} \right)' \right) = 1 - a (q_0 - F^{-1} c_0 a)^2 - \nu k_0^2 c_0 (a^{-2} a')', \quad (3.7)$$

and $b = q_0 - F^{-1} c_0 a$, q_0 constant. Linearizing (3.5) with $\alpha = -2$ about such an X_0 -periodic profile (\bar{a}, \bar{b}) yields the associated rescaled spectral problem

$$\begin{aligned} F^{-2} \lambda a - k_0 c_0 F^{-2} a' - k_0 F^{-1} b' &= 0 \\ F \lambda b - k_0 c_0 F b' - 3k_0 \left(\bar{a}^{-3} a \right)' & \\ &= -a \bar{b}^2 - 2\bar{a} \bar{b} + \nu k_0^2 F (-2\bar{a} \bar{b}' a + \bar{a}^{-2} b')' \end{aligned} \quad (3.8)$$

to be considered for (a, b) satisfying suitable Bloch boundary conditions. Sending $F \rightarrow \infty$ above, it follows that the profile equation is a regular perturbation of the limiting system

$$\left(k_0 c_0^2 a' + k_0 \left(\frac{a^{-2}}{2} \right)' \right) = 1 - a q_0^2 - \nu k_0^2 c_0 (a^{-2} a')', \quad (3.9)$$

while the above spectral problem is a regular perturbation of

$$\begin{aligned} \lambda a - k_0 c_0 a' - k_0 \check{b}' &= 0, \\ \lambda \check{b} - k_0 c_0 \check{b}' - k_0 (\bar{a}_\infty^{-3} a') &= -a q_0^2 + k_0^2 \nu (\bar{a}_\infty^{-2} \check{b}' + 2c_0 \bar{a}_\infty^{-3} \bar{a}'_\infty a'), \end{aligned} \quad (3.10)$$

where $(\bar{a}_\infty, \bar{b}_\infty)$, necessarily solutions of (3.9), denote the limiting profiles of (\bar{a}, \bar{b}) as $F \rightarrow \infty$, and $\check{b} = F \bar{b}$. The limiting profile Eq. (3.9) is numerically seen to admit periodic orbits existing in a two-parameter family, parametrized by the period X_0 and the discharge rate q_0 . The stability of these profiles may then be investigated by means of the spectral problem (3.10): This is discussed in Sect. 3.2 below.

3.1.2 Case $\alpha > -2$

When $\alpha > -2$, it is readily seen that the profile Eq. (3.6) is a regular perturbation of the ODE

$$0 = 1 - q_0^2 a - \nu k_0^2 c_0 (a^{-2} a')', \quad (3.11)$$

which is Hamiltonian in the unknown $1/a$. Indeed, denoting $h := q_0^{-2} a^{-1}$ and rescaling space via $x = s/\sqrt{\nu k_0 c_0 q_0^2}$, the above ODE reads as

$$0 = 1 - h^{-1} + h'', \quad (3.12)$$

where $'$ denotes differentiation with respect to s . This is clearly seen to be Hamiltonian and, upon integrating, is equivalent to

$$\mu = h - \ln(h) + \frac{1}{2}(h')^2, \tag{3.13}$$

where μ is a constant of integration. Elementary phase plane analysis shows that (3.12) admits a one-parameter family of periodic orbits parametrized by the constant μ . Indeed, for each $\mu > 1$ Eq. (3.13) admits a unique (up to spatial translations) periodic solution h_μ , whose period we denote X_μ . Returning to the original variables then, we see that, choosing k_0 to satisfy $\nu k_0^2 c_0 q_0^2 X_\mu^2 = 1$, the profile Eq. (3.11) admits a three-parameter family of periodic orbits with unit period parametrized by μ, c_0 , and q_0 . Clearly, a necessary condition for such a 1-periodic orbit of (3.11) to persist as a solution of (3.6) for $F \gg 1$ is that the (α -independent) orthogonality condition

$$0 = \int_0^1 \left(\frac{1}{a}\right)' \times \left(k_0 c_0^2 a' + k_0 \left(\frac{a^{-2}}{2}\right)'\right) dx$$

be satisfied. Note that this yields a selection principle for the wavespeed via

$$c_0^2 = -\frac{1}{2} \frac{\int_0^1 (a^{-1})' \times (a^{-2})' dx}{\int_0^1 (a^{-1})' \times a' dx} = \frac{\int_0^1 a^{-5} \times (a')^2 dx}{\int_0^1 a^{-2} \times (a')^2 dx} = \frac{\int_0^1 a^{-1} \times ((a^{-1})')^2 dx}{\int_0^1 ((a^{-1})')^2 dx}.$$

Generically zeros of the above selection function are simple, and in this case, as in Sect. 2.1, it follows from elementary bifurcation analysis that the Hamiltonian profile Eq. (3.11) admits a two-parameter family of periodic orbits, parametrized by μ and q_0 that persist as periodic orbits of (3.6) for $F \gg 1$. In particular, note that for $\alpha > -2$, the specific value of α does not enter into either the limiting profile equation nor the selection principle.

Finally, taking $F \rightarrow \infty$ in (3.5), we see that the spectral stability of the 1-periodic traveling wave solutions (\bar{a}, q_0) of (3.5) constructed above is determined via the spectral problem

$$\begin{aligned} \Lambda a - k_0 \check{b}' &= 0, \\ 0 &= -a q_0^2 + \nu k_0^2 (2c_0 \bar{a}^{-3} \bar{a}' a + \bar{a}^{-2} \check{b}') \end{aligned}$$

where here (a, b) denotes perturbation, $\Lambda = F^{1/2} \lambda$, and $\check{b} = Fb$. The former system may also be written as

$$\begin{aligned} \Lambda a - k_0 \check{b}' &= 0, \\ 0 &= -a q_0^2 + \Lambda \nu k_0^2 c_0 (\bar{a}^{-2} a)' - \nu k_0^2 c_0 (\bar{a}^{-2} a)'' . \end{aligned}$$

Therefore, in this case we investigate the spectral problem

$$0 = h_\mu^{-2} \check{a} - \check{\Lambda} \check{a}' + \check{a}'' \tag{3.14}$$

for $\check{\Lambda} = (X_\mu)^{-1} \Lambda$ and $\check{a}(\cdot) = q_0^{-2} (\bar{a}^{-2} a) ((X_\mu)^{-1} \cdot)$ where h_μ and X_μ are associated with \bar{a} as described above. As above, we point out that for $\alpha > -2$, the spectral problem governing the spectral stability of the limiting $F = \infty$ profiles is independent of the value of α . As a consequence, spectral instability of the limiting periodic traveling wave solutions constructed above implies spectral instability of the (α -dependent) large- F profiles of the system (3.5) for any $\alpha > -2$.

3.2 Numerical Investigation as $F \rightarrow \infty$

With the above preparations, we report our numerical results concerning the existence and spectral stability of the profiles introduced in the previous section for the limiting systems in the $F \rightarrow \infty$ limit.

In the case $\alpha > -2$, elementary phase plane analysis indicates that for each $h_- \in (0, 1)$, there exists a unique (up to translations) periodic solution with $h(0) = h_-$. These profiles were numerically computed for 1000 equally spaced values of h_- in $[0.05, 0.95]$ using the MATLAB functions `bvp5c` and `bvp6c`, with absolute and relative error tolerances both set to 10^{-8} in the `bvp` solver. To this end, we utilized a bisection method to approximate the value $h_+ > h_-$ such that $h_+ - \log(h_+) = \mu$ and then approximated the corresponding period by computing $\sqrt{2} \int_{h_- - 10^{-13}}^{h_+ + 10^{-13}} (\mu - x + \log(x))^{-1/2} dx$.

As a first attempt to study the $L^2(\mathbb{R})$ -spectrum associated with (3.14), we utilized a Galerkin truncation method known as Hill’s method. For each $\xi \in [-\pi/X_\mu, \pi/X_\mu)$, Hill’s method proceeds by expanding both the unknown \check{a} as well as the background wave h_μ in the associated Bloch eigenvalue problem as a Fourier series and then truncating all expansions at some finite order to reduce the problem to finding, for each $\xi \in [-\pi/X_\mu, \pi/X_\mu)$ the eigenvalues of a finite-dimensional matrix; see Appendix 1 for more details. For each of the profiles numerically constructed above, unstable spectra were present; see Fig. 6d for an example. In addition, we verified the existence of unstable spectra of (3.14) by numerically computing winding number for the associated periodic Evans function on a closed contour in the open right half complex plane verifying that the winding number is indeed greater than zero for some Bloch frequency ξ . Employing Theorem 1.11, his study suggests that all periodic traveling wave solutions of (3.2) are *spectrally unstable* for $F \gg 1$. Note, in our study of spectral problem (3.14) via Hill’s method, we used 41 Fourier modes and 1000 Floquet parameters.

Concerning the case $\alpha = -2$, the profile Eq. (3.9) was solved by using the MATLAB functions `bvp5c` and `bvp6c`, where we treated c_0 as a free parameter in the `bvp` solver and used numerical continuation to solve the profile as k_0 was varied. Our numerical investigation of the associated spectral problem (3.10) covered $q_0 \in [1.6, 2.2]$ for $\nu = 2$ and $q_0 \in [1.2, 2.7] \cup [0.3, 0.45]$ for $\nu = 0.1$ with step size 0.1 in q_0 and varying,

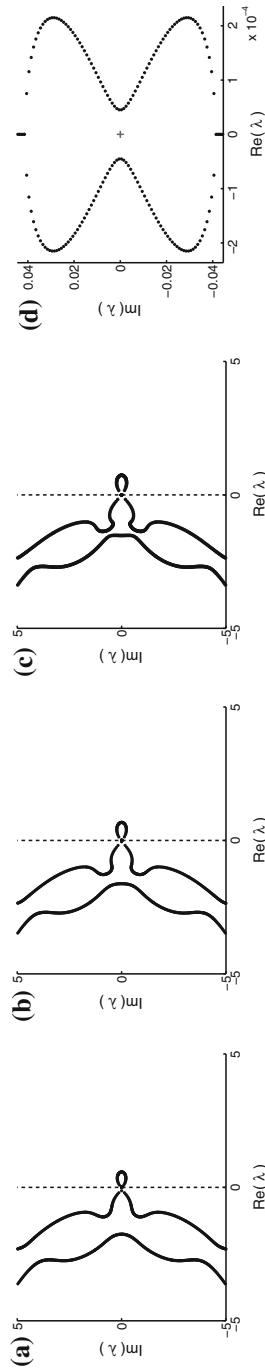


Fig. 6 In **a**, **b**, we plot, respectively, for $F = 38$ and $F = 100$, the spectrum corresponding to eigenvalue problem (3.8) with $\alpha = -2$, and in **c** the spectrum corresponding to the limiting spectral problem (3.10). Here $\nu = 0.1$, $q_0 = 0.4$, $X = 437.6$, $c = 84.0$, and **a** $X_0 = 0.303$, **b** $X_0 = 0.044$. In **d**, we plot a numerical sampling (via Hill's method) of the unstable spectrum corresponding to the spectral problem 3.14, corresponding to the case $\alpha > -2$, for a representative periodic stationary solution of (3.12)

but smaller, steps in k_0 in the region where we could solve profiles numerically. Again, we found that all these waves have unstable spectra; see Fig. 6c for an example. In Fig. 6, we also plot the spectrum as determined using the “ $\alpha = -2$ ” scaling given in Sect. 3.1.1 and show that in this scaling the spectrum is unstable for large F as well as in the $F = \infty$ eigenvalue problem (3.10). Instability in the $F = \infty$ case was thus confirmed by multiple numerical checks, providing strong evidence of instability.

In conclusion, our numerical calculations strongly indicate that for F , sufficiently large, spectrally stable periodic traveling wave solutions of the St. Venant system (1.11) do not exist. This justifies Numerical Observation 1 described in 1.2.2.

3.3 Numerical Investigation for Intermediate F

In order to better understand the stability of periodic traveling wave solutions of (1.11) away from the distinguished limits $F \rightarrow 2^+$ and $F \rightarrow \infty$, we also carried out a numerical investigation for some “intermediate” Froude numbers.

To solve the profile equation numerically, we expand (2.2) to obtain the profile ODE equation,

$$\tau'' = \left(\frac{-\tau^2}{c\nu} \right) \left(c^2\tau' - \frac{\tau'}{F^2\tau^3} - 1 + \tau(q - c\tau)^2 - 2c\nu(\tau')^2/\tau^3 \right), \tag{3.15}$$

and then proceed the same way as described in the studies of the limiting $F \rightarrow \infty$ systems described above, this time using a relative error tolerance between 10^{-6} and 10^{-10} in the bvp solver. Checking the slope condition (1.12) across numerically determined profiles, we found that it is satisfied for profiles with $F \lesssim 3.5$ but violated for those with larger F . As discussed in the introduction, however, the slope condition is no longer required for the nonlinear analysis thanks to the recent work [Rodrigues and Zumbrun \(2016\)](#).

To study the spectrum, we worked with the original (unrescaled) eigenvalue system (2.12), associating parameters with those under the rescaling (1.15). We found that the results for Hill’s method were more accurate using these original coordinates as opposed to the rescaled coordinates (1.15), even for large F . For $q_0 = 0.4$, k_0 ranging in the parameter space where profiles could be solved, and for F ranging from 10 to either 20 or 30 by 1, we examined, via Hill’s method and the Taylor expansion of the Evans function, the cases $\alpha = -0.7, -1, -1.4, -1.5, -1.6, -1.7, -1.8, -1.9, -2$. We used 201–3000 Fourier modes and 21–31 Floquet parameters in Hill’s method and 33–201 Chebyshev nodes for the integral in the Taylor expansion. For each value of α , we found that a lower stability boundary curve and an upper high-frequency instability curve meet at some value $F^*(\alpha)$ after which no waves are stable. See Figures 4. In addition, we find that the upper and lower stability boundaries appear to have a linear relationship of the form $\log(X/\nu) = b_1 \log(F) + b_2 \log(q) + b_3$; see Fig. 7. We used a combination of Hill’s method and Evans function computations to determine stability or instability. However, as the period X increases, a small loop of spectra parameterized by the whole interval of Floquet parameters $\xi \in [-\pi/X, \pi/X)$ shrinks until eventually neither the Evans function nor Hill’s method can definitively

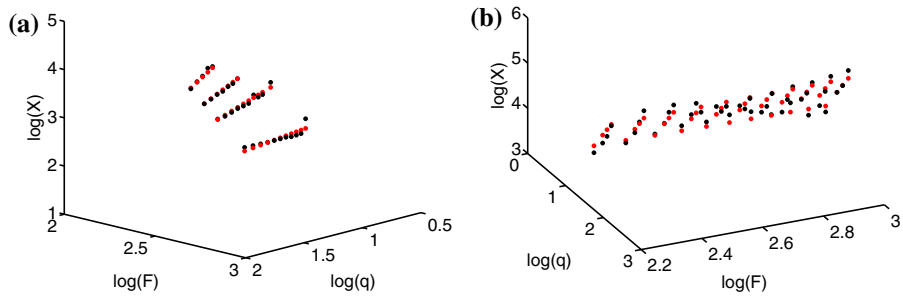


Fig. 7 In **a**, **b**, *black dots* mark the computed boundary and *pale dots* (red in color plates) mark the best least curve fit. We hold $\nu = 0.1$ constant. **a** Lower stability boundary. We have $\log(X) \approx b_1 \log(F) + b_2 \log(q) + b_3$ where $b_1 = -0.692$, $b_2 = 3.46$, and $b_3 = 0.3$. Here $\alpha = -1.6, -1.8, -1.9, -2$. The maximum error is 0.200, and the maximum relative error is 0.056. The average relative error is 0.012, and the average absolute error is 0.041. **b** High-frequency stability boundary. We have $\log(X) \approx b_1 \log(F) + b_2 \log(q) + b_3$ where $b_1 = -0.791$, $b_2 = 1.73$, and $b_3 = 3.92$. Here $\alpha = -1.6, -1.8, -1.9, -2$. The maximum error is 0.228, and the maximum relative error is 0.052. The average relative error is 0.024, and the average absolute error is 0.103

determine small frequency stability at which point we rely on Hill's method for the overall behavior of the spectrum; in this region, analytic verification of the stability regions as $F \rightarrow \infty$ would be beneficial. However, for the lower intermediate F region where the period is smaller, the stability picture appears clear. In particular, for $\alpha = -2$ our numerical study, though not a numerical proof, strongly suggests the stability region shown in Fig. 4a. As F continues to increase, it becomes easier again to compute the spectrum with Hill's method as the spectrum approaches that of the limiting system given in Eq. (3.9); see Fig. 6a–c for an illustration. For $F = 38$, we examined the full set of periods corresponding to those examined in Fig. 4, and found no stability region, confirming that by this point, the upper and lower stability boundaries have met.

Acknowledgements The numerical stability computations in this paper were carried out using the STABLAB package developed by Jeffrey Humpherys and the first and last authors; see [BHZ] for documentation. We gratefully acknowledge his contribution. We thank also Indiana University Information Technology Service for the use of the Quarry computer with which some of our computations were carried out. Authors in various combinations also acknowledge the kind hospitality of ÉNS Paris, Indiana University, INSA Toulouse and Université Lyon 1 that hosted them during parts of the preparation of the present paper. Finally, we thank Sergey Gavriluk for a helpful exchange regarding the experimental literature. Finally, we thank the two anonymous referees for their careful review and helpful comments improving the exposition.

Appendix 1: Notation for High-Frequency Bounds

The proof of Lemma 2.2 in Sect. 2.2.1 relied heavily on computations previously carried out in detail in Section 4.1 of Barker et al. (2011). There the authors were concerned with the stability analysis of traveling *solitary* wave solutions of the viscous St. Venant equation (1.11), i.e., those traveling wave solutions that decay exponentially fast to zero as $x - \bar{c}t \rightarrow \pm\infty$. By a straightforward adaptation of this analysis to the periodic

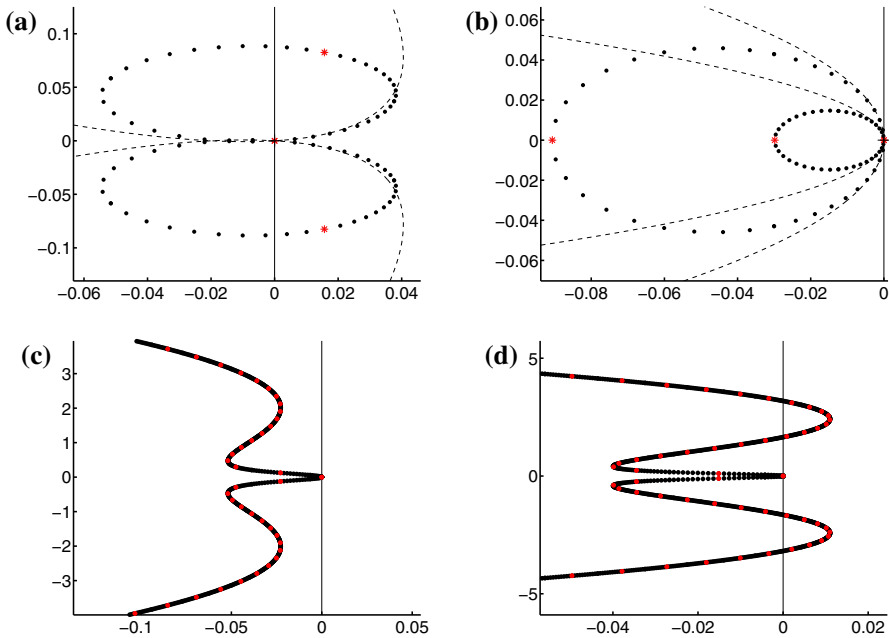


Fig. 8 Plot of spectra for the intermediate eigenvalue problem. We plot the approximations returned by Hill’s method with *black dots* and those obtained by Taylor expanding the Evans function with *light dashes*. We plot the spectra corresponding to Floquet parameter zero with a *pale star (red in color plates)*. The *solid line* indicates the imaginary axis. In all cases, $\alpha = -2$, $\nu = 0.1$, and $q_0 = 0.4$. Other parameters are **a** $F = 6$, $X = 7.83$, **b** $F = 6$, $X = 8.78$, **c** $F = 10$, $X = 76.9$, **d** $F = 10$, $X = 90.9$

case,²⁴ it follows that, for each $k \in \mathcal{P}$, there exists an X_δ -periodic change in variables $W(\cdot) = P(\cdot; \lambda, \delta)Z(\cdot)$ that transforms the spectral problem (2.13) into an equivalent system of the form $W'(x) = (D(x, \lambda) + \Theta(x, \lambda))W(x)$, supplemented with the boundary conditions $W(X_\delta) = e^{i\xi}W(0)$ for some $\xi \in [-\pi/X_\delta, \pi/X_\delta)$, where the 3×3 matrix-valued D is defined via $D(\cdot, \lambda) = \text{diag} \left(\frac{\lambda}{c} + \theta_0 + \frac{\theta_1}{\lambda}, \bar{\tau}\sqrt{\frac{\lambda}{\nu}}, -\bar{\tau}\sqrt{\frac{\lambda}{\nu}} \right)$, where $\theta_0 = \frac{\bar{\alpha}\bar{\tau}^2}{c\nu}$ and $\theta_1 = -\frac{\bar{\tau}^2(q - c\bar{\tau})^2}{\nu} - \frac{c\bar{\alpha}}{\sqrt{\nu}}\frac{\bar{\tau}^3}{\nu^{3/2}}$ with $\bar{\alpha} := \bar{\tau}^{-3}(F^{-2} + 2c\nu\bar{\tau}')$. Moreover, the 3×3 matrix $\Theta(x, \lambda)$ has the block structure $\Theta = \begin{pmatrix} \Theta_{++} & \Theta_{+-} \\ \Theta_{-+} & \Theta_{--} \end{pmatrix}$, where Θ_{++} is a 2×2 matrix. The individual blocks of the matrix Θ can be expanded as cubic polynomials in $\lambda^{-1/2}$ with matrix-valued coefficients. More precisely, they expand as

$$\begin{cases} \Theta_{++}(\cdot, \lambda) = \Theta_{++}^0 + \lambda^{-1/2}\Theta_{++}^1 + \lambda^{-1}\Theta_{++}^2 + \lambda^{-3/2}\Theta_{++}^3 \\ \Theta_{+-}(\cdot, \lambda) = \Theta_{+-}^0 + \lambda^{-1/2}\Theta_{+-}^1 + \lambda^{-1}\Theta_{+-}^2 + \lambda^{-3/2}\Theta_{+-}^3 \\ \Theta_{-+}(\cdot, \lambda) = \Theta_{-+}^0 + \lambda^{-1/2}\Theta_{-+}^1 + \lambda^{-1}\Theta_{-+}^2 + \lambda^{-3/2}\Theta_{-+}^3 \\ \Theta_{--}(\cdot, \lambda) = \Theta_{--}^0 + \lambda^{-1/2}\Theta_{--}^1 + \lambda^{-1}\Theta_{--}^2 + \lambda^{-3/2}\Theta_{--}^3 \end{cases}$$

²⁴ Namely, using formally identical coordinate changes depending on the profile and its derivatives.

with

$$\begin{aligned} \Theta_{++}^0 &= \begin{pmatrix} 0 & -\frac{\bar{\tau}^2}{v} \\ -\frac{\bar{\alpha}\bar{\tau}^2}{2v} & \frac{\bar{\tau}'}{\bar{\tau}} - \frac{\bar{c}\bar{\tau}^2}{2v} \end{pmatrix}, & \Theta_{+-}^1 &= \begin{pmatrix} -\frac{2\bar{\tau}'}{\sqrt{v}} + \frac{\bar{\tau}^3}{v^{3/2}} \left(\frac{\bar{\alpha}}{\bar{c}} + \bar{c}\right) \\ -\frac{\bar{\tau}^2(q-\bar{c}\bar{\tau})}{\sqrt{v}} - \frac{\bar{\alpha}}{2} \frac{\bar{\tau}^3}{v^{3/2}} \end{pmatrix}, \\ \Theta_{++}^1 &= \begin{pmatrix} 0 & -\frac{2\bar{\tau}'}{\sqrt{v}} + \frac{\bar{\tau}^3}{v^{3/2}} \left(\frac{\bar{\alpha}}{\bar{c}} + \bar{c}\right) \\ \frac{\bar{\tau}}{2\sqrt{v}} \left((q-\bar{c}\bar{\tau})^2 + c\bar{\alpha} \frac{\bar{\tau}^2}{v} \right) & \frac{\bar{\tau}^2(q-\bar{c}\bar{\tau})}{\sqrt{v}} + \frac{\bar{\alpha}}{2} \frac{\bar{\tau}^3}{v^{3/2}} \end{pmatrix}, \\ \Theta_{++}^2 &= \begin{pmatrix} 0 & -\frac{2\bar{\tau}^3(q-\bar{c}\bar{\tau})}{v} \\ 0 & \frac{\bar{\tau}^2(q-\bar{c}\bar{\tau})^2}{2v} + \frac{\bar{c}\bar{\alpha}}{2\sqrt{v}} \frac{\bar{\tau}^3}{v^{3/2}} \end{pmatrix}, \\ \Theta_{++}^3 &= \begin{pmatrix} 0 & -\frac{\bar{\tau}^3(q-\bar{c}\bar{\tau})^2}{v^{3/2}} - \frac{\bar{c}\bar{\alpha}}{\sqrt{v}} \frac{\bar{\tau}^4}{v^2} \\ 0 & 0 \end{pmatrix}, & \Theta_{+-}^0 &= \begin{pmatrix} \frac{\bar{\tau}^2}{v} \\ \frac{\bar{\tau}'}{2\bar{\tau}} - \frac{\bar{c}}{2} \frac{\bar{\tau}^2}{v} \end{pmatrix}, \\ \Theta_{+-}^2 &= \begin{pmatrix} \frac{2\bar{\tau}^3(q-\bar{c}\bar{\tau})}{v} \\ \frac{\bar{\tau}^2(q-\bar{c}\bar{\tau})^2}{2v} + \frac{\bar{c}\bar{\alpha}}{2\sqrt{v}} \frac{\bar{\tau}^3}{v^{3/2}} \end{pmatrix}, & \Theta_{+-}^3 &= \begin{pmatrix} -\frac{\bar{\tau}^3(q-\bar{c}\bar{\tau})^2}{v^{3/2}} - \frac{\bar{c}\bar{\alpha}}{\sqrt{v}} \frac{\bar{\tau}^4}{v^2} \\ 0 \end{pmatrix}, \\ \Theta_{-+}^0 &= \begin{pmatrix} \frac{\bar{\alpha}\bar{\tau}^2}{2v} & \frac{\bar{\tau}'}{\bar{\tau}} - \frac{\bar{c}\bar{\tau}^2}{2v} \end{pmatrix}, & \Theta_{-+}^2 &= \begin{pmatrix} 0 & \frac{\bar{\tau}^2(q-\bar{c}\bar{\tau})^2}{2v} + \frac{\bar{c}\bar{\alpha}}{2\sqrt{v}} \frac{\bar{\tau}^3}{v^{3/2}} \end{pmatrix}, \\ \Theta_{-+}^1 &= \begin{pmatrix} \frac{\bar{\tau}}{2\sqrt{v}} \left((q-\bar{c}\bar{\tau})^2 + \bar{c}\bar{\alpha} \frac{\bar{\tau}^2}{v} \right) & \frac{\bar{\tau}^2(q-\bar{c}\bar{\tau})}{\sqrt{v}} + \frac{\bar{\alpha}}{2} \frac{\bar{\tau}^3}{v^{3/2}} \end{pmatrix}, & \Theta_{--}^0 &= \begin{pmatrix} \frac{\bar{\tau}'}{\bar{\tau}} - \frac{\bar{c}\bar{\tau}^2}{2v} \end{pmatrix}, \\ \Theta_{--}^1 &= \begin{pmatrix} -\frac{\bar{\tau}^2(q-\bar{c}\bar{\tau})^2}{2v} + \frac{\bar{c}\bar{\alpha}}{2\sqrt{v}} \frac{\bar{\tau}^3}{v^{3/2}} \end{pmatrix}, & \Theta_{--}^2 &= \begin{pmatrix} \frac{\bar{\tau}^2(q-\bar{c}\bar{\tau})^2}{2v} + \frac{\bar{c}\bar{\alpha}}{2\sqrt{v}} \frac{\bar{\tau}^3}{v^{3/2}} \end{pmatrix}. \end{aligned}$$

From this, the matrices $N_{D,D}$, $N_{H,D}$, $N_{D,H}$ in (2.17) are obtained through the identification

$$\begin{pmatrix} \Theta_{++} & \Theta_{+-} \\ \Theta_{-+} & \Theta_{--} \end{pmatrix} = \begin{pmatrix} 0 & N_{H,D} \\ N_{D,H} & N_{D,D} \end{pmatrix},$$

where N_{DD} is a 2×2 matrix.

Appendix 2: Computational Methods

For completeness, we very briefly describe the computational methods utilized in our investigations reported in Sects. 3.2 and 3.3 above. For more details, the interested reader is referred to Barker et al. (2013) where an analogous numerical study is performed on the generalized Kuramoto–Sivashinsky equation.

3.4 Hill’s Method

To determine the global picture of spectrum of a linear X -periodic operator L , we use Hill’s method. The linear operator L takes the form $L_{j,k} = \sum_{q=1}^{m,jk} f_{j,k,q}(x) \frac{\partial^q}{\partial x^q}$ where the $f_{j,k,q}(x)$ are X periodic. Following Deconinck et al. (2007), we represent the coefficient functions $f_{j,k,q}(x)$ as a Fourier series $f_{j,k,q}(x) = \sum_{j=-\infty}^{\infty} \hat{\phi}_{j,k,q} e^{i2\pi jx/X}$.

We use MATLAB’s fast Fourier transform to determine the coefficients $\hat{\phi}_{j,k,q}$. The generalized eigenfunctions are represented as²⁵ $v(x) = e^{i\xi x} \sum_{j=-\infty}^{\infty} \hat{v}_j e^{i\pi jx/X}$, where $\xi \in [-\pi/2X, \pi/2X]$ is the Floquet exponent. Upon substituting the Fourier expansions into the eigenvalue problem, fixing ξ , and equating the coefficients of the resulting Fourier series, we arrive at the eigenvalue problem $\hat{L}^\xi \hat{v} = \lambda \hat{v}$ where \hat{L}^ξ is an infinite-dimensional matrix. The spectrum of the operator L is given by $\sigma(L) = \bigcup_{\xi \in [-\pi/2X, \pi/2X]} \sigma(L_\xi)$. Truncating the Fourier series at N terms leads to a finite-dimensional eigenvalue problem $L_N^\xi \hat{v} = \lambda \hat{v}$. The matrix L_N^ξ is of the form $M_2^{-1} M_1$ where $M_1 \hat{v} = \lambda M_2 \hat{v}$ is the original eigenvalue problem. Typically M_2 is the identity, but in (3.14), M_2 is diagonal with j th diagonal entry $i(j + \xi)$; hence, we avoid $\xi = 0$ in that case so that M_2 is invertible. We compute $\sigma(L_N^\xi)$ on a mesh to approximate the spectral curves of L . For our numerical studies, we used the implementation of Hill’s method built into STABLAB [BHZ]. For discussion of Hill’s method and its convergence, see Curtis and Deconinck (2010), Deconinck and Nathan Kutz (2006), Johnson and Zumbrun (2012).

3.5 Evans Function

Our results for Hill’s method are augmented by use of the Evans function. To this end, note all the spectral problems we study, such as the one given in (3.14), may be written as a first-order system of the form $W'(x) = \mathbb{A}(x; \lambda)W(x)$ and that, further, $\lambda \in \mathbb{C}$ belongs to the essential spectrum of the associated linearized operator L if and only if this first-order system admits a nontrivial solution satisfying

$$Y(x + X; \lambda) = e^{i\xi X} Y(x; \lambda), \quad \forall x \in \mathbb{R}$$

where here X denotes the period of the coefficients of L . Following Gardner (1993), the Evans function is defined as $D(\lambda, \xi) := \det(\Psi(X, \lambda) - e^{i\xi X})$ where the matrix $\Psi(x, \lambda)$ satisfies $\partial_x \Psi(x, \lambda) = \mathbb{A}\Psi(x, \lambda)$ and $\Psi(0, \lambda) = \text{Id}$. By construction then, the roots of $D(\cdot; \xi)$ agree in location and algebraic multiplicity with the eigenvalues of the associated ξ -dependent spectral problem. Unfortunately, the Evans function as described here is poorly conditioned for numerical computation. To remedy this, as in Barker et al. (2013), we use the observation of Gardner (1993) that

$$D(\lambda, \xi) := \det(\Psi(X) - e^{i\xi X} \text{Id}) = \det \begin{pmatrix} \Psi(X) & e^{i\xi X} \text{Id} \\ \text{Id} & \text{Id} \end{pmatrix},$$

to express the Evans function as an exterior product of solutions of

$$\begin{pmatrix} Y \\ \alpha \end{pmatrix}' = \begin{pmatrix} \mathbb{A}(\cdot, \lambda)Y \\ 0 \end{pmatrix},$$

²⁵ Mark that in the standard implementation of Hill’s method a periodic wave is treated as a periodic function of twice its fundamental period. As recalled in (Rodrigues 2013, Section 3.1, p.67), this is originally motivated by the fact that in applications to self-adjoint second-order scalar operators, the Floquet-zero spectrum will then provide edges of spectral bands.

with data $(\text{Id}, \text{Id})^T$ at $x = 0$ and $(e^{i\xi X}\text{Id}, \text{Id})^T$ at $x = X$; for details see [Barker et al. \(2013\)](#). We then use the *polar coordinate method* of [Humpherys and Zumbrun \(2006\)](#) to evolve the solutions. This algorithm is numerically well conditioned [Zumbrun \(2009\)](#). All computations were carried out using STABLAB [BHZ].

As mentioned above, Hill’s method is ideal for obtaining a global picture of the spectrum and the Evans function can be evaluated on contours and the winding number evaluated to determine the presence of zeros. However, neither method determines definitively whether unstable spectra of arbitrarily small size exist, due to numerical error. In particular, such methods cannot be used to determine the spectrum of the associated linearized operators in a sufficiently small neighborhood of the origin, i.e., they cannot resolve the modulational instability problem. A strategy for rigorously computing *stability*, which we utilize in our intermediate F numerical studies reported in 3.3 above, involves a Taylor expansion of the Evans function as we now briefly describe; see [Barker et al. \(2013\)](#) for details.

Due to the presence of a conservation law in the governing system (see [Serre \(2005\)](#), [Johnson et al. \(2011\)](#), [Johnson et al. \(2014\)](#), [Rodrigues \(2013\)](#)) the Evans function has a double root at the origin when $\xi = 0$. As such, the Taylor expansion of the Evans function about the origin $(\lambda, \xi) = (0, 0)$ takes the form $D(\lambda, \xi) = c_{2,0}\lambda^2 + c_{1,1}\lambda\xi + c_{0,2}\xi^2 + c_{3,0}\lambda^3 + c_{2,1}\lambda^2\xi + c_{1,2}\lambda\xi^2 + c_{0,3}\xi^3 + O(|\lambda|^4 + |\xi|^4)$ where the coefficients $c_{k,j}$ may be determined via Cauchy’s integral formula,

$$c_{k,j} = -\frac{1}{4\pi^2} \oint_{\partial B(0,r)} \oint_{\partial B(0,r)} D(\lambda, \xi)\lambda^{-k-1}\xi^{-j-1}d\lambda d\xi \tag{3.16}$$

with $r > 0$ sufficiently small. Setting $\alpha_j = \frac{-c_{1,1}+(-1)^{j+1}\sqrt{c_{1,1}^2-4c_{2,0}c_{0,2}}}{2c_{2,0}}$, $\beta_j = \frac{-c_{3,0}\alpha_j^3+c_{2,1}\alpha_j^2+c_{1,2}\alpha_j+c_{0,3}}{2c_{2,0}\alpha_j+c_{1,1}}$, one readily checks that the roots of the Evans function near $(\lambda, \xi) = (0, 0)$ may be continued for $|\xi| \ll 1$ as

$$\lambda_j(\xi) = \alpha_j\xi + \beta_j\xi^2 + \frac{\xi^3}{2} \int_0^1 (1-s)^2 \lambda_j'''(s\xi) ds.$$

The spectral curves at the origin are thus approximated by $\alpha_j\xi + \beta_j\xi^2$ with spectral stability corresponding to the case $\alpha_j \in \mathbb{R}i$ and $\Re(\beta_j) < 0$; see [Barker et al. \(2013\)](#) for details.

In practice, to compute the Taylor expansion coefficients, rather than to compute the Evans function on the contour integral in the variable λ for fixed ξ given in (3.16), we interpolate with $\sum_{k=0}^K e^{ik\xi x}$ ($K = 3$ is the largest power of $e^{i\xi x}$ that appears) and then use the Taylor expansion $e^{ik\xi x} = 1 + (ik\xi x) + (ik\xi x)^2/2 + \dots$ yielding $D(\lambda, \xi) = \sum_{k=0}^\infty c_k \xi^k$, from which the contour integral can be determined simply by reading off the corresponding coefficient. Calling the quantity just determined \tilde{D} , we see

$$\frac{1}{2\pi i} \oint_{|\lambda|=R_1} \frac{\tilde{D}(\lambda)}{\lambda^{r+1}} d\lambda = \frac{1}{2\pi} \int_{-\pi}^\pi \frac{\tilde{D}(Re^{i\theta})}{R^r e^{ir\theta}} d\theta = \frac{1}{2R^r} \int_{-1}^1 \tilde{D}(Re^{i\pi\theta}) e^{-ir\pi\theta} d\theta,$$

which we compute by approximating the integrand with Chebyshev interpolation and integrating.

4 Computational Effort

4.1 Computational Environment

In carrying out our numerical investigations, we used a MacBook laptop with 2GB memory and a duo core Intel processor with 2GHz processing speed, a 2009 Mac Pro with 16GB memory and two quad-core Intel processors with 2.26 GHz processing speed, and Quarry, a supercomputer at Indiana University consisting of 140 IBM HS21 Blade servers with two 2GH quad-core Intel Zeon 5335 processors per node and delivering 8.96 teraflops processing speed. All computations were done using MATLAB and the MATLAB-based stability package STABLAB.

4.2 Computational Time

We begin by providing computational statistics for the representative parameter set $\alpha = -2$, $q_0 = 0.4$, $F = 10$, and $X = 50$. We compute the Evans function, $D(\lambda, \xi)$, on a semicircular contour, Ω , of radius $R = 0.2$ with 42 evenly spaced Floquet parameters $\xi \in [-\pi/X, -\pi/(10X)] \cup [\pi/(10X), \pi/X]$. We require the relative error between contour points of the image contour, $Y_\xi, D(\cdot, \xi) : \Omega \rightarrow Y_\xi$, not exceed 0.2 so that Rouché's theorem implies the winding number of Y_ξ corresponds to the number of roots of $D(\cdot, \xi)$ in Ω . We use 277 points in Ω , chosen adaptively, to achieve 0.2 relative error in each Y_ξ at a computational cost of 56.0s using 8 MATLAB workers on Quarry to determine the winding number is zero. Computing the Taylor expansion of the Evans function at the origin requires 61.7s on Quarry, while computing the spectrum via Hill's method using 603 Fourier modes and 21 Floquet parameters comes at a computational cost of 143 s.

As the period X increases or as F increases, the number of Fourier modes needed in Hill's method increases. Using 600 Fourier modes typically takes around 3 min on the Mac Pro, while using 1600 Fourier modes takes about 77 min, and using 3000 Fourier modes requires approximately 8 h.

In creating Fig. 4a, it took 4.36 days of computation time to evaluate the Taylor coefficients and 34.5 days to compute the spectrum using Hill's method, while the Evans function required an estimated 58 h. A typical profile requires only a few seconds to compute, but we must use continuation whereby we use a nearby profile as an initial guess in the boundary value solver, so that computing the profiles also required a great computational effort. Overall, taking into account the use of parallel computing and all values of α investigated, we estimate that total computational time for the project exceeds a year.

References

- Abd-el Malek, M.B.: Approximate solution of gravity-affected flow from planar sluice gate at high Froude number. *J. Comput. Appl. Math.* **35**(13), 83–97 (1991)

- Aung Win, H.: Model equation of surface waves of viscous fluid down an inclined plane. *J. Math. Kyoto Univ.* **33**(3), 803–824 (1993)
- Balmforth, N.J., Mandre, S.: Dynamics of roll waves. *J. Fluid Mech.* **514**, 1–33 (2004)
- Barker, B., Humpherys, J., Zumbrun, K.: STABLAB: A MATLAB-based numerical library for Evans function computation. <http://impact.byu.edu/stablab/>
- Barker, B., Johnson, M., Noble, P., Rodrigues, L.M., Zumbrun, K.: Whitham averaged equations and modulational stability of periodic traveling waves of a hyperbolic-parabolic balance law. *Journées Équations aux Dérivées Partielles* **6**, 1–24 (2010). <http://eudml.org/doc/116384>
- Barker, B., Johnson, M.A., Rodrigues, L.M., Zumbrun, K.: Metastability of solitary roll wave solutions of the St. Venant equations with viscosity. *Phys. D* **240**(16), 1289–1310 (2011)
- Barker, B., Johnson, M.A., Noble, P., Rodrigues, L.M., Zumbrun, K.: Stability of periodic Kuramoto–Sivashinsky waves. *Appl. Math. Lett.* **25**(5), 824–829 (2012)
- Barker, B., Johnson, M.A., Noble, P., Rodrigues, L.M., Zumbrun, K.: Nonlinear modulational stability of periodic traveling-wave solutions of the generalized Kuramoto–Sivashinsky equation. *Phys. D* **258**, 11–46 (2013)
- Barker, B.: Numerical proof of stability of roll waves in the small-amplitude limit for inclined thin film flow. *J. Differ. Equ.* **257**(8), 2950–2983 (2014)
- Bar, D.E., Nepomnyashchy, A.A.: Stability of periodic waves governed by the modified Kawahara equation. *Phys. D* **86**(4), 586–602 (1995)
- Benzoni-Gavage, S., Mietka, C., Rodrigues L.M.: Co-periodic stability of periodic waves in some Hamiltonian PDEs. Nonlinearity (to appear). [arXiv:1505.01382](https://arxiv.org/abs/1505.01382)
- Benzoni-Gavage, S., Noble, P., Rodrigues, L.M.: Slow modulations of periodic waves in Hamiltonian PDEs, with application to capillary fluids. *J. Nonlinear Sci.* **24**(4), 711–768 (2014)
- Bottman, N., Deconinck, B.: KdV cnoidal waves are spectrally stable. *Discrete Contin. Dyn. Syst.* **25**(4), 1163–1180 (2009)
- Boudlal, A., Yu Liapidevskii, V.: Stability of regular roll waves. *J. Comput. Technol.* **10**(2), 3–14 (2005)
- Brock, R.R.: Development of roll-wave trains in open channels. *J. Hydraul. Div.* **95**(4), 1401–1428 (1969)
- Brock, R.R.: Periodic permanent roll waves. *J. Hydraul. Div.* **96**(12), 2565–2580 (1970)
- Chang, H.-C., Demekhin, E.A., Kopelevich, D.I.: Laminarizing effects of dispersion in an active-dissipative nonlinear medium. *Phys. Rev. D* **63**(3–4), 299–320 (1993)
- Chang, H.-C., Demekhin, E.A.: *Complex Wave Dynamics on thin Films, Studies in Interface Science*, vol. 14. Elsevier Science B.V, Amsterdam (2002)
- Collet, P., Eckmann, J.-P.: *Instabilities and Fronts in Extended Systems*, Princeton Series in Physics. Princeton University Press, Princeton (1990)
- Curtis, C.W., Deconinck, B.: On the convergence of Hill’s method. *Math. Comput.* **79**(269), 169–187 (2010)
- Deconinck, B., Kiyak, F., Carter, J.D., Nathan Kutz, J.: SpectrUW: a laboratory for the numerical exploration of spectra of linear operators. *Math. Comput. Simul.* **74**(4–5), 370–378 (2007)
- Deconinck, B., Kapitula, T.: The orbital stability of the cnoidal waves of the Korteweg–de Vries equation. *Phys. Lett. A* **374**(39), 4018–4022 (2010)
- Deconinck, B., Nathan Kutz, J.: Computing spectra of linear operators using the Floquet–Fourier–Hill method. *J. Comput. Phys.* **219**(1), 296–321 (2006)
- Dressler, R.F.: Mathematical solution of the problem of roll-waves in inclined open channels. *Commun. Pure Appl. Math.* **2**, 149–194 (1949)
- Ercolani, N.M., McLaughlin, D.W., Roitner, H.: Attractors and transients for a perturbed periodic KdV equation: a nonlinear spectral analysis. *J. Nonlinear Sci.* **3**(4), 477–539 (1993)
- Freeze, B., Smolentsev, S., Morley, N., Abdou, M.: Characterization of the effect of froude number on surface waves and heat transfer in inclined turbulent open channel water flows. *Int. J. Heat Mass Transf.* **46**(20), 3765–3775 (2003)
- Frisch, U., She, Z.-S., Thual, O.: Viscoelastic behaviour of cellular solutions to the Kuramoto–Sivashinsky model. *J. Fluid Mech.* **168**, 221–240 (1986)
- Gardner, R.A.: On the structure of the spectra of periodic travelling waves. *J. Math. Pure Appl.* (9) **72**(5), 415–439 (1993)
- Gardner, R.A.: Spectral analysis of long wavelength periodic waves and applications. *J. Reine Angew. Math.* **491**, 149–181 (1997)
- Gardner, R.A., Zumbrun, K.: The gap lemma and geometric criteria for instability of viscous shock profiles. *Commun. Pure Appl. Math.* **51**(7), 797–855 (1998)

- Guckenheimer, J., Holmes, P.: *Nonlinear Oscillations, Dynamical Systems, and Bifurcations of Vector Fields*, Volume 42 of *Applied Mathematical Sciences*. Springer, New York (1990). Revised and corrected reprint of the 1983 original
- Hărăguș, M., Kapitula, T.: On the spectra of periodic waves for infinite-dimensional Hamiltonian systems. *Phys. D* **237**(20), 2649–2671 (2008)
- Hong Hwang, S., Chang, H.-C.: Turbulent and inertial roll waves in inclined film flow. *Phys. Fluids* **30**(5), 1259–1268 (1987)
- Humpherys, J., Zumbrun, K.: An efficient shooting algorithm for Evans function calculations in large systems. *Phys. D* **220**(2), 116–126 (2006)
- Jeffreys, H.: Lxxxiv. the flow of water in an inclined channel of rectangular section. *Philos. Mag. Ser. 6* **49**(293), 793–807 (1925)
- Johnson, M.A., Zumbrun, K.: Nonlinear stability of periodic traveling wave solutions of systems of viscous conservation laws in the generic case. *J. Differ. Equ.* **249**(5), 1213–1240 (2010)
- Johnson, M.A., Zumbrun, K.: Nonlinear stability of periodic traveling-wave solutions of viscous conservation laws in dimensions one and two. *SIAM J. Appl. Dyn. Syst.* **10**(1), 189–211 (2011)
- Johnson, M.A., Zumbrun, K.: Convergence of Hill’s method for nonselfadjoint operators. *SIAM J. Numer. Anal.* **50**(1), 64–78 (2012)
- Johnson, M.A., Zumbrun, K., Noble, P.: Nonlinear stability of viscous roll waves. *SIAM J. Math. Anal.* **43**(2), 577–611 (2011)
- Johnson, M. A., Noble, P., Rodrigues, L.M., Zumbrun, K.: Behavior of periodic solutions of viscous conservation laws under localized and nonlocalized perturbations. *Invent. Math.* **197**(1), 115–213 (2014)
- Johnson, M.A., Noble, P., Rodrigues, L.M., Zumbrun, K.: Spectral stability of periodic wave trains of the Korteweg-de Vries/Kuramoto-Sivashinsky equation in the Korteweg-de Vries limit. *Trans. Am. Math. Soc.* **367**(3), 2159–2212 (2015)
- Jun, Y., Yang, Y.: Evolution of small periodic disturbances into roll waves in channel flow with internal dissipation. *Stud. Appl. Math.* **111**(1), 1–27 (2003)
- Kapitula, T., Promislow, K.: *Spectral and Dynamical Stability of Nonlinear Waves*, Volume 185 of *Applied Mathematical Sciences*. Springer, New York (2013) With a foreword by Christopher K. R. T. Jones
- Kuramoto, Y.: *Chemical Oscillations, Waves, and Turbulence*, Springer Series in Synergetics, vol. 19. Springer, Berlin (1984)
- Kuramoto, Y., Tsuzuki, T.: On the formation of dissipative structures in reaction-diffusion systems, reductive perturbation approach. *Prog. Theor. Phys.* **54**(3), 687–699 (1975)
- Kuznetsov, E.A., Spector, M.D., Fal’kovich, G.E.: On the stability of nonlinear waves in integrable models. *Phys. D* **10**(3), 379–386 (1984)
- Mielke, A.: The Ginzburg–Landau equation in its role as a modulation equation. In: Fiedler, B. (ed.) *Handbook of Dynamical Systems*, vol. 2, pp. 759–834. North-Holland, Amsterdam (2002)
- Mielke, A.: Instability and stability of rolls in the Swift–Hohenberg equation. *Commun. Math. Phys.* **189**(3), 829–853 (1997)
- Mielke, A.: Mathematical analysis of sideband instabilities with application to Rayleigh–Bénard convection. *J. Nonlinear Sci.* **7**(1), 57–99 (1997)
- Mikyong Hur, V., Johnson, M.A.: Modulational instability in the Whitham equation for water waves. *Stud. Appl. Math.* **134**(1), 120–143 (2015)
- Noble, P.: On the spectral stability of roll-waves. *Indiana Univ. Math. J.* **55**(2), 795–848 (2006)
- Noble, P., Rodrigues, L.M.: Whitham’s modulation equations and stability of periodic wave solutions of the Korteweg-de Vries-Kuramoto-Sivashinsky equation. *Indiana Univ. Math. J.* **62**(3), 753–783 (2013)
- Oh, M., Zumbrun, K.: Stability and asymptotic behavior of periodic traveling wave solutions of viscous conservation laws in several dimensions. *Arch. Ration. Mech. Anal.* **196**(1), 1–20 (2010). Erratum. *Arch. Ration. Mech. Anal.* **196**(1), 21–23 (2010)
- Pego, R.L., Schneider, G., Uecker, H.: Long-time persistence of Korteweg-de Vries solitons as transient dynamics in a model of inclined film flow. *Proc. R. Soc. Edinb. Sect. A* **137**(1), 133–146 (2007)
- Plaza, R., Zumbrun, K.: An Evans function approach to spectral stability of small-amplitude shock profiles. *Discrete Contin. Dyn. Syst.* **10**(4), 885–924 (2004)
- Reed, M., Simon, B.: *Methods of Modern Mathematical Physics. IV. Analysis of Operators*. Academic Press [Harcourt Brace Jovanovich, Publishers], New York, London (1978)
- Richard, G.L., Gavriluk, S.L.: A new model of roll waves: comparison with Brock’s experiments. *J. Fluid Mech.* **698**, 374–405 (2012)

- Richard, G.L., Gavriluk, S.L.: The classical hydraulic jump in a model of shear shallow-water flows. *J. Fluid Mech.* **725**, 492–521 (2013)
- Rodrigues, L.M.: Asymptotic stability and modulation of periodic wavetrains, general theory & applications to thin film flows. Habilitation à diriger des recherches, Université Lyon 1 (2013). <https://tel.archives-ouvertes.fr/tel-01135522v1>
- Rodrigues, L.M., Zumbrun, K.: Periodic-coefficient damping estimates, and stability of large-amplitude roll waves in inclined thin film flow. *SIAM J. Math. Anal.* **48**(1), 268–280 (2016)
- Sandstede, B., Scheel, A.: On the stability of periodic travelling waves with large spatial period. *J. Differ. Equ.* **172**(1), 134–188 (2001)
- Schneider, G.: Nonlinear diffusive stability of spatially periodic solutions—abstract theorem and higher space dimensions. In *Proceedings of the International Conference on Asymptotics in Nonlinear Diffusive Systems (Sendai, 1997)*, Volume 8 of Tohoku Mathematical Publications, pp 159–167. Tohoku University, Sendai (1998)
- Schneider, G.: Diffusive stability of spatial periodic solutions of the Swift–Hohenberg equation. *Commun. Math. Phys.* **178**(3), 679–702 (1996)
- Serre, D.: Spectral stability of periodic solutions of viscous conservation laws: large wavelength analysis. *Commun. Partial Differ. Equ.* **30**(1–3), 259–282 (2005)
- Sivashinsky, G.I.: Nonlinear analysis of hydrodynamic instability in laminar flames. I. Derivation of basic equations. *Acta Astronaut.* **4**(11–12), 1177–1206 (1977)
- Sivashinsky, G.I.: Instabilities, pattern formation, and turbulence in flames. *Ann. Rev. Fluid Mech.* **15**(1), 179–199 (1983)
- Spektor, M.D.: Stability of conoidal [cnoidal] waves in media with positive and negative dispersion. *Zh. Èksper. Teoret. Fiz.* **94**(1), 186–202 (1988)
- Yang, Z., Zumbrun, K.: Stability of periodic traveling waves in the homoclinic limit (in preparation) (2016)
- Zumbrun, K.: Numerical error analysis for Evans function computations: a numerical gap lemma, centered-coordinate methods, and the unreasonable effectiveness of continuous orthogonalization. ArXiv e-prints (2009)
- Zumbrun, K., Howard, P.: Pointwise semigroup methods and stability of viscous shock waves. *Indiana Univ. Math. J.* **47**(3), 741–871 (1998)